Journal of Medicinal Chemistry



Article

# Design and Synthesis of Janus Kinase 2 (JAK2) and Histone Deacetlyase (HDAC) Bispecific Inhibitors Based on Pacritinib and Evidence of Dual Pathway Inhibition in Hematological Cell Lines

Eugene Guorong Yang, Nurulhuda Mustafa, Eng Chong Tan, Anders Poulsen, Pondy Murugappan Ramanujulu, Wee Joo Chng, Jeffrey J. Y. Yen, and Brian W. Dymock

*J. Med. Chem.*, **Just Accepted Manuscript** • DOI: 10.1021/acs.jmedchem.6b00157 • Publication Date (Web): 19 Aug 2016



ACS Publications

Journal of Medicinal Chemistry is published by the American Chemical Society. 1155 Sixteenth Street N.W., Washington, DC 20036

# Design and Synthesis of Janus Kinase 2 (JAK2) and Histone Deacetlyase (HDAC) Bispecific Inhibitors Based on Pacritinib and Evidence of Dual Pathway Inhibition in Hematological Cell Lines

Eugene Guorong Yang,[1] Nurulhuda Mustafa,[2‡] Eng Chong Tan,[3‡] Anders Poulsen,[4,5] Pondy Murugappan Ramanujulu,[1,6] Wee Joo Chng,[2,7,8] Jeffrey J. Y. Yen,[3] Brian W. Dymock[1,*]

[1] Department of Pharmacy, National University of Singapore, 18 Science Drive 4, Singapore 117543.

[2] Department of Medicine, Yong Loo Lin School of Medicine, National University of Singapore, 1E Kent Ridge Road, NUHS Tower Block Level 10, Singapore 119228.

[3] Institute of Biomedical Sciences, Academia Sinica, Taiwan, 11529.

[4] Experimental Therapeutics Centre, 31 Biopolis Way, 03-01 Nanos, Singapore 138669.

[5] Department of Chemistry, National University of Singapore, 3 Science Drive 3, Singapore 117543

[6] Life Sciences Institute, Centre for Life Sciences Level 5, 28 Medical Drive, National University of Singapore, Singapore 117456.

[7] Cancer Science Institute, Singapore, National University of Singapore

[8] National University Cancer Institute of Singapore, National University Health System

[#]these authors contributed equally

KEYWORDS: Dual inhibitor, Designed Multiple Ligand, Janus Kinase Inhibitor, Histone Deacetylase Inhibitor.

**ABSTRACT:** Blockage of more than one oncoprotein or pathway is now a standard approach in modern cancer therapy. Multiple inhibition is typically achieved with two or more drugs. Herein we describe a pharmacophore merging strategy combining the JAK2/FLT3 inhibitor pacritnib with the pan-HDAC inhibitor, vorinostat, to create bispecific single molecules with both JAK and HDAC targeted inhibition. A preferred ether hydroxamate, **51** inhibits JAK2 and HDAC6 with low nanomolar potency, is <100 nM potent against HDACs 2 and 10, sub-micromolar potent against HDACs 1, 8 and 11, and >50 fold selective for JAK2 in a panel of 97 kinases. Broad cellular antiproliferative potency is supported by demonstration of JAK-STAT and HDAC pathway blockade in several hematological cell lines, inhibition of colony formation in HEL cells, and analysis of apoptosis. This study provides new tool compounds for further exploration of dual JAK-HDAC pathway inhibiton achieved with a

single molecule.

## INTRODUCTION

Cancer is a multi-faceted disease often requiring multiple therapeutic interventions for successful long term outcomes.[1] Traditional approaches to combating cancer, still in widespread use today, are non-selective such as radiation or chemotherapy.[2] At the other extreme, targeted treatment of cancer typically aims to target cancer cells via blockage of a single biological target. However, more intensive evaluation of typical 'targeted' drugs often reveals multiple-target mechanisms.[3, 4] Realization that simultaneous inhibition of multiple mechanisms can lead to additive effects, or even synergy, has led to a rise in combinations of targeted therapies with each other and with non-selective regimens.[2] In today's therapeutic armoury, an increasing array of complex combination strategies tailored to individual diseases, and increasingly, individual patients, is available.[5] Despite many significant improvements, it is clear that less complex approaches are required for multiple pathway intervention to tackle challenging or resistant tumors.

There are generally three methods to achieve multi-target knockdown – use of a cocktail of separate drugs, a multicomponent drug and the multiple ligand approach.[6-8] Drug cocktails, specifically combinations of single agents each targeted to specific mechanisms, are associated with poor patient compliance, complex pharmacokinetics and the challenge of drug-drug interactions.[9]

Similarly, the multicomponent drug regimen, where two or more separate agents are formulated into a single tablet can suffer from drug-drug interactions and differing physicochemical properties between components that can affect the efficacy of the drugs administered. Polypharmacology is recognized as an approach where more than one therapeutic pathway can be modulated by a *single* molecule. Specific strategies to combine targeted mechanisms together are referred to as the multiple ligand, multi-component ligand, or designed multiple ligand (DML) approaches. In these cases a single drug molecule has multiple, but targeted, pharmacology.[10, 11] With this approach, once the potency ratio is determined is it fixed within the molecule hence the variable pharmacokinetics usually seen with combinations of two single agents will not affect the potency ratio of a DML in the same way. However it should be noted that DMLs are just as susceptible to metabolism as any other drug, reducing or eliminating the biological activity or pharmacodynamic profile of the compound. Being single molecules DMLs will not suffer from drug-drug interactions, unless combined with another drug. There is also opportunity for structural novelty – design of a DML is not just a matter of joining two pharmacophores together, it is a creative process to balance multiple SARs while maintaining drug-like properties. Development costs for a DML are likely to be significantly lower than development of a multiple drug combination, but this must be balanced with other potential downsides such as molecular weight inflation, the challenge of balancing multiple SARs and potentially more

challenging synthesis are all present dangers. DMLs are not new, in fact, multi-GPCR modulators, as well as multi-kinase inhibitors, have been known for many years.[12] In this work we focus on DMLs that target *two different classes* of enzyme, rather than two enzymes performing the same type of transformation. Deliberate strategies to adopt such a DML approach at the outset for enzyme inhibitors in cancer are not commonly reported. Recent progress has been most successful combining the histone deacetylase (HDAC) pharmacophore with other enzyme inhibitor activities, such as kinases. Examples of successful kinase-HDAC DMLs have now reached the clinic in oncology pioneered by Curis, although none are yet approved by the FDA. CUDC-101[13-17] (HDAC/EGFR2 inhibitor) and CUDC-907[18] (PI3K/HDAC inhibitor) have both entered phase I clinical trials (Figure 1). Inspired by this progress we have been focused on designed combinations of JAK2 kinase / HDAC DMLs for study in cancer, using **1** (vorinostat / SAHA) and **2** (pacritinib / SB1518) as initial templates.

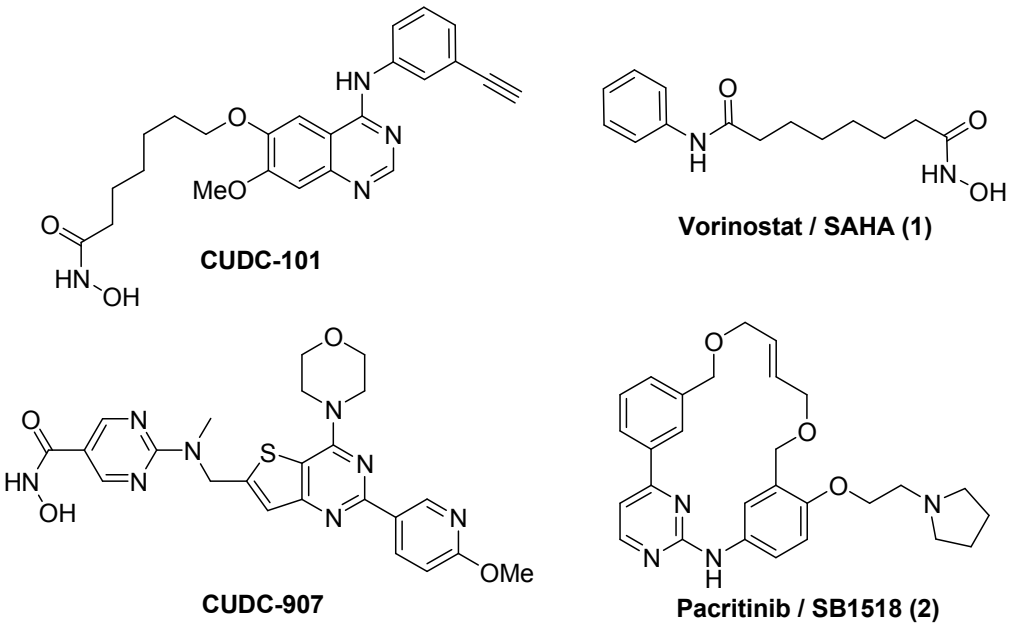


**Figure 1**. Structures of dual inhibitors, HDAC inhibitor **1** and JAK2/FLT3 inhibitor **2**.

Janus Kinase (JAK) inhibitors[19, 20] have been developed rapidly following the discovery of the JAK2-V617F[21-24] mutation in patients with myeloproliferative neoplasms (MPNs). This has led to the approval of (3*R*)-3-cyclopentyl-3-[4-(7*H*-pyrrolo[2,3-*d*]pyrimidin-4-yl)pyrazol-1-yl]propanenitrile (ruxolitinib/INCB018424) and 3-[(3*R*,4*R*)-4-methyl-3-[methyl(7*H*-pyrrolo[2,3-*d*]pyrimidin-4-yl)amino]piperidin-1-yl]-3-oxopropanenitrile (tofacitinib/CP690550) as JAK inhibitors for the treatment of myelofibrosis (MF)[25, 26] and rheumatoid arthritis[27], respectively. Compound **2** (Figure 1) has been developed[28, 29] as a dual JAK2 and fms-like tyrosine kinase-3 (FLT3) selective inhibitor and has successfully completed its first phase 3 trial, PERSIST-1, as an orphan drug[30] for myelofibrosis (MF) patients with

thrombocytopenia (low platelet levels).[31] On the basis of the phase 3 data, an NDA filing of **2** was recently initiated at the US FDA.[32] Soon after this filing compound **2** was put on full clinical hold by the FDA while investigations of patient deaths are investigated. At the time of writing FDA reinstated use of **2** via an individual patient application protocol. Another clinical concern is the onset of resistance which has been shown in the case of ruxolitinib to be due to the reactivation of JAK-STAT signaling where heterodimerisation between activated JAK2 and JAK1 or TYK2 occurs; and not due to mutation or change in the active site of JAK2 itself.[33] JAK2 inhibitor resensitisation occurred upon withdrawal of treatment. More importantly JAK2 inhibitor resistant cells still remain dependent on JAK2 protein expression. Alternative therapies that degrade JAK2 indirectly are also effective and have been postulated to be good combinations with JAK2 inhibitors. Some of the possible targets for potentially synergistic JAK2 combination therapy include histone deacetylase (HDAC)[34-36], Heat Shock Protein 90 (HSP90)[34-36], phosphoinositide 3-kinase (PI3K)[37, 38], and B-cell lymphoma 2 (Bcl2).[39] With this in mind we postulated that a drug-like DML which could inhibit JAK2 and HDAC in a cell in a similar concentration range could be created and would be effective in JAK2-sensitive or resistant cells.

HDAC enzymes were initially discovered to deacetylate histones affecting how tightly the DNA is bound to the histone and subsequently regulation of gene expression.[40] There are four classes of HDAC enzymes based on their function

and DNA sequence similarity.[41] However HDACs have also been found to interact with non-histone proteins,[42] thus they are implicated in a wide range of biological functions. HDAC inhibitors have been shown to be clinically effective as single agents[43] and entered the market earlier than the JAK inhibitors with the approval of **1** in 2007,[44] romidepsin (FK228)[45] and the recently approved belinostat (PXD101, FDA approval July 2014)[46] and panobinostat (LBH589, FDA approval February 2015).[47] However HDAC inhibitors have experienced slow and difficult clinical development as single agents due to limitations of toxicity.[48] Selective inhibition of individual HDAC isoforms, or smaller groups of isozymes, could prove beneficial in cancer therapy with some evidence of an improved therapeutic window in clinical studies, such as with the class-I selective benzamides.[49] Obtaining selectivity between individual HDAC isoforms has generally been challenging, but there have been reports of HDAC3, 6 and 8 selective compounds.[49-53] Selective HDAC6 inhibitors are achievable by optimisation of the cap region of the inhibitor taking advantage of the larger lip of the substrate binding pocket.[54-58] Overexpression of HDAC6 correlates with oncogenesis and improved survival. Some effects of HDAC6 inhibition have been to prevent migration and invasion of cancer cells by acetylation of α-tubulin and cortactin leading to a decrease in cell motility[59, 60], sensitisation of cancer cells to known DNA damaging agents[61] and induction of apotosis in cancerous cells.[62, 63] Increased HDAC activity has been observed in patients with MPN.[64, 65] Specifically, HDAC inhibitors have

been shown to be effective against MPN both as a single agent[66-68] and in combination[69-71] with JAK2 inhibitors. JAK2-selective TG101209 exerts synergistic toxic effects in MPN cell lines when combined with panobinostat.[69] Ruxolitinib and panobinostat in combination lead to improved efficacy in a mouse model of $JAK2^{V617F}$ driven disease.[71] In preclinical mouse models of AML, a combination of **2** and pracinostat (SB939) were found to be synergistic.[70] Thus, we hypothesised that a single compound that selectively inhibits both JAK2 as well as HDAC enzymes could have utility, especially in resistant MPN and AML, but perhaps also more broadly in solid tumors, compared to a single inhibitor alone. A weaker inhibitor of either enzyme in a dual acting DML could also potentially lead to lower toxicity levels while maintaining therapeutic efficacy leading to an overall safer profile.[72] In summary, our goal was to design and synthesise molecules, which inhibit *both* JAK2 and HDAC enzymes, seeking to explore selectivity between these two families of diverse enzymes.

Design of Dual Inhibitors

Substrate competitive HDAC inhibitors consist of a zinc binding functional group, a long chain or extended heterocycle and a cap group (Figure 2). The zinc binding group can be a bidentate group (eg. hydroxamic acid, benzamide, keto-thiol) which bind more strongly to the zinc cation or a monodentate group (eg. carboxylic acid, thiols).[73] With monodentate functional groups, the

importance of the "cap" increases as the interaction with the inhibitor increases relative to the zinc binding group. It was envisioned that we could achieve some selectivity for HDAC6 which is slightly wider in the "cap" region relative to HDAC1.[54] Some selective HDAC6 inhibitors that have been reported include tubacin[74], tubastatin A[54] and a small molecule hydroxamic acid without a cap group.[75] A lead compound was reported by Auzzas *et al*, where the HDAC selectivity is reversed to achieve 10 times HDAC6 ($IC_{50}$ 0.4 nM) selectivity over HDAC1.[76] Even more potent compounds, with HDAC6 $IC_{50}$ down to 2 pM, have been reported based on a phenylisoxazole cap. These compounds were 10 fold more potent than **1** in pancreatic cells.[65] Several natural products (and analogues) containing macrocycles have been discovered as HDAC inhibitors with most of them having moderate to high selectivity for HDAC1 over HDAC6. These are mainly macrocyclic tetrapeptides[64, 77-80], depsipeptides[81-83] (eg. romidepsin), azumamides[84] and peptidomimetics.[76, 85, 86]

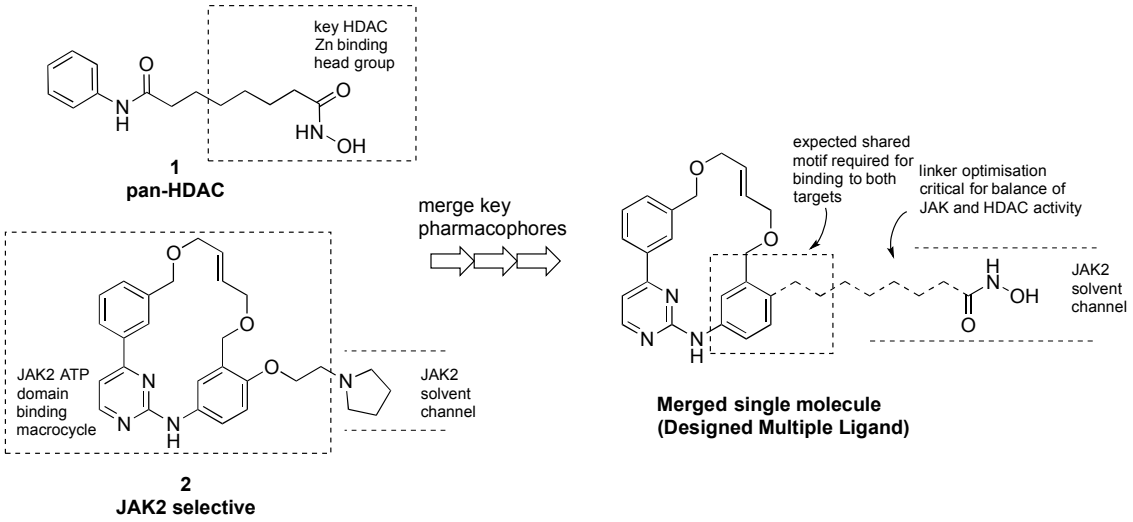

**Figure 2.** Schematic showing plans for merged JAK-HDAC pharmacophore taking advantage of the solvent binding channel in JAK2 and the probable interactions to be gained by a merged inhibitor at the entrance to the HDAC substrate binding pocket.

Aminopyrimidine **2**, which contains a macrocycle as its core JAK2-binding scaffold provides a suitable moiety to explore our hypothesis as it possesses key features required in both JAK2 and the cap of a potentially selective HDAC inhibitor. Furthermore, **2** is selective for JAK2 and FLT3, both enzymes which have been shown to be beneficial in MPN and AML, and it has been shown to be synergistic in both cellular and *in vivo* studies in combination with an HDAC inhibitor.[28, 29, 70] A recent study has shown that JAK2/FLT3 kinase-HDAC dual inhibitors derived from the potent cyclin dependant kinase (CDK) inhibiting macrocycle TG02 can be prepared, however HDAC selectivity was not explored.[87] Rather than linking two known inhibitors together with a long chain, which will typically result in a compound with high molecular weight (addition of both compound's molecular weight as well as the linker), a merged pharmacophore is more desirable.[6] For **2**, it is known that the pyrolidine ring is located in a solvent exposed region when binding to the enzyme and its main purpose is to improve the aqueous solubility of the compound.[28, 88] Thus it was postulated that inserting the HDAC binding group here will retain JAK2 activity while giving rise to potentially selective HDAC inhibition activity. We then

planned to study the resulting JAK-HDAC inhibitors in a range of both solid tumor and hematological cancer cell lines seeking evidence of target modulation ideally within the same concentration range.

## Chemistry

Starting from macrocycle chloride **3**[28] (Scheme 1), substitution with Boc-protected anilines **4a**, **5a** and **7a**, phenol **6a** and piperidine-4-methyl ester **8a** gave esters **4**-**6** and **8** and nitro **7**. Boc protection was required to increase the acidity of the anilines, performing the reaction at 100 °C for 24 h or at 120 °C for 18 h in DMF. Higher temperature leads to degradation of the product (Scheme 1). Reaction with **8a** was slower requiring heating for 3 days at 80 °C in acetonitrile. Nitro substituted aniline **7** provided a route to install a longer linker for the hydroxamic acid, similar to **1**. Reduction of nitro **7**, followed by coupling with monoester acids **10a**-**12a** bearing chain lengths of 4-6 methyenes gave boc-protected esters **10**-**12**. A more convergent approach attempted was to perform the substitution with 4-NHBoc substituted **10a** (Supplemental Scheme S1) but this gave a mixture of the desired product **12** and amide alkylation product **10b**, thus it was abandoned in favour of the longer but more practical route using **7**.

Following a merged pharmacophore strategy, compounds with long chain hydroxamic acids connected directly to the macrocycle ring, were synthesised

from commercially available **13** (Scheme 3). The common intermediate phenol **14** was prepared using two strategies. The first was a 3 step protocol, without purification or protecting groups, entailing the reduction of aldehyde **13** to the primary benzyl alcohol followed by chlorination using thionyl chloride. However this chlorination reaction was capricious and does not go to completion. Furthermore, the benzylic chloride is susceptible to reaction with water and must be used quickly. Refluxing in neat allyl alcohol gives the desired allyl ether **14** in 35% yield over 3 steps. A cleaner method was to use methoxymethyl (MOM) as a temporary phenol protecting group, with concomitant reduction of the aldehyde, followed by alkylation of the benzyl alcohol with allyl bromide under phase transfer conditions. Finally, deprotection of the phenol is achieved by refluxing in aqueous 4 M hydrochloric acid in THF. This 4-step protocol, while longer, gives a better overall yield of 72%. An alternative protecting group, 4-methoxybenzyl (PMB) gave only a 47% yield over 4 steps. Aside from the higher yield, the former was preferred due to the ease of purification of the product from the ether by-product arising from cleavage of the protecting group. Alkylation of phenol **14** with the appropriate bromo esters **15a**-**19a** gave compounds **15**-**19**. As per the reported[28] synthesis of **3**, the nitro group was reduced using iron and ammonium chloride. The crude aniline was stirred with the pyrimidine at 95 °C in dioxane for 18 h to give the diallyl compounds **21**-**25**. Ring closing metathesis with the Grubbs II catalyst[89]

in DCM with aqueous 4 M hydrochloric acid gave macrocycles **26-30** in good yields as approximately 85:15 mixtures of *trans* to *cis* isomers of the alkene.

Attempts to directly convert esters **26-30** to the hydroxamic acids using hydroxylamine hydrochloride and base such as sodium methoxide or sodium hydroxide at 0 °C or room temperature were not successful, with only the starting material being recovered. Attempted hydrolysis of the ester with lithium hydroxide was also not successful. Subsequently, it was found that by treating the ester with potassium trimethylsilanoate the acid could be successfully obtained. Attempts to couple the acids with *O*-THP protected hydroxylamine were ultimately successful using (1-[Bis(dimethylamino)methylene]-1H-1,2,3-triazolo[4,5-*b*]pyridinium 3-oxidhexafluorophosphate (HATU) but not 1-ethyl-3-(3-dimethylaminopropyl)carbodiimide (EDC). Deprotection of the THP using anhydrous hydrogen chloride in dioxane released the free hydroxamic acids in low to moderate yield.

**Scheme 1.** Preparation of intermediates **4-8**[a]

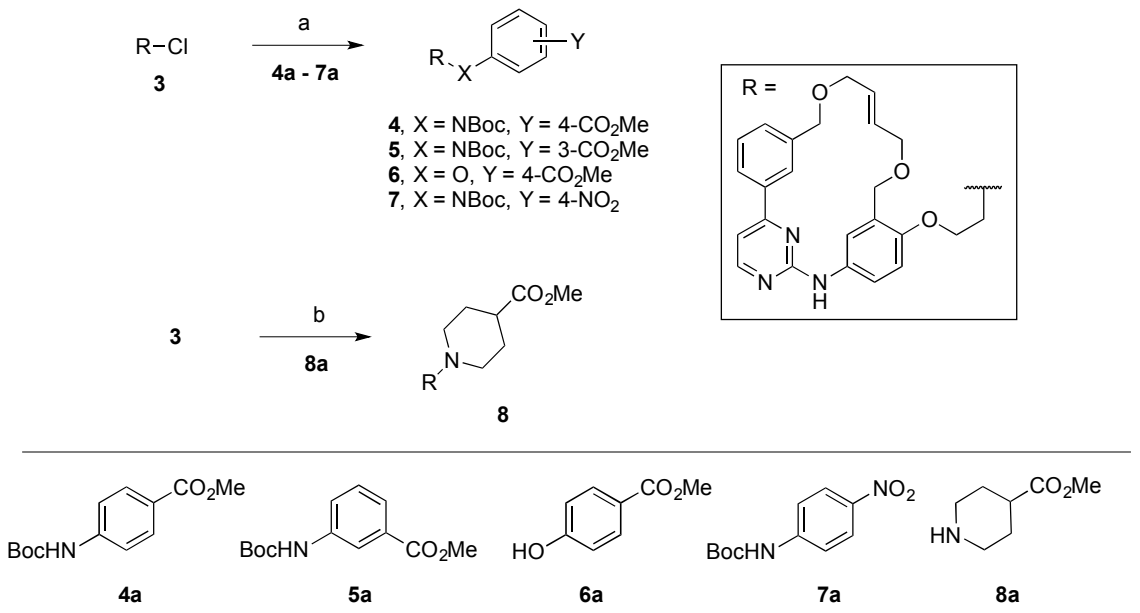


[a]Reagents and Conditions: (a) **4a-7a**, $Cs_2CO_3$, TBAI, DMF, 120 °C, 18 h, 45 to 82% yield; (b) **8a**, TBAI, MeCN, reflux, 72 h, 62% yield.

**Scheme 2.** Preparation of intermediates **10-12**[a]

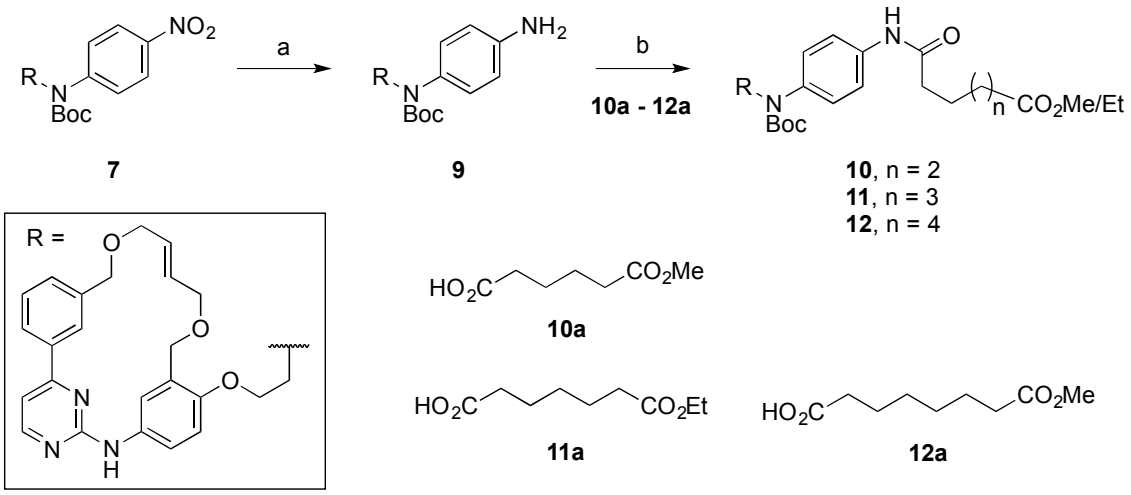


[a]Reagents and Conditions: (a) Fe, $NH_4Cl$, EtOH/$H_2O$ (2:1), reflux, 3 h; (b) **10a** – **12a**, NMM, $ClCO_2Et$, DCM, O °C to RT,18 h, 59 to 79% (over 2 steps).

**Scheme 3.** Preparation of intermediates **26-30**[a]

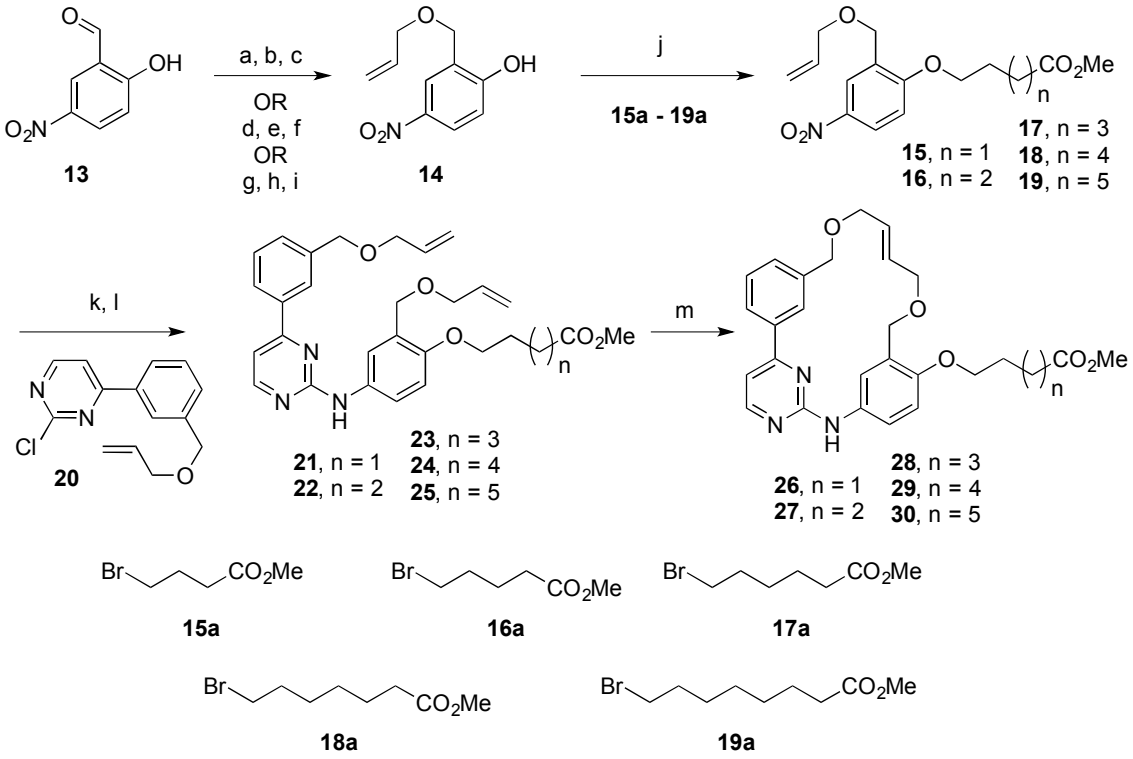


[a]Reagents and Conditions: (a) $NaBH_4$, MeOH, RT, 2 h; (b) $SOCl_2$, DCM, RT, 18 h ; (c) Allyl alcohol, reflux, 3 h, 35% (3 steps); (d) MOMCl, $NaBH_4$, MeOH, RT, 2 h; (e) *c.*NaOH, $NEt_3BnCl$, Allyl bromide, RT, 72 h; (f) 4M HCl, THF, reflux, 3 h, 72% yield (3 steps); (g) $NaBH_4$, MeOH, RT, 2 h; (h) $PPh_3$, $CCl_3CN$, DCM, RT, 16 h; (i) Allyl alcohol, reflux, 4 h, 35% (3 steps); (j) $K_2CO_3$, MeCN, reflux, 18 h, 84-100%; (k) **20**, Fe, $NH_4Cl$, EtOH/$H_2O$ (2:1), reflux, 3 h; (l) $TsOH.H_2O$, Dioxane, 95 °C, 18 h, 28-62% (2 steps); (m) Grubbs II, DCM, 4M HCl, reflux, 3 h, 62 to 83% yield.

**Scheme 4.** Preparation of test compounds **31**-**52**[a]

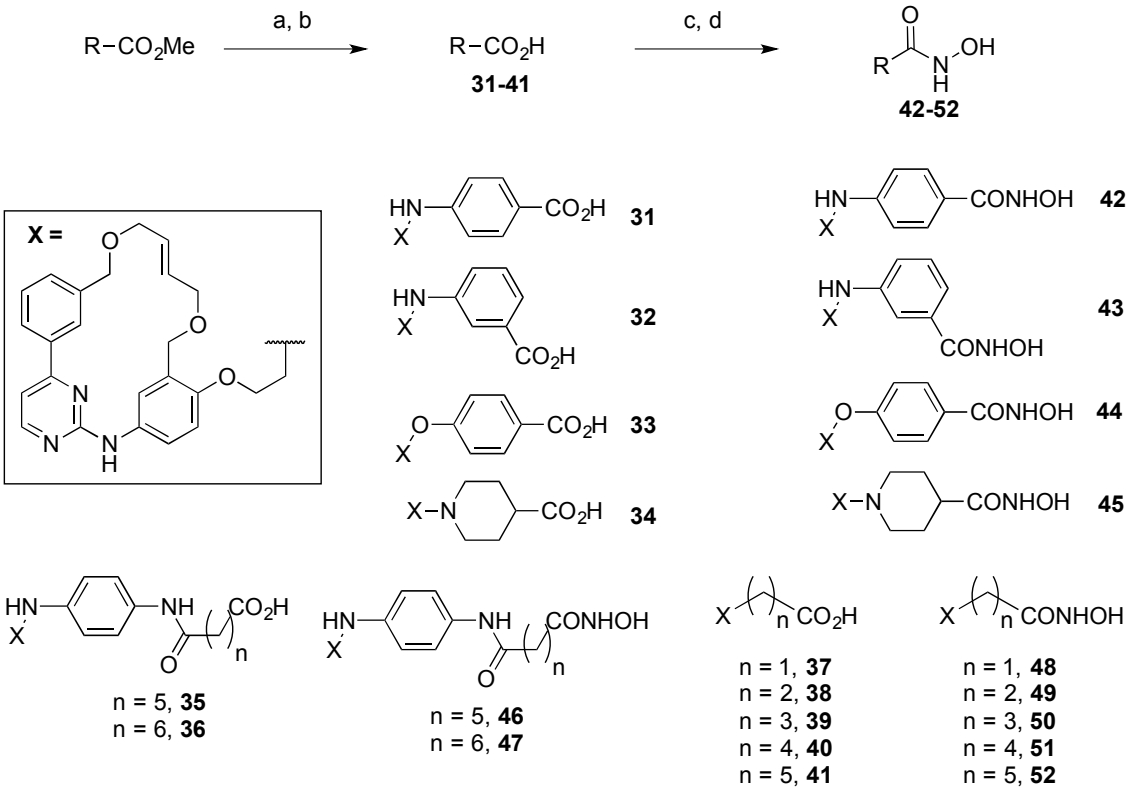


[a]Reagents and Conditions: (a) KOTMS, THF, RT, 2 h; (b) *c.*HCl, RT, 18 h, 44 to 83% yield (2 steps); (c) HATU, $NH_2OTHP$, $NEt_3$, DMSO, RT, 3 d; (d) 4M HCl in dioxane, RT, 18 h, 12-62% yield.

## RESULTS AND DISCUSSION

### Enzyme Inhibitory Activity

Carboxylic acids, such as valproic acid, are known to be weak HDAC inhibitors due to the weak chelating effect of the carboxylic acid to the zinc cation in the HDAC active site.[90] Thus, the carboxylic and hydroxamic acids were both tested in enzymatic and cellular assays. Reference compounds include **1** (pan-HDAC), **2** (JAK2 selective) and Tubastatin A (HDAC6 selective). Data for acids is shown in Table 1 and hydroxamates in Table 2. JAK2, HDAC1 and HDAC6 were selected for initial SAR studies, the latter due to the large macrocyclic cap group which we hypothesised would form additional interactions at the lip of the HDAC pocket potentially conferring HDAC isoform selectivity.[91] Unsurprisingly, given the common macrocyclic ring, significant inhibition of JAK2 enzymatic activity was observed with acids **31**-**34** ($IC_{50}$ <39 nM). Of these compounds only aminobenzoic acids **31** and **32** afforded weak HDAC6 inhibition and were completely inactive against HDAC1 at the highest concentration tested (10 μM). Likewise ether **33** and piperidine **34** were not HDAC active, probably due to the short distance between the acid and the bulky macrocycle. JAK2 potency was expected based on our design of the hybrid molecules whereby the zinc chelating functional group was in the

solvent exposed region of the JAK2 enzyme, while retaining the key binding features of **2** in the JAK2 enzyme binding pocket. Lengthening the distance between the Zn chelating group and macrocycle using an aniline linker yielded progressively more HDAC6 inhibition with a 5 methylene spacer (**35**, 20% inhibition at 10 μM) and with 6 methylenes (**36**, $IC_{50}$ = 2.6 μM). It is perhaps not entirely surprising that **36** would have HDAC activity, however, it is completely inactive against HDAC1 at 10 μM. Compound **36** was potent against JAK2 ($IC_{50}$ = 2.3 nM), similar to **2**, reassuring us that a wide range of HDAC-binding side chains were fully compatible with our targeted levels of JAK2 activity. We believed the observed high HDAC6/HDAC1 selectivity is due to the aforementioned differences in the cap binding region of the HDACs. Structure activity relationships seen with **35**/**36** are mirrored in compounds **37**-**41** with aliphatic linkers of increasing length directly attached to the macrocycle. Again, **40** (HDAC6 $IC_{50}$ = 2.8 μM) with 6 methylene groups proved to be the optimal length for HDAC6 activity.[17] Following the trend observed with **35**/**36**, the inhibition of HDAC6 activity increases as the chain length increases to 6 methylenes before it decreases with an additional methylene. No HDAC inhibition could be detected with the shortest 3 and 4 carbon linkers in compounds **37** and **38**, whereas the 5 carbon linked **39** was weakly active (HDAC6 $IC_{50}$ = 45 μM). Increasing the chain length to 7 methylenes decreased the HDAC6 activity to 10 μM. Potency against JAK2 was maintained although with some variations. Shortening the linker as in

**37** brings the negatively charged carboxylate closer to the JAK2 pocket decreasing JAK2 potency nearly 20 fold from 2.6 nM (**40**) to 47 nM (**37**).

This HDAC6 selectivity and SAR profile is mirrored in the enzymatic activity of the hydroxamic acids but with significantly greater HDAC6 activity (>1000-fold in the most active cases). Thus, by changing the zinc binding group it is possible to 'tune' the HDAC activity to explore the effect of different levels of HDAC activity in these multi-ligand compounds in biological systems. Aminobenzhydroxamates **42** and **43** had much improved HDAC6 activity as did piperidine **45**, however phenol ether **44** had the most surprising sub-micromolar potency against HDAC6 ($IC_{50}$ = 66 nM) and also had weak HDAC1 activity (56% at 10 μM), especially when compared with its acid derivative **33** (HDAC6 $IC_{50}$ >100 μM), representing at least a 1,500-fold improvement. With JAK2 $IC_{50}$ of 1.3 nM this was the most promising compound to date. However, we were most interested in achieving compounds with potency in the same concentration range for both JAK2 and HDAC isoforms. We were heartened to discover that the longer **1**-like side chains in **46** and **47** conferred high HDAC6 potency, $IC_{50}$s of 2.5 and 2.3 nM, respectively. HDAC1 potency was still not detectable at the highest concentration tested (10 μM). Furthermore, **46**, displayed a high level of JAK2 potency with an $IC_{50}$ of 6.9 nM, while **47** was approximately 4-fold lower at 30 nM. However, although **46** and **47** had reached our initial potency goals against these two different enzyme targets, they were not active in cells (with the exception of

MDA-MB231 breast cancer cells for **47** ($GI_{50}$ = 3.74 μM) (Table 2 – further discussion below). Although **46** had a desirable LLE[92] [LLE = −Log$IC_{50}$−cLogP] of 5.2, it had a high molecular weight of 666 and 5 hydrogen bond donors. Nevertheless we were excited to find that the direct linking of the hydroxamate to the macrocycle, as in compounds **48**-**52**, addressed both issues while maintaining our target enzyme inhibition profile. With the long chain aliphatic hydroxamic acids **48**-**52**, JAK2 activity was similar ($IC_{50}$'s from 1 to 5 nM) but they had striking differences in their HDAC6 $IC_{50}$s ranging from 2.1 to 510 nM. This data again illustrates the critical nature of the chain length, with 5-fold improvement in HDAC6 potency on going from 3 carbons (**48**) to 4 carbons (**49**), a further 4-fold with an additional methylene (**50**) then a further 10-fold with a sixth carbon in the linker giving **51**, which had the best HDAC6 activity of the series with an $IC_{50}$ of 2.1 nM. Approximately 8 fold HDAC6 potency is lost with a seventh carbon (**52**). HDAC1 potency roughly tracks that of HDAC6 with **51** having the highest ($IC_{50}$ = 221 nM) and, although not as high as the HDAC6/1 selectivity seen with other compounds, is still significant at 100-fold. Importantly, these compounds all maintain very strong JAK2 potency with **51** being the most potent with an $IC_{50}$ of 1.4 nM. Compound **51** had a LLE of 5.2 (cLogP 3.5) matching that of **47** but with a lower MWt of 518 and two fewer hydrogen bond donors. This is probably a contributing reason to the significant cellular activity seen with **51** and **52** compared with **46** and **47**. We were curious to understand the reasons for the very high HDAC6 potency

and selectivity hence we undertook molecular modelling studies against the 3 target enzymes focusing on the JAK2/HDAC6 equipotent **51**.

**Table 1. Enzyme inhibition data for carboxylic acids**

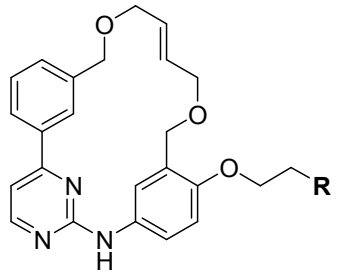

| Compound | R | Enzyme $IC_{50}$ (μM)[a] (% Inhibition at 10μM) | | |
|---|---|---|---|---|
| | | HDAC1 | HDAC6 | JAK2 |
| Tubastatin | HDAC6 selective | (37%) | 0.0035 | - |
| 1 | (pan-HDAC inhibitor) | 0.306[b] | 0.020[b] | - |
| 2 | 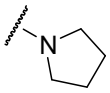 | - | - | 0.001 |
| 31 | 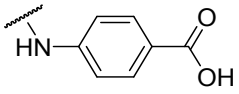 | (0%) | 64 | <0.039[c] |
| 32 | 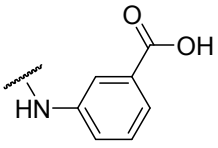 | (0%) | 53 | <0.039[b] |
| 33 | 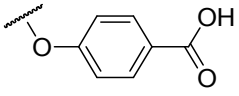 | (0%) | >100 | <0.039[b] |

| Compound | R | Enzyme $IC_{50}$ (μM)[a] (% Inhibition at 10μM) HDAC1 | HDAC6 | JAK2 |
|---|---|---|---|---|
| 34 | 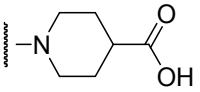 | (0%) | >100 | <0.039[b] |
| 35 | 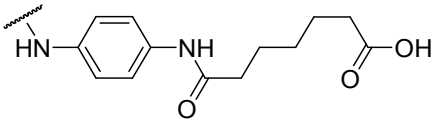 | (10.4%) | (20.4%) | - |
| 36 | 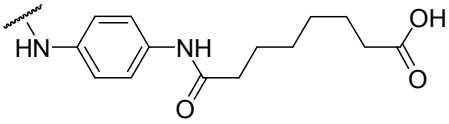 | (0%) | 2.6 | 0.00231 ±0.0001 |
| 37 | 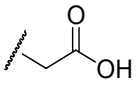 | (0%) | - | 0.047 ±0.002 |
| 38 | 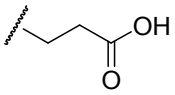 | (0%) | - | <0.039[b] |
| 39 | 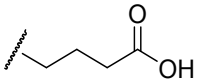 | (0%) | 45 | <0.039[b] |
| 40 | 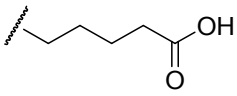 | (2.8%) | 2.8 | 0.00257 ±0.0001 |
| 41 | 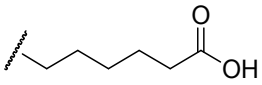 | (3.8%) | 10 | <0.039[b] |

[a] all compounds tested in the same assay format. $IC_{50}$ data are reported as the average of two independent determinations (see Supporting Information for $IC_{50}$

curves for **36** and **40**). Note that reported literature values vary depending on assay format. [b]Reported values.[119] [c]lowest concentration tested 39 nM.

**Table 2. Enzyme Inhibition data for hydroxamic acids**

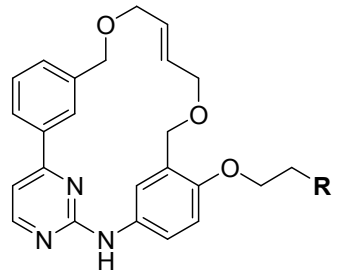


| Compound | R | Enzyme assay $IC_{50}$ (μM)[a] (% inhibition at 10μM) | | |
|---|---|---|---|---|
| | | HDAC1 | HDAC6 | JAK2 |
| Tubastatin | (HDAC6 selective) | (37%) | 0.0035[b] | - |
| 1 | (pan-HDAC inhibitor) | 0.306[c] | 0.020[c] | - |
| 2 | 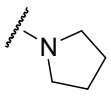 | - | - | 0.001 |
| 42 | 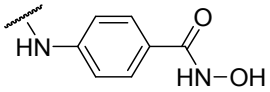 | (18%) | 0.395 ±0.013 | 0.00171 ±0.0003 |
| 43 | 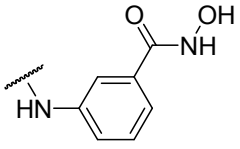 | (9%) | 2.90 ±0.31 | 0.009 ±0.0005 |
| 44 | 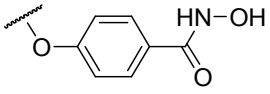 | (56%) | 0.066 | 0.00127 |

| Compound | R | Enzyme assay $IC_{50}$ (μM)[a] (% inhibition at 10μM) | | |
|---|---|---|---|---|
| | | HDAC1 | HDAC6 | JAK2 |
| | | | ±0.024 | ±0.00005 |
| 45 | 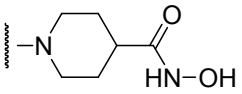 | (20%) | 0.899 ±0.319 | 0.00097 ±0.00001 |
| 46 | 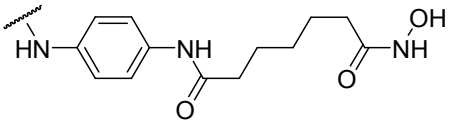 | (16%) | 0.0025 ±0.0014 | 0.0069 ±0.00015 |
| 47 | 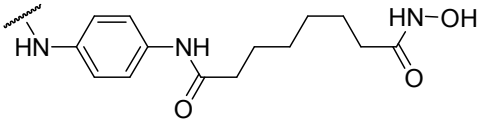 | (14%) | 0.0023 ±0.0009 | 0.030 ±0.009 |
| 48 | 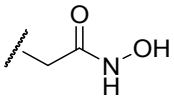 | 2.40 ±0.43 | 0.510 ±0.004 | 0.0047 ±0.00055 |
| 49 | 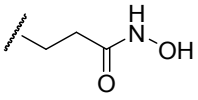 | 3.09 ±0.15 | 0.107 ±0.014 | 0.00245 ±0.00001 |
| 50 | 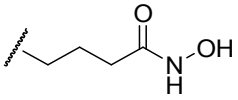 | 4.07 ±0.21 | 0.028 ±0.0007 | 0.0043 ±0.0005 |

| Compound | R | Enzyme assay $IC_{50}$ (μM)[a] (% inhibition at 10μM) | | |
|---|---|---|---|---|
| | | HDAC1 | HDAC6 | JAK2 |
| 51 | 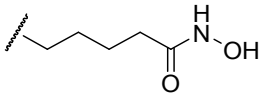 | 0.222 ±0.06 | 0.0021 ±0.00001 | 0.0014 ±0.0003 |
| 52 | 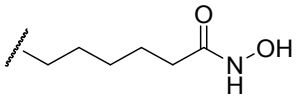 | 2.34 ±0.02 | 0.0158 ±0.0013 | 0.005 ±0.0002 |

[a]Tested in the same assay. $IC_{50}$ data are reported as the average of two independent determinations (see Supporting Information for $IC_{50}$ curves). Note that reported literature values vary depending on assay format. [b]Literature values range from 11-15 nM.[54, 93] [c]Reported values.[119]

Modeling Studies

In an attempt to determine the reasons for the HDAC6 selectivity of the compounds, we docked compound **51** into a homology model of the HDAC6 protein. This model was derived from a crystal structure of the HDAC4 catalytic domain (PDB code 2VQW) (Figure 3). Both the N-terminal and C-terminal catalytic domains of HDAC6 modelled very similarly, not unexpected given they have 49% sequence similarity and 67% homology. As well as the expected zinc-hydroxamate interactions, the macrocycle of **51** was found to complement the surface of the cap region of HDAC6 very closely. In particular, a pocket unique to HDAC6 was formed by proline 748 and leucine 749 (proline 352 and lysine 353 in the N-terminal catalytic domain) into which the linker of **51** bound with many close contacts. A hydrogen bond appears to be formed between the aminopyrimidine NH of the macrocycle and the backbone carbonyl of Ser498. Given that this NH is critical for hinge binding to JAK2 (Figure 5) it is satisfying to find that it may also be serving a similar role in its interactions with HDAC6. From this point of view **51** displays attributes of a truly merged bispecific pharmacophore. It must also be noted that the residues at the rim region of HDAC6 are quite flexible and the observed docking interactions cannot therefore be easily quantified and must be interpreted in this light.

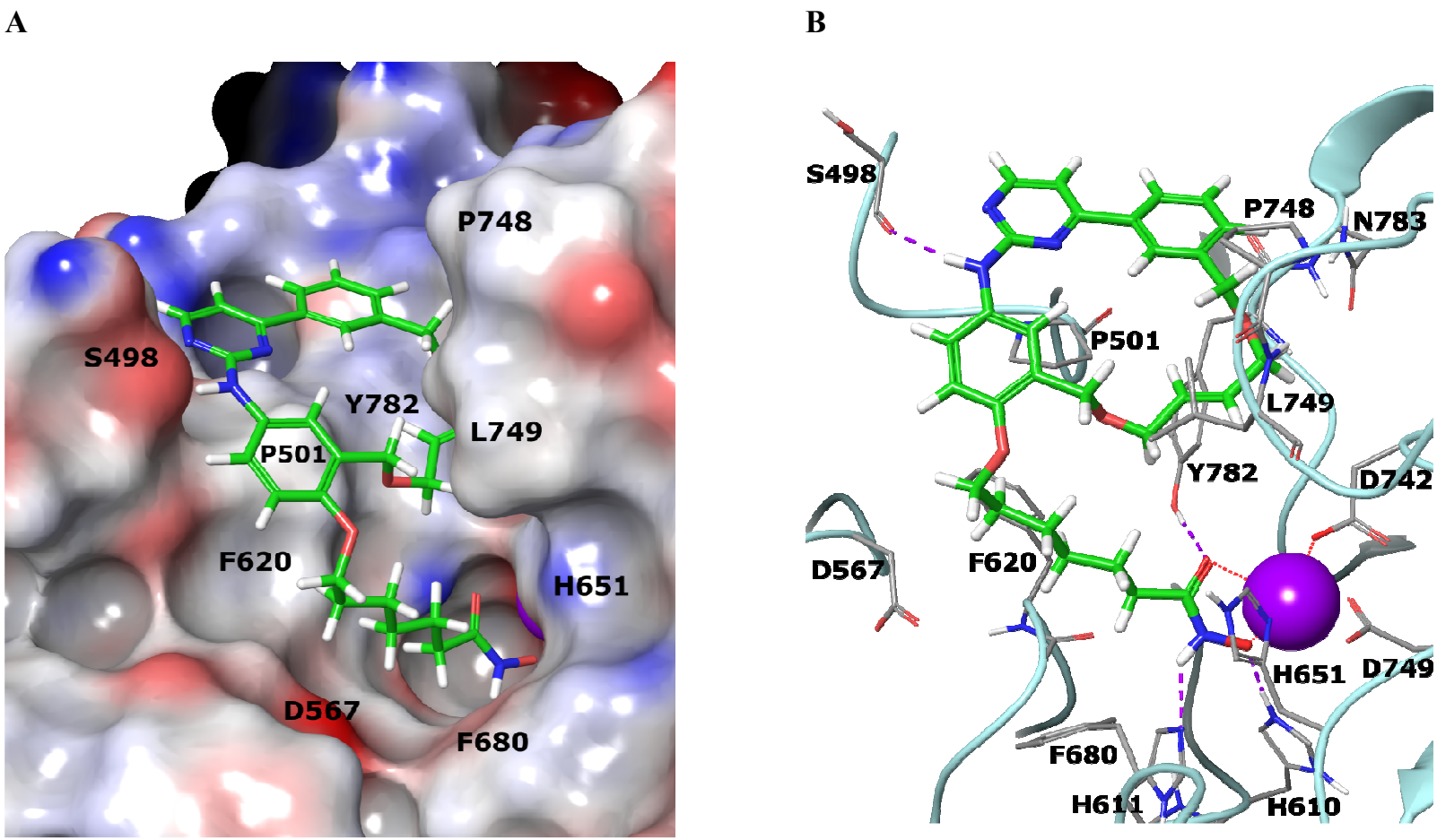


**Figure 3.** Docking of **51** into HDAC6. A: electrostatic surface of HDAC6 shown with blue indicating positively charged areas and red indicating negatively charged areas. The hydroxamate is bound deep in the Zn pocket while the large

macrocyclic cap forms very good surface complementarity. A pocket unique to HDAC6 is formed by Pro748 and Leu749 into which the hydrophobic linker of the macrocyle is bound. B: Detailed interactions between **51** and HDAC6 residues Tyr782, His610 and His611 of HDAC6, form hydrogen bonds with the hydroxamate that also coordinates the catalytic Zn in a bidentate manner. Tyr782 together with Pro501 also forms part of the surface for macrocycle binding. A possible hydrogen bond between the kinase hinge-binding pyrimidine NH can be seen with the backbone carbonyl of Ser498.

A

B

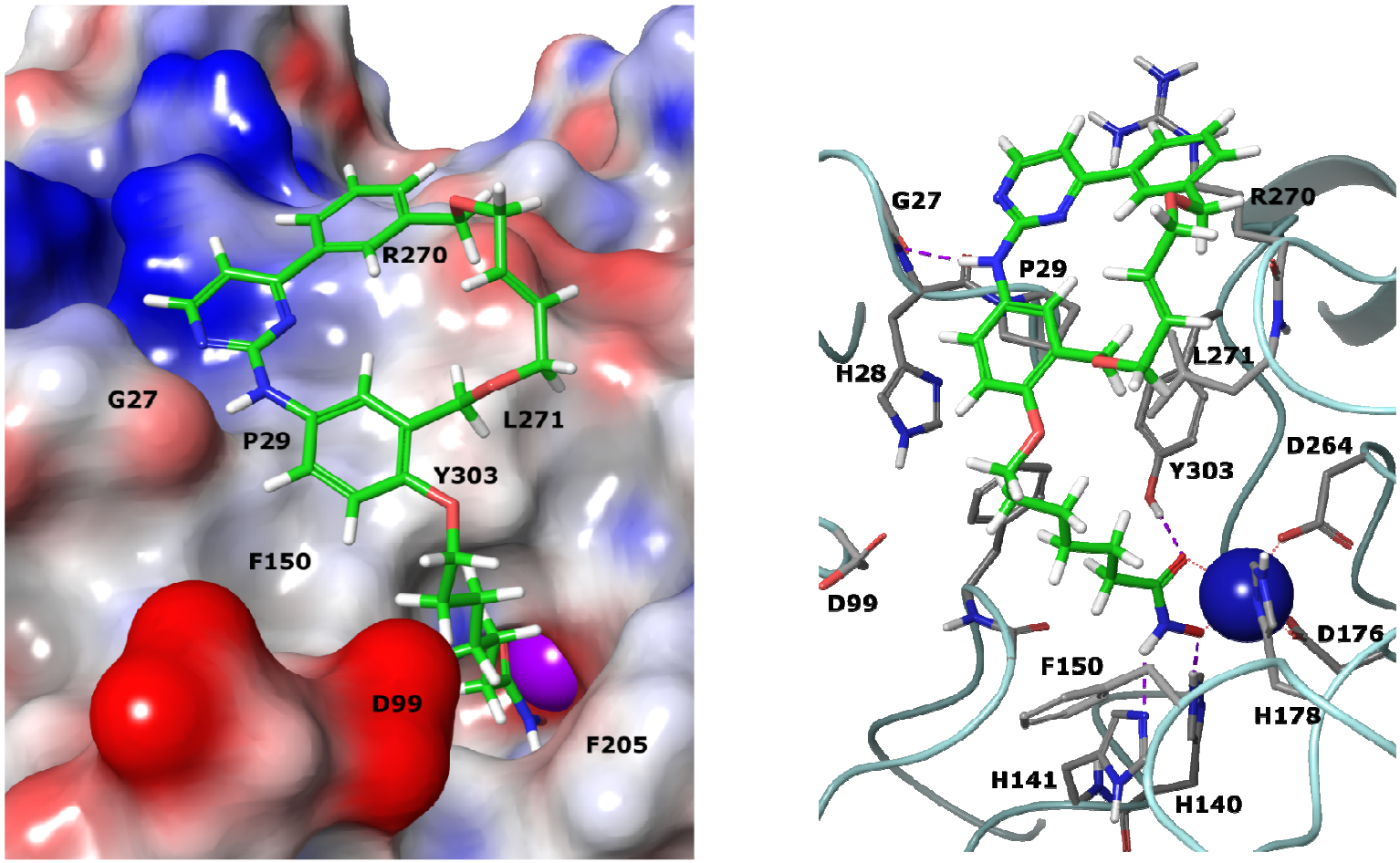


**Figure 4.** Docking of **51** into HDAC1. A: electrostatic surface of HDAC1 shown with blue indicating positively charged areas and red indicating negatively charged areas. The hydroxamate is bound in the Zn pocket while the large macrocyclic

cap is positioned on the highly solvent exposed surface. B: Detailed interactions between **51** and HDAC1 residues Tyr303, His140 and His141 of HDAC1, form hydrogen bonds with the hydroxamate that also coordinates the catalytic Zn in a bidentate manner. There also appears to be a hydrogen bond formed between the pyrimidine NH and the backbone carbonyl of Gly27, possibly explaining the mid-nanomolar potency of **51** against HDAC1.

A

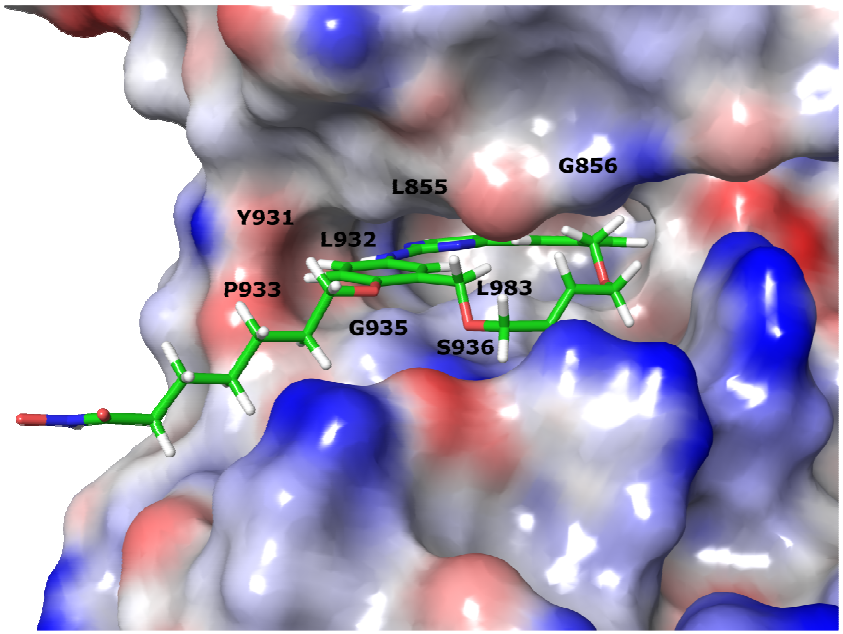
L855
G856
Y931
L932
P933
L983
G935
S936

B

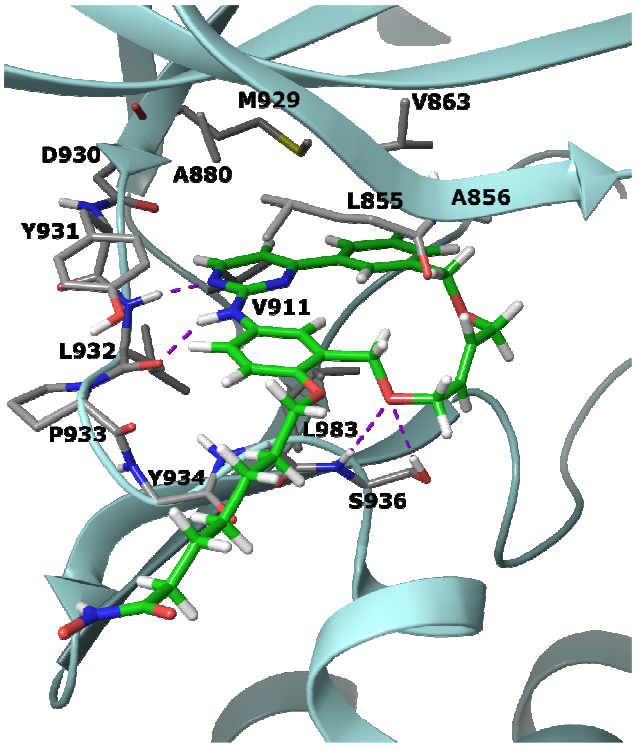
M929
V863
D930
A880
L855
A856
Y931
V911
L932
P933
L983
Y934
S936

**Figure 5.** Docking of **51** into JAK2. A: electrostatic surface of JAK2 shown with blue indicating positively charged areas and red indicating negatively charged areas. The macrocycle is binding in the ATP cavity with very good surface complementarity, very similar to the reported orientation of **2**.[88] B: Detailed interactions with the protein residues. The aminopyrimidine binds to the backbone of the hinge residue Leu932 with a donor-acceptor hydrogen bond arrangement. The oxygen of the macrocyclic linker of **51** makes close contacts, possibly hydrogen bonds, with both sidechain hydroxyl and backbone NH of Ser936.

In HDAC1, there is a complete absence of the pocket formed by Pro352/Lys353 as seen in HDAC6 (see Figure 4). Hence the macrocycle does not form good interactions with HDAC1 as it is binding to a solvent exposed surface with only the hydroxamate side chain buried inside HDAC1. This striking difference between the two proteins appears to account for the observed experimental selectivity. Work by Wiest *et al* studying class II HDAC selectivity, specifically HDAC6, supports the notion that HDAC6 selectivity vs HDAC1 can be achieved by efficient non-convalent interactions at the opening to the active site.[94] However, **51** does still inhibit HDAC1 in the mid-nanomolar range (HDAC1/6 about 100 fold). It is possible that an apparent hydrogen bond formed between the pyrimidine NH and the backbone carbonyl of Gly27 contributes to it's binding affinity. This is a similar interaction to the postulated hydrogen bond seen with the corresponding residue of HDAC6, Ser498.

In JAK2 the aminopyrimidine binds to the hinge region of the enzyme with hydrogen bonds to Leu932 while a number of important hydrophobic interactions are made between the aromatic rings and linker of the macrocycle as expected from the reported binding analysis of **2** (Figure 5).[88] Furthermore a bidentate interaction between one of the ether oxygens of **51** and Ser936 of JAK2 also matches that reported for **2**. Fewer interactions are seen between JAK2 and the hydroxamic acid linker as it is positioned in the solvent exposed channel. Taken

together, the interactions assessed from the modelling of **51** bound to HDAC1/6 and JAK2 support the observed SAR between these 3 proteins.

Isoform Selectivity

Potency in favour of one enzyme isoform is often sought where there is a strong possibility of toxicity via inhibition of too many isozymes. In the case of a multi-component JAK-HDAC ligand this challenge is significant since there are 4 JAK family members as well as over 500 other potential kinases, and 11 HDAC isoforms. With a merged DML design the interplay between the various pharmacophores and enzyme binding sites is complex increasing the difficulty of carrying out structure based design. We were intrigued to understand how selectivity would change when the pharmacophores of **1** and **2** are merged. Hence we tested compound **51** in a biochemical kinase assay, similar to the JAK2 assay, at a concentration of 100 nM (about 70 fold over JAK2 $IC_{50}$) against the 4 JAK isoforms JAK1, JAK2, JAK3 and TYK2 as well as FLT3, an important kinase in AML and targeted by **2** (Table 3). We also tested **51** against 11 HDAC isoforms covering the 4 classes of zinc utilising deacetylases, class I, IIA, IIB and IV (Table 4). We did not test **51** against the distinctly different class III NAD-dependent sirtuins, which are not inhibited by **1**.

**Table 3. Isoform selectivity of 51 against the JAK and FLT3 kinases[a]**

| Isoform | $IC_{50}$ (μM) or % inhibition | JAK2 SI[b] | HDAC6 SI[c] |
|---|---|---|---|
| JAK1 | 8.7% @ 0.1 μM | >100 | >100 |
| JAK2 | 0.0014 | 1 | 1.5 |
| JAK3 | 55% @ 0.1 μM | >50 | >25 |
| TYK2 | 56% @ 0.1 μM | >50 | >25 |
| FLT3 | 67% @ 0.1 μM | >50 | >25 |

[a] kinases were tested in duplicate at 100 nM concentration. [b] JAK2 SI = fold less potent compared to JAK2 $IC_{50}$ (1.4 nM). [c] HDAC6 SI = fold less potent compared to HDAC6 $IC_{50}$ (2.1 nM).

We were pleased to discover that **51** is selective for JAK2 against all the tested kinases. JAK1 was especially insensitive to **51** with less than 10% inhibition at the test concentration of 100 nM, corresponding to a selectivity of much greater than 100 fold against both JAK2 and HDAC6. Inhibition of JAK3 and TYK2 is 55% and 56% at 100 nM, significantly greater than for JAK1. Selectivities for JAK3

and TYK2 over JAK2 are higher than **2** at over 50 fold, and over 25 fold over HDAC6. A surprisingly low potency against FLT3 of only 67% inhibition at 100 nM corresponded to over 50 fold selectivity and over 25 fold against HDAC6. Within the 5 tested kinases compound **51** was over 50 fold selective in favour of JAK2.

Having established selectivity within the JAK family of kinases we also tested **51** in a kinase panel composed of 97 kinases from across the kinome. This data depicts binding to the ATP sites of the tested kinases, as opposed to biochemical inhibition of the phosphate transfer reaction, in the well-known TREE*spot*™ interaction map[95] and in tabular format for the kinases which **51** bound to most tightly (Figure 6). Remarkably, **51** only fully binds JAK2 at the test concentration of 100 nM. There are no kinases inhibited in the 0.1-1.0% control range or 1-5% range giving a low 'S' score of <0.1 indicating a high degree of kinase selectivity for this compound. Eight other non-mutant kinases were bound by **51** at lower levels including TYK2 and JAK3, with 4.9 and 7.9% of control, respectively. These data correlate with biochemical $IC_{50}$s in the 100's of nanomolar, which is consistent with the data depicted in Table 3. Phosphoinositol-dependent kinase gamma (PI3K-λ) was also hit (5.7% of control). PI3K-λ is itself a relevant cancer target with no reports of selective compounds yet published in the literature.[96] The other 5 kinases hit by **51** were all significantly less active.

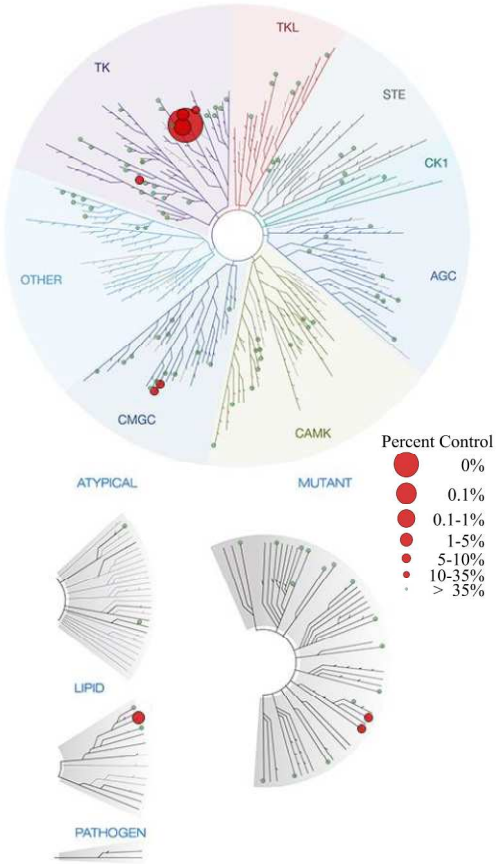


| Kinase | Percent Control[a] |
|---|---|
| JAK2 | 0 |
| TYK2 | 4.9 |
| PI3K-λ | 5.7 |
| JAK3 | 7.9 |
| NTRK1 | 13 |
| KIT | 21 |
| MAPK8 | 26 |
| MAPK10 | 29 |
| KIT(V559D,T670I) | 31 |

[a]lower numbers equate to stronger hits; values of 5-10 approximately equate to $IC_{50}$s of 10-1000nM; values above 10 approximately equate to $IC_{50}$s of 1->10 μM

| Selectivity Score[a] | Number of Hits | Number of Non-Mutant Kinases | Selectivity Score[b] |
|---|---|---|---|
| S(35) | 8 | 90 | 0.089 |
| S(10) | 4 | 90 | 0.044 |
| S(1) | 1 | 90 | 0.011 |

[a]the 'S' score is defined as the number of kinases bound by the compound divided by the total number of kinases tested, excluding mutant kinases. [b]The selectivity

score can be understood by comparing with other well-known kinase inhibitors such as sunitinib (0.65), sorafenib (0.22) and Imatinib (0.12).[97]

**Figure 6.** Kinase panel screening data of compound **51** against 97 kinases (DiscoveRx) tested at a concentraiton of 100 nM. The TREE*spot*™ map indicates the very high selectivity of compound **51**. From 90 non-mutated kinases only 9 were hit with <35% of control binding remaining (approximately equates to an $IC_{50}$ of around 10 μM). 'S' scores are all less than 0.1 indicating a high degree of kinase selectivity.

Of 11 tested HDAC isoforms compound **51** was very weakly active against the four class IIA HDACs 4, 5, 7 and 9 with less than 20% inhibition at 10 μM corresponding to >7,000 fold selectivity over JAK2 and over 5,000 fold over HDAC6 (Table 4). Low micromolar potency against the class I isoform HDAC3 ($IC_{50}$ = 2.17 μM) still represented a high selectivity of >1,000 fold for both JAK2 and HDAC6. The next most active isoforms were HDACs 11 and 8 with $IC_{50}$s of 0.93 μM and 0.74 μM, respectively (SI of 352-664 for JAK2 and HDAC6). HDAC1 was next most potently inhibited followed by HDACs 2, 10 and 1 with $IC_{50}$s of 49, 80 and 222 nM, respectively. It is perhaps not surprising that **51** is potent against HDAC10, a class IIB isoform like HDAC6. However the selectivities within the class I isoforms HDACs 1, 2, 3 and 8 are more varied than

expected with HDAC2 having the lowest $IC_{50}$ of 49 nM (23 fold selective versus HDAC6).

**Table 4. Isoform selectivity of 51 against the class I, II and IV HDAC enzymes**[a]

| Isoform | Class | $IC_{50}$ (μM) or % inhibition | JAK2 SI[b] | HDAC6 SI[c] |
|---|---|---|---|---|
| HDAC1 | I | 0.222 | 158 | 111 |
| HDAC2 | I | 0.049 | 35 | 23 |
| HDAC3 | I | 2.17 | 1,550 | 1,033 |
| HDAC4 | IIA | 8.6% @ 10 μM | >7,000 | >5,000 |
| HDAC5 | IIA | 16.1% @ 10 μM | >7,000 | >5,000 |
| HDAC6 | IIB | 0.0021 | 1.5 | 1 |
| HDAC7 | IIA | 1.3% @ 10 μM | >7,000 | >5,000 |
| HDAC8 | I | 0.74 μM | 528 | 352 |
| HDAC9 | IIA | 14% @ 10 μM | >7,000 | >5,000 |

| Isoform | Class | $IC_{50}$ (μM) or % inhibition | JAK2 SI[b] | HDAC6 SI[c] |
|---|---|---|---|---|
| HDAC10 | IIB | 0.080 μM | 57 | 38 |
| HDAC11 | IV | 0.93 μM | 664 | 443 |

[a] HDAC enzymes were tested in a 10-dose $IC_{50}$. [b] JAK2 SI = fold less potent compared to JAK2 $IC_{50}$ (1.4 nM). [c] HDAC6 SI = fold less potent compared to HDAC6 $IC_{50}$ (2.1 nM).

This enzyme inhibition data indicates that **51** is >50 fold selective for JAK2 over a broad panel of other kinases and >20 fold selective over HDAC6 compared to HDACs 2 and 10, and >100 fold selective over other HDAC isoforms. Compound **51** demonstrates that it is possible to achieve high potency with good selectivity for one member of each class from two distinctly different families of enzymes. Whether or not the observed selectivity transfers to cell lines was next explored with cancer cell proliferation and apoptosis assays, in both solid tumor and hematological cell lines, the latter characterised via specific pharmacodynamic biomarkers quantifying inhibitor modulation of the JAK2 and HDAC pathways.

Cellular Assays

Single agent JAK or HDAC inhibitors have been successfully launched in two indications: the JAK2-driven hematological malignancy myelofibrosis (ruxolitinib) and HDAC inhibitor sensitive T-cell lymphomas (including compound **1**, and belinostat). Recently panobinostat was approved as the first targeted HDAC agent to treat multiple myeloma.[47] Broadening of therapy into leukemias/lymphomas and solid tumors is highly desirable and with this aim in mind much effort has been expended in the clinic to evaluate compounds inhibiting either the JAK or HDAC families with varying degrees of isoform selectivity. Notably, ruxolitinib has recently received wide coverage of its encouraging initial responses in combination with capecitabine (a prodrug of 5-FU) in patients with recurrent or treatment refractory metastatic pancreatic cancer, hinting at the potential value of JAK inhibitors in difficult to treat solid tumors.[98] Combination of ruxolitinib with panobinostat is being studied in the clinic for myelofibrosis with the expectation that this combination could be extended to other indications if successful.[99]

*Solid Tumor Cell Lines*. Given the emerging broader potential for a combination approach we focused our initial efforts on the evaluation of our JAK-HDAC dual inhibitors in 4 solid tumor cell lines: breast cancer (MDA-MB-231, MCF-7), colorectal cancer (HCT-116) and prostate cancer (PC-3). Each compound was evaluated in a dose response study to establish their ability to inhibit cell proliferation (Tables 5 and 6). Compounds **1** and **2** were used as references with

tubastatin as an HDAC6 selective inhibitor. $IC_{50}$ values obtained for these three reference compounds were generally in the low to sub-micromolar range and were within 3-5 fold of the reported values.

Due to the high polarity of the negatively charged carboxylic acids we did not expected those compounds (**31**-**41**) to exhibit strong inhibition of cell proliferation. Despite this, even the poorly soluble JAK2-selective acids **31**-**33** had moderate $IC_{50}$'s in two cell lines. However the zwitterionic piperidine acid **34** was more active possibly due to improved solubility. Acid **36**, potent against JAK2 ($IC_{50}$ = 2.3 nM) and inhibiting HDAC6 in the low micromolar range ($IC_{50}$ = 2.6 μM) was more active against HCT-116 cells but in other cell lines the dose response was poor, with no sigmoidal curve fit possible. Short aliphatic chain acids **37**-**39** were tested in two cell lines and found to be weakly active. A longer 6 carbon linker (**40**) conferred low micromolar HDAC6 inhibition and slightly improved cell activity while one carbon more (**41**) was less active against HDAC6 and slightly less active than **40** in all 4 cell lines. Clearly carboxylic acids are not potent in solid tumor cells.

**Table 5. Solid tumor cell proliferation data for carboxylic acids**

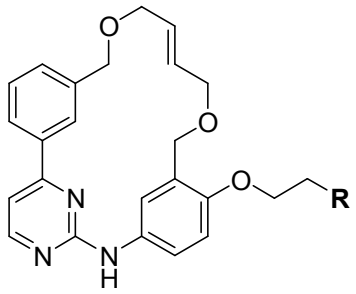


| Compound | R | Solid tumor cell proliferation $IC_{50}$ (μM)[a] | | | |
|---|---|---|---|---|---|
| | | MDA-MB-231 | HCT-116 | PC-3 | MCF-7 |
| 1 | (pan-HDAC inhibitor) | 1.19 ±0.18[b] | 1.85 ±0.52[b] | 0.85 ±0.37[b] | 0.65 ±0.08[b] |
| 2 | 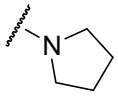 (JAK2 inhibitor) | 2.43 ±0.53 | 0.88 ±0.06[c] | 2.41 ±0.05[c] | 0.29 ±0.07[c] |
| 31 | 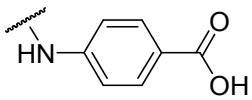 | 46.0 ±7.9 | - | - | - |
| 32 | 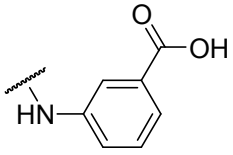 | 21.4 ±2.5 | 59.2[d] | - | - |
| 33 | 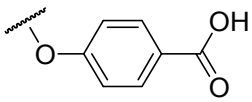 | 54.2 ±5.5 | 29.7[d] | - | - |

| Compound | R | Solid tumor cell proliferation $IC_{50}$ (μM)[a] | | | |
|---|---|---|---|---|---|
| | | MDA-MB-231 | HCT-116 | PC-3 | MCF-7 |
| 34 | 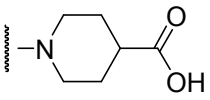 | 10.7 ±2.3 | 8.2 ±1.0 | - | - |
| 35 | 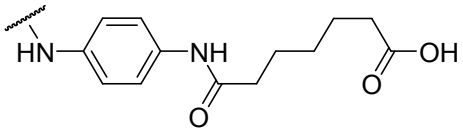 | - | - | - | - |
| 36 | 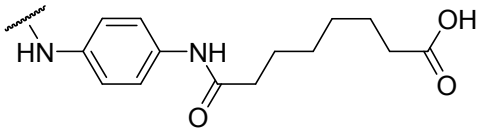 | NC | 2.7 ±1.4 | NC | NC |
| 37 | 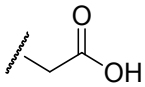 | 53.5 ±28 | 124[d] | - | - |
| 38 | 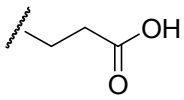 | 25.9 ±12.6 | 36[d] | - | - |
| 39 | 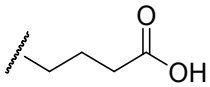 | 19.9 ±3.4 | 41[d] | - | - |
| 40 | 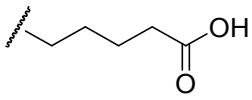 | 12.0 ±1.2 | 6.06 ±0.38 | 8.76 ±1.19 | 20.0 ±2.6 |
| 41 | 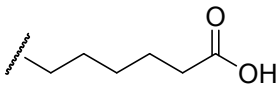 | 17.1 ±0.6 | 8.04 ±2.0 | 22.8 ±2.5 | 27.7 ±1.9 |

[a]Values are the mean ± SD of at least 3 determinations unless noted. [b]Reported $IC_{50}$ values for **1**: MCF-7 (*c*.6 μM)[100], MDA-MB-231 (*c*.4.5 μM)[101], HCT-116 (2.85 μM) and PC-3 (1.21 μM).[102] Note that reported literature values vary depending on assay format. [c]Reported $IC_{50}$ values for **2**: 1.69, 0.77 and 0.85 μM for HCT-116, PC-3 and MCF-7, respectively.[29] Compound **2** has not been reported for MDA-MB231. [d]10-point dose response. NC = no dose response curve.

We next studied the more HDAC potent hydroxamic acids in the same four cell lines. Aromatic hydroxamate **42** was more potent than expected, whereas its meta analogue, **43**, was only active against HCT-116 cells, perhaps due to poor physicochemical properties. Similarly, although phenolic ether **44** was potent against PC-3 cells, its poor solubility hampered studies in other cells. In general a similar trend was seen as for the carboxylic acid analogues: the basic piperidine **45** was quite potent across all cell lines, most likely driven by its very potent JAK2 activity and higher solubility. This compound is a close analogue of **2**, with a tertiary amine two carbons distant from the oxygen in the side chain. This amine is well placed to form an electrostatic interaction with Asp939 in JAK2, similar to **2** as demonstrated in extensive modeling studies[28] that will account for it having the best JAK2 potency of all the compounds. However, it had very weak HDAC6 inhibition (HDAC6 $IC_{50}$ is only 899 nM) compared to the other compounds with

similar length indicating the HDAC channel does not tolerate the tertiary amine so close to the hydroxamic acid. Despite being highly potent against both JAK2 and HDAC6, long chain analogues **46** and **47**, direct analogues of **1**, were only weakly active in these cells. The only exception was **47** with an $IC_{50}$ of 3.43 μM in MB-MDA-231 cells. More positive results were obtained with directly attached aliphatic side chains of 3 to 7 carbons for compounds **48** to **52**, respectively. The best solid tumor cell potency of these analogues was obtained for 6 carbon linked **51**, also the most potent inhibitor of JAK2 and HDAC6 with $IC_{50}$ values of 1.4 and 2.1 nM, respectively. Compound **51** had the lowest $IC_{50}$ values in all cell lines tested with the exception of HCT-116, where piperidine **45** and short chain **49** were more potent.

**Table 6. Solid tumor cell proliferation data for hydroxamic acids**[a]

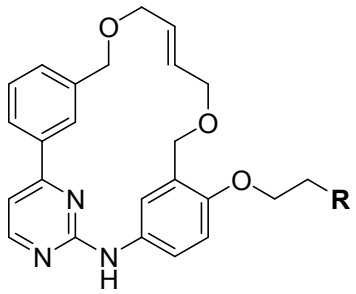


| Compound | R | Solid tumor cell proliferation $IC_{50}$ (μM)[a] |
|---|---|---|

| | | MDA-MB-231 | HCT-116 | PC-3 | MCF-7 |
|---|---|---|---|---|---|
| Tubastatin | (HDAC6 selective) | 10.4 | 2.0 | 8.6 | 3.7 |
| **1** | (pan-HDAC inhibitor) | 1.58 ±0.26 | 1.85 ±0.52[a] | 0.85 ±0.37[a] | 0.65 ±0.08[a] |
| **2** | 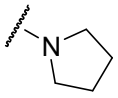 | 2.50 ±0.31 | 0.88 ±0.06[a] | 2.41 ±0.05[a] | 0.29 ±0.07[a] |
| **42** | 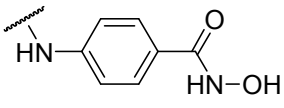 | 8.69 ±0.13 | 3.20 ±0.67 | 4.58 ±0.76 | 3.84 ±0.41 |
| **43** | 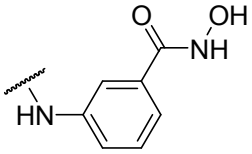 | >50 | 2.01 ±0.83 | >100 | NC |
| **44** | 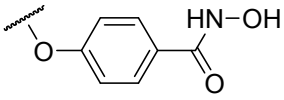 | - | - | 1.6 ±0.23 | NC |
| **45** | 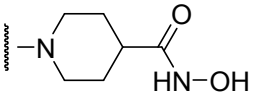 | 3.41 ±0.20 | 1.20 ±0.35 | 4.58 ±0.76 | 1.68 ±0.14 |
| **46** | 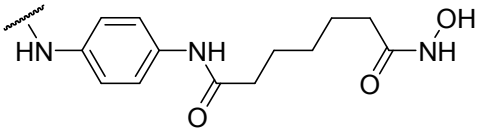 | NC | NC | > 100 | NC |
| **47** | 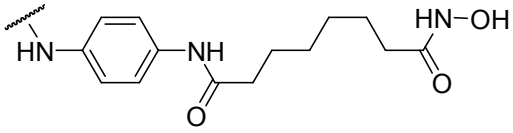 | 3.43 ±1.36 | NC | > 100 | NC |

| Compound | R | Solid tumor cell proliferation $IC_{50}$ (μM)[a] | | | |
|---|---|---|---|---|---|
| | | MDA-MB-231 | HCT-116 | PC-3 | MCF-7 |
| **48** | 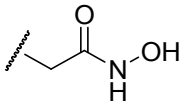 | 5.91 ±0.71 | 3.64 ±2.62 | 4.61 ±0.58 | 2.78 ±0.32 |
| **49** | 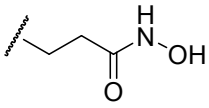 | 12.7 ±0.32 | 1.41 ±0.21 | 10.1 ±0.8 | 7.87 ±0.75 |
| **50** | 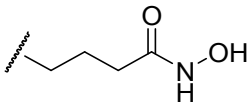 | 8.07 ±0.81 | 2.56 ±0.12 | 8.11 ±0.37 | 4.81 ±0.40 |
| **51** | 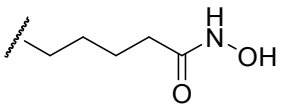 | 1.43 ±0.53 | 2.23 ±0.63 | 1.7 ±0.3 | 1.47 ±0.37 |
| **52** | 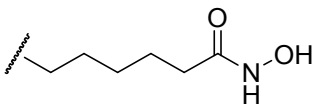 | 6.44 ±0.52 | 6.23 ±0.58 | 10.1 ±1.1 | 9.48 ±0.80 |

[a]See Table 5 footnotes. NC = no dose response curve.

*Hematological Cell Lines*. We studied the potency of selected compounds in a range of blood/bone marrow derived cancer cells. JAK and HDAC inhibitors have wide application to blood cancers as discussed previously and are expected to be sensitive to dual pathway inhibition. Dual inhibitors were selected on the basis of

their $IC_{50}$ against *both* JAK2 and HDAC6 of less than 50 nM. Hence compounds **46**, **47**, **50**, **51** and **52** were assessed in three hematological cells lines: the AML cell line HL-60, the erythroleukemia (EL) cell line HEL92.1.7 (expressing mutated $JAK2^{V617F}$) and the acute T-cell leukemia cell line Jurkat (Table 7). All compounds were more potent in these cell lines than in solid tumor cell lines. Compound **51**, having the strongest profile in vitro, was the most potent compound with around 1 μM $IC_{50}$ values in the HEL and Jurkat cell lines and about 4 μM in the FLT-3 sensitive HL-60 AML cell line. The JAK1/2 selective inhibitor ruxolitinib was not potent in these cells indicating a lack of sensitivity to JAK pathway inhibition. However they are sensitive to HDAC blockade indicated by the activity of **1**. Tubastatin is not potent indicating lack of sensitivity to HDAC6. Compound **51** has similar potency to **1** and **2** in HEL and Jurkat cells probably driven by its HDAC/FLT-3 potency. This data suggests that the broad potency of **51** could be due to its ability to block multiple pathways but not necessarily eliciting synergy between those pathways in terms of inhibition of proliferation.

**Table 7. Cell proliferation inhibition assay data of selected compounds in three leukemia cell lines**

| Compound | $IC_{50}$ (μM) [a] | | |
|---|---|---|---|
| | HL-60[b] | HEL92.1.7[c] | Jurkat[d] |
| Tubastatin[e] | >>4[i] | >>2[i] | >>4[i] |
| **1**[f] | 2.28 ±1.28 | 0.49 ±0.10 | 0.59 ±0.17 |
| **2**[g] | 1.78 ±0.62 | 1.17 ±0.03 | 1.09 ±0.08 |
| Ruxolitinib[h] | >4[i] | >4[i] | >>4[i] |
| 46 | >>4[i] | >>2[i] | >4[i] |
| 47 | >4[i] | >>2[i] | >4[i] |
| 50 | >4[i] | >2[i] | 2.90 ±0.11 |
| 51 | c.4[i,j] | 0.94 ±0.22 | 1.19 ±0.22 |
| 52 | >4[i] | >2[i] | 2.48 ±0.21 |

[a]Anti-proliferative inhibitory activities are the average of at least 3 determinations. [b]Acute Myeloid Leumekia. [c]Erythroleukemia ($JAK2^{V617F}$). [d]Acute T-Cell Leukemia. [e]HDAC6 selective inhibitor. [f]pan-HDAC inhibitor. [g]JAK2/FLT3 selective inhibitor. Literature data[29]: HL-60 0.52 μM; HEL92.1.7: 1.726 μM; Jurkat: 0.839 μM. Note that other JAK2 inhibitors are similar.[103] [h]JAK1/JAK2 selective. [i]top concentration tested. [j]47% inhibition at 4 μM.

Given the clear superiority of **51** we continued our studies in an expanded range of cell lines. Hence **51** was tested against the multiple myeloma (MM) cell lines KMS-12-BM and OPM-2, with different translocations in MM (t4:14 and t11:14) respectively, both being translocations which correspond to poor prognosis in MM[104, 105] (Table 8). An additional two AML cell lines, KG-1 and MOLM-14 were selected, where MOLM-14 has a FLT3-ITD mutation while KG1 does not. MOLM-14 is a M5 stage (FAB) cancer while KG-1 is a M6 stage (FAB) cancer.[106, 107] Finally, two natural killer T-cell lymphoma (NKTCL) cell lines NKYS and KHYG,[108] with positive and negative EBV status,[109] respectively, were tested against **51**. NK cell neoplasms have been shown to be sensitive to compound **1** due to suppression of the JAK-STAT pathway suggesting that a combination of both JAK and HDAC inhibition could be an effective strategy.[110] Anti-proliferative potency of **51** in these 6 cell lines ranged from 1.08 to 2.11 μM with the most

potent cell lines being the NK T-cell lymphoma. Compound **51** was broadly potent at low micromolar concentrations potentially supporting dual pathway blockage as an efficacious strategy. Most likely the very high potency of **2** in MOLM-14 cells is largely due to the very potent FLT-3 activity of these compounds.

**Table 8. Cell proliferation inhibition assay data of 51 and reference standards in a range of hematological cell lines**

| Compound | $IC_{50}$ (μM)[a] | | | | | |
|---|---|---|---|---|---|---|
| | KMS-12-BM[b] | OPM-2[b] | KG-1[c] | MOLM-14[c] | NKYS[d] | KHYG[d] |
| **1**[e] | 0.94 ±0.24 | 2.91 ±0.87 | - | - | - | - |
| **2**[f] | 0.75 ±0.24 | 1.21 ±0.65 | 1.48[g] | 0.079[g] | 1.60[g] | 1.24[g] |
| **51** | 2.11 ±0.91 | 2.05 ±0.89 | 1.63 ±0.53 | 1.14 ±0.39 | 1.08 ±0.22 | 1.09 ±0.45 |

[a]Anti-proliferative inhibitory activities are the average of at least 3 determinations unless noted. [b]Multiple Myeloma. [c]Acute Myeloid Leumekia. [d]Natural Killer T-Cell Lymphoma. [e]pan-HDAC inhibitor. [f]JAK2/FLT3 inhibitor. [g] Single determination of an 8-dose response in triplicate. Blank cells = not tested.

A more physiologically relevant measure of a compound's anti-proliferative potential is to study its effects in blocking the formation of colonies of tumor cells growing in a 3D matrix. Compound **51** was tested against HEL92.1.7 cells grown

over 14-16 days in methylcellulose and effectively blocked colony formation in a dose dependent manner and at concentrations similar to its $IC_{50}$ against cells growing in 2D culture (Figure 7A). Visually, photographs of selected colonies clearly indicate the potent anti-growth effects of compound **51**.

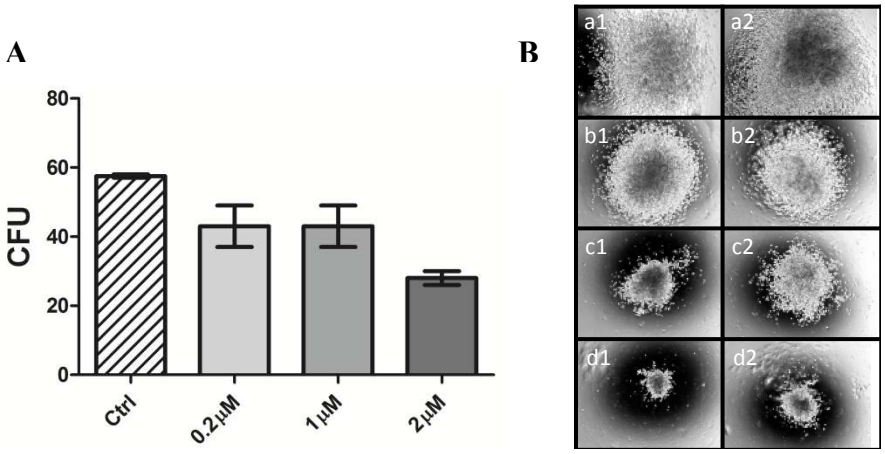


**Figure 7.** *Compound 51 effectively blocks colony formation in the erythroleukemia cell line HEL92.1.7 expressing endogenous JAK2$^{V617F}$.* HEL92.1.7 cells were grown in methylcellulose (ClonaCell™-TCS Medium) and treated with compound **51** at the respective concentrations. After 14-16 days colonies were counted. (A) bar graph indicating dose response based on total cell populations. Data is presented as mean ± SEM. (B) Photographs of selected colonies indicating controls (a1, a2), treatment with **51** at 0.2 μM (b1, b2), 1.0 μM (c1, c2) and 2.0 μM (d1, d2).

Having identified compound **51** as a preferred dual inhibitor we wondered if it would be as toxic to a normal cell as is it is to the range of cancer cells tested. Hence we tested both **51** and **52** in Transforming growth factor-α Mouse Hepatocytes (TAMH) (Table 9), comparing with 1 and 2 as controls. Compound **51** inhibited the proliferation of TAMH cells with an $IC_{50}$ of 9.57 μM, whereas **2** was nearly 3 times more potent ($IC_{50}$ of 3.68 μM). Compounds **1** and **52** were also slightly more potent than **51**. This data suggests that dual inhibitors are not simply toxic to every cell line.

**Table 9. Cell proliferation assay data of compounds in a normal cell line**

| Compound | TAMH $IC_{50}$ (μM)[a] | Therapeutic window (TAMH $IC_{50}$ / Cancer cell $IC_{50}$)[d] |
|---|---|---|
| **1**[b] | 7.86 ± 2.2 | 13.1 |
| **2**[c] | 3.68 ± 0.88 | 3.1 |
| **51** | 9.57 ± 1.00 | 8.7 |
| **52** | 5.26 ± 0.24 | 1.8 |

[a]Average of 4 determinations. [b]pan-HDAC. [c]JAK2/FLT3. [d]based on the most sensitive cell lines with average $IC_{50}$s of 0.6 μM for **1**, 1.2 μM for **2** (excluding MOLM-14), 1.1 μM for **51** and 2.9 μM for **52**.

Cell proliferation is a phenotypic readout that could result from off target effects, hence we next set out to prove that **51** blocked both the JAK-STAT pathway and HDAC mediated deacetylation in cells.

Intracellular Mechanism of Action

To investigate whether the dual enzyme inhibition profile of **51** translates into intracellular inhibition against both the JAK-STAT and HDAC pathways, we studied the effects of **51** in the MM cell line KMS12BM and the AML cell line MOLM-14. Compound **51** was tested at approximately 2 x $IC_{50}$ where it showed increased histone-3 acetylation (Ac-H3 (Lys9/Lys14)), mediated by HDACs 1,2 and 3[111], and potent increase of acetylated tubulin (Ac-tubulin), mediated by HDAC6.[112] The HDAC6 selective inhibitor tubastatin (15 μM)[54] was used as a positive control and indicated a significant increase in Ac-tubulin but no increase in Ac-H3 (Figure 8A,B). Exposure of the cells to **51**, in a time course from 0 to 48 h, led to an increase of Ac-H3 indicating strong blockade of HDAC1/2/3 signaling.

The in vitro selectivity profile of **51**, showing sub-micromolar activity for HDACs 1, 2, 8, 10 and 11, is apparently sufficient to induce inhibition of histone deacetylation in cells. Increase of **51**-induced Ac-H3 peaked at 16 and 4 h in KMS12BM and MOLM-14 cells, respectively, and was still detectable at 48 hours (Figures 8A and B). Similar effects were seen in both cell lines for Ac-tubulin where **51** showed strong and constant induction of Ac-tubulin up to 48 h in KMS-12-BM cells and peaking at 16 h in MOLM-14 cells. Having shown that the HDAC enzyme inhibition profile led to the induction of Ac-H3 and Ac-tubulin by **51** in cells, we next studied the effects of **51** on the JAK-STAT pathway. Using **2** as a positive control at its $IC_{50}$ value in KMS12BM and MOLM-14 cells, STAT3 levels were significantly reduced (Figure 8C and D). Similarly, a dose response study with **51** revealed progressively increased suppression of STAT3 levels with increasing concentrations of the dual inhibitor. At concentrations around the proliferation $IC_{50}$ level, 1.5 μM, STAT3 was completely inhibited in both cell lines.

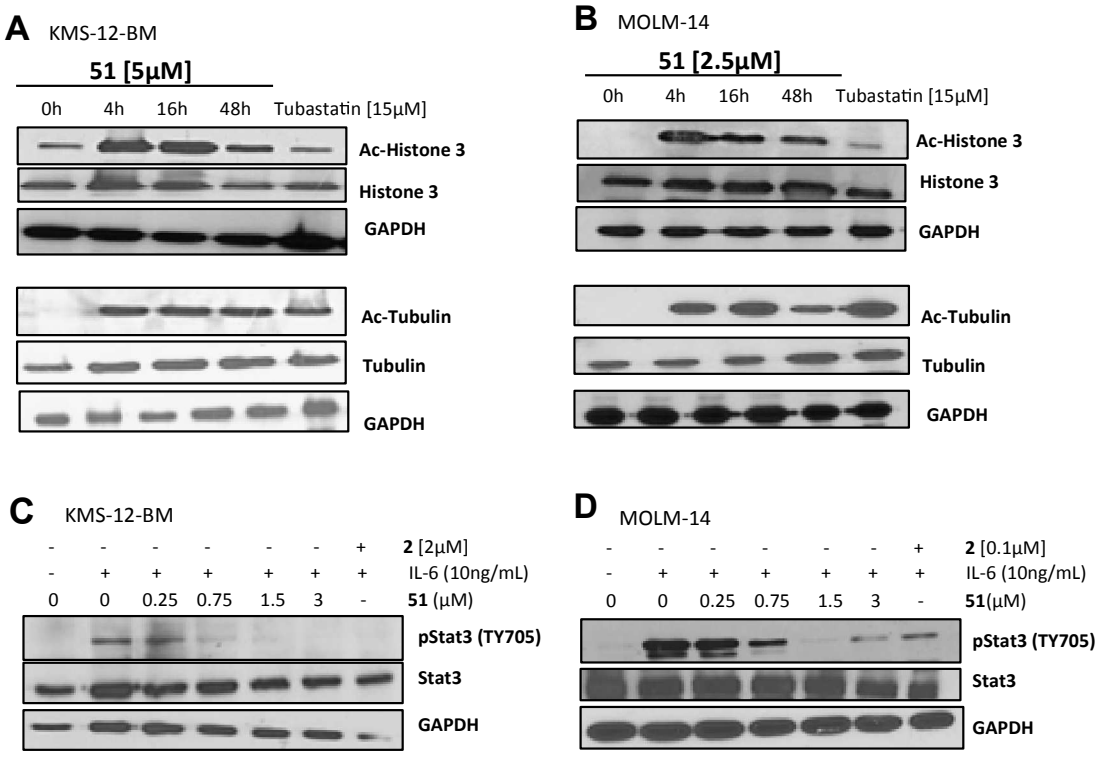


**Figure 8**. *Compound 51 effectively blocks dual signalling pathways in MM and AML cell lines.* (A) KMS-12-BM and (B) MOLM-14 were treated with **51** at the respective concentrations and timepoints. Tubastatin was used as a positive control for HDAC6 inhibition (48 hour treatment). After lysis, acetylated tubulin (Ac-Tubulin) and acetylated histone 3 (Ac-H3) were detected by immunoblotting. Subsequently, as a loading control the same membranes were re-probed with Tubulin and H3 respectively. (C) KMS-12-BM and (D) MOLM-14 were pre-treated with **51** for 3h and then were treated with 10ng/mL of IL-6 for 15 minutes. Compound **2** was used as a positive control for the inhibition of the JAK2 pathway in each cell line at approximately its $IC_{50}$ concentration (2 μM for KMS-12-BM

and 0.1 μM for MOLM-14). After lysis, p-STAT3(TY705) was detected by immunoblotting. The same membranes were re-probed with STAT3 to detect total protein levels.

We also studied the effects of **51** in V617F-expressing HEL92.1.7 cells (Figure 9). Using **1** as a positive control, a strong increase in Ac-H3 was seen at 0.1, 0.5 and 1.0 μM. Compound **51** gave a dose response but with lower responses at the same concentrations, indicating effective HDAC1/2/3 pathway blockade but requiring higher concentrations compared to **1**. Approximately a 10 fold higher concentration of **51** was required to elicit the same Ac-H3 response as **1**. As expected from its potent HDAC6 inhibition, Ac-tubulin was more sensitive to the effects of **51** with significant increases at the lowest concentration tested and a clear dose response. Even at 0.1 μM increase of Ac-tubulin could be seen with **51** but not with **1**. Hence **51** is 2 fold more sensitive than **1** for Ac-tubulin response. Comparing Ac-H3 to Ac-tubulin for compound **51** indicates that it is 20 fold more selective for HDAC6 in cells compared to SAHA. Considering that Ac-H3 is affected by HDAC1, 2 and 3 isoforms, and Ac-tubulin is only affected by HDAC6 this data is consistent with the enzyme inhibitory profile of **51**. JAK-STAT pathway inhibition is clearly evident upon treatment of HEL92.1.7 cells with **51** (Figure 9C). Upregulation of phospho-JAK2 (p-JAK2) has been reported using the Y1007/8 p-JAK2 antibody described in studies with pacritnib in HEL92.1.7 cells.[29] Although phosphorylation

of the specific Y1007/8 residue(s) increases, phosphorylation of the critical Y221 decreases as does total phosphorylation levels.[29] Compound **51** gives the same increase in p-JAK2 (Y1007/8) as **2** in this assay. Furthermore, upon treatment with **51**, STAT5 is decreased in this cell line at around its proliferation $IC_{50}$, providing direct evidence for JAK pathway inhibition in HEL92.1.7 cells. Taken together, these data in 3 hematological cell lines provides strong evidence for dual JAK-STAT and HDAC pathway inhibition in cells induced by a single compound, **51**.

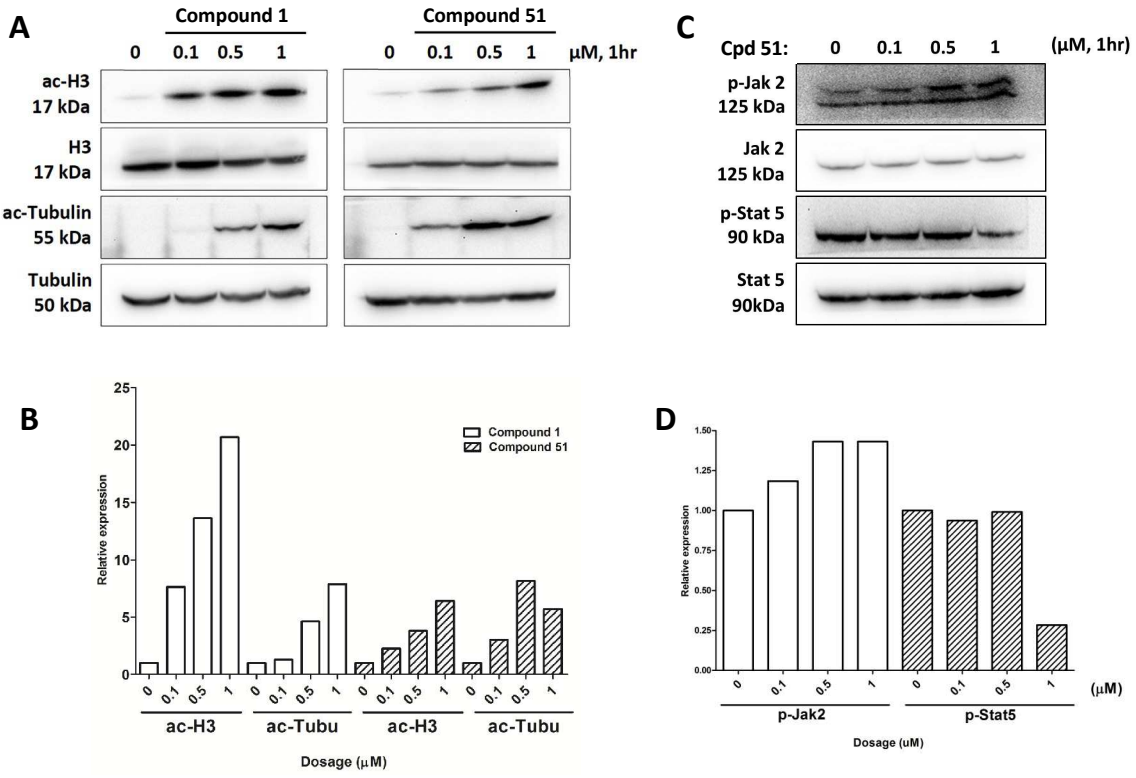


**Figure 9**. *Compound **51** effectively blocks dual signalling pathways in the erythroleukemia cell line HEL92.1.7 expressing endogenous $JAK2^{V617F}$.* (A) HEL92.1.7 cells were treated with **1** and **51** at the respective concentrations for 1

hour. After lysis, acetylated tubulin (Ac-Tubulin) and acetylated histone 3 (Ac-H3) were detected by immunoblotting. Subsequently, as a loading control the same membranes were re-probed with Tubulin and H3 respectively. (B) Quantification of HDAC inhibitory responses by densitometry. (C) HEL92.1.7 cells were treated with **51** at the respective concentrations for 1 hour. After lysis, p-JAK2 and p-STAT5 were detected by immunoblotting. The same membranes were re-probed with JAK2 and STAT5 to detect total protein levels. (D) Quantification of JAK inhibitory responses by densitometry.

**Mechanism of Cell Death**

We next wanted to confirm that the phenotypic observations of cell death induced by **51** were specifically due to apoptosis.[113] Early apoptosis involves translocation of membrane phosphatidylserine (PS) from the inner side of the plasma membrane to the surface. Annexin V, a $Ca^{2+}$-dependent phospholipid-binding protein, has high affinity for PS, and fluorochrome-labeled Annexin V can be used for the detection of exposed PS using flow cytometry.[114] In the early stages of apoptosis the cell membranes are still largely intact hence Annexin V can enter and bind exposed PS, whereas propidium iodide (PI) cannot. In the later stages of apoptosis, the cell membrane is not intact and propidium iodide (PI) can also enter giving a specific readout for dead cells. Conversely, viable cells with intact membranes exclude PI,

therefore, cells that are considered viable are both Annexin V and PI negative, while cells that are in early apoptosis are Annexin V positive and PI negative, and cells that are in late apoptosis or already dead are both Annexin V and PI positive. An effective strategy is to track the progress of cells over time through early to later phases of apoptosis which further supports the assertion that the mechanism of cell death is indeed via apoptosis. Compound **51** was hence studied in a time course dose response experiment in the AML cell line MOLM-14 using doxorubicin as a positive control (Figure 10. Figure 10B shows only 48 h data. For 4 h and 24 h timepoints see Supporting Information.) Both an increase in dose and time led to an increase in Annexin V positive cells indicating early apoptotic events. At 24 h it became evident that cells were dying shown by the increased levels of PI+ cells. At this timepoint a dose response was achieved for both Annexin V and PI, whereas at the earlier timepoint of 4 h no dose response was observed. At the later timepoint of 48 h more cells were PI+ indicating late apoptosis (Figure 10A,B).

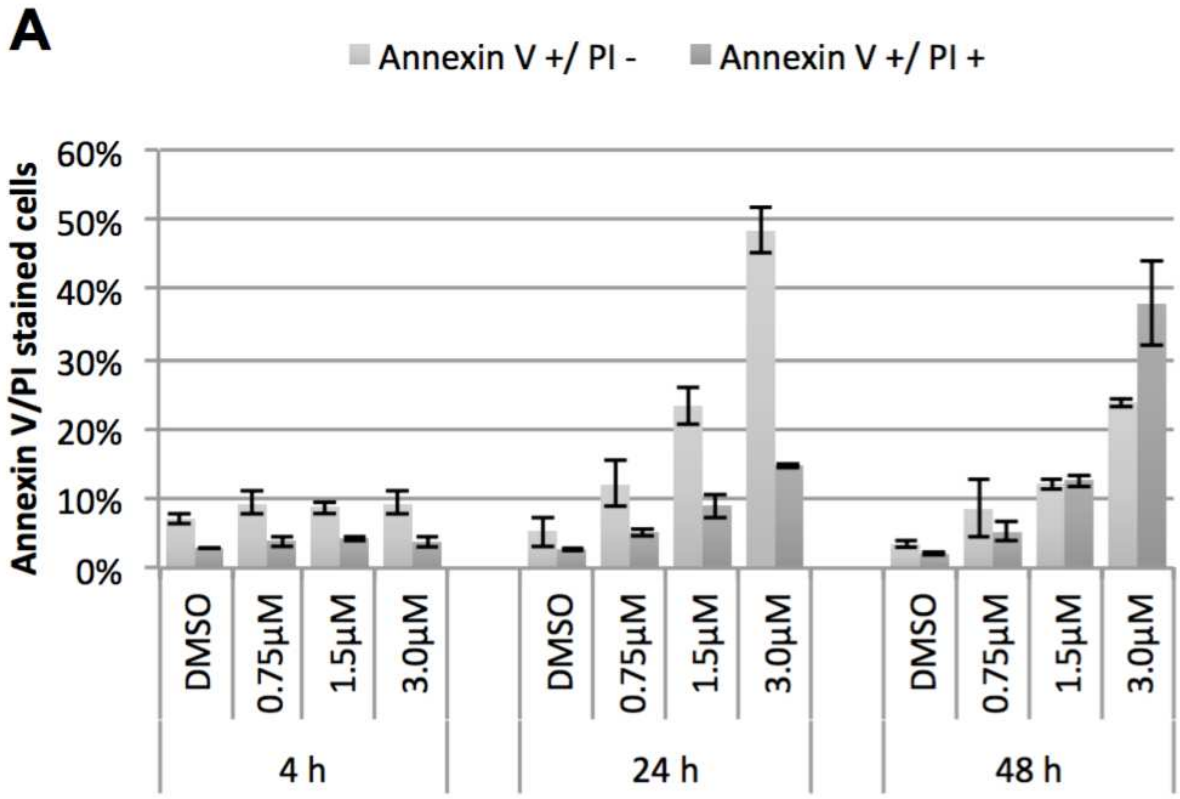
A
Annexin V +/ PI -
Annexin V +/ PI +
Annexin V/PI stained cells
60%
50%
40%
30%
20%
10%
0%
DMSO
0.75µM
1.5µM
3.0µM
4 h
24 h
48 h

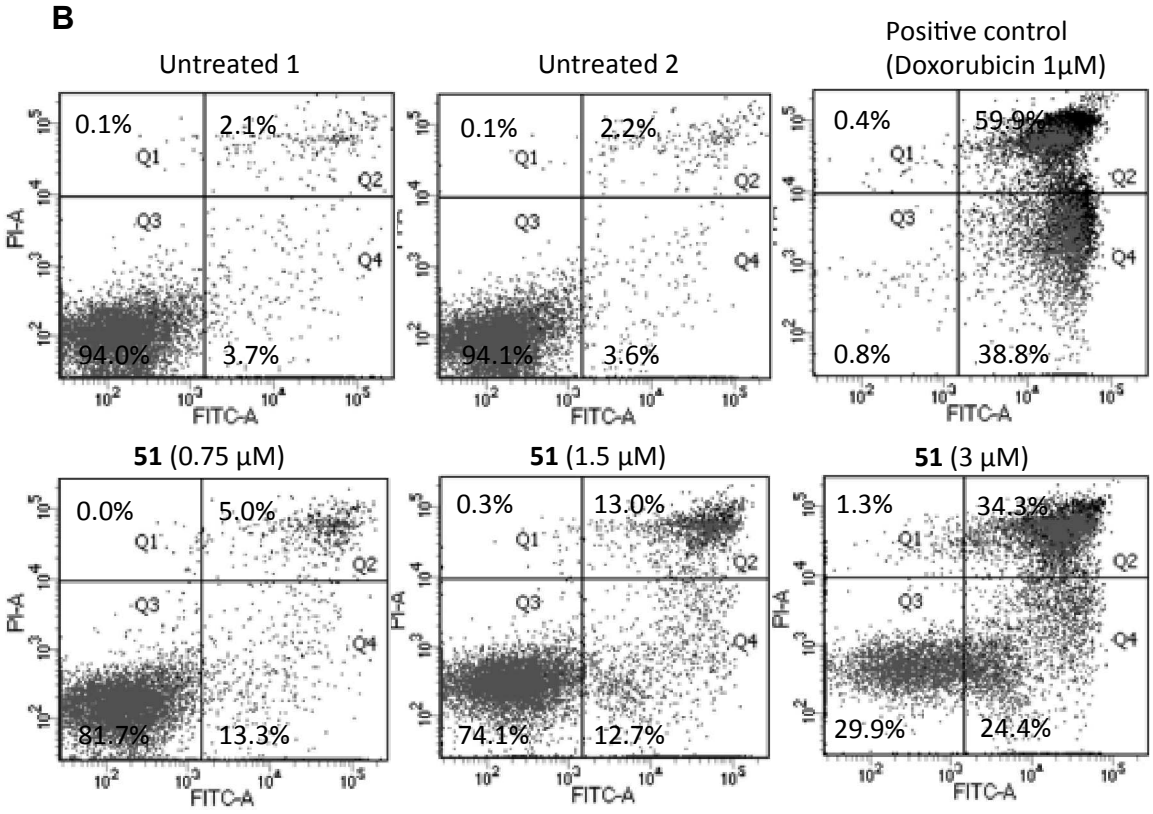
B
Untreated 1
Untreated 2
Positive control
(Doxorubicin 1µM)
0.1%
2.1%
94.0%
3.7%
0.1%
2.2%
94.1%
3.6%
0.4%
59.9%
0.8%
38.8%
51 (0.75 µM)
51 (1.5 µM)
51 (3 µM)
0.0%
5.0%
81.7%
13.3%
0.3%
13.0%
74.1%
12.7%
1.3%
34.3%
29.9%
24.4%
Q1
Q2
Q3
Q4
PI-A
FITC-A

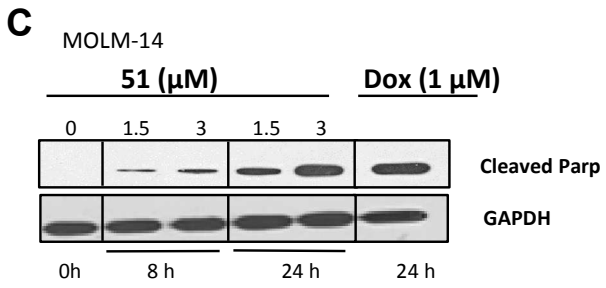


Figure 10. *Compound **51** triggers apoptosis in AML cell line, MOLM-14.* (A) MOLM-14 cells were treated with compound **51** for 4 h, 24 h and 48 h at the concentrations indicated and subsequently stained by Annexin-V FITC and Propidium Iodide (PI). Fluorescence was measured via flow cytometry (LSRII) and at least 10,000 events were analysed. (B) Annexin V FITC vs Propidium Iodide-plots from the gated cells show the populations corresponding to viable and non-apoptotic (Annexin V–PI–), early (Annexin V+PI–), and late (Annexin V+PI+) apoptotic cells following 48 h treatment of compound **51** (for 4 h and 24 h timepoints see Supporting Information) (C) MOLM-14 cells were treated with **51** at the respective concentrations and timepoints and then lysed. Doxorubicin (1μM) was utilised as a positive control for induction of PARP cleavage. Cleaved PARP was detected by immunoblotting.

Poly(ADP-ribose) polymerase (PARP) has been implicated in cell death pathways via apoptosis.[115, 116] During apoptosis PARP is cleaved by caspases to give a N-terminal DNA binding domain. Increase in cleaved PARP upon drug treatment indicates cell death via apoptosis. Treatment of MOLM-14 cells with compound **51**

led to dose related increases in cleaved PARP at both the 8 h and 24 h timepoints (Figure 10C). Taking all the data together, compound **51** has been shown to induce cell death via apoptosis.

Assessment of In Vitro Metabolism

Having identified compound **51** as a suitable dual inhibitor template we tested it and homologue **52** in male and female rat liver microsomes to assess the propensity of the template towards degradation by phase I metabolism. In female rat liver microsomes, **51** had a half life of 26.3 minutes (apparent clearance of 10.7 L/h/kg) and was cleared more rapidly in male microsomes. Compound **52** showed no significant difference between male and female microsomes (Figure 11). Although **51** and **52** are rapidly cleared, this data compares favourably with 2 which is reported to have a half life in rat liver microsomes of 18 minutes.[28]

A

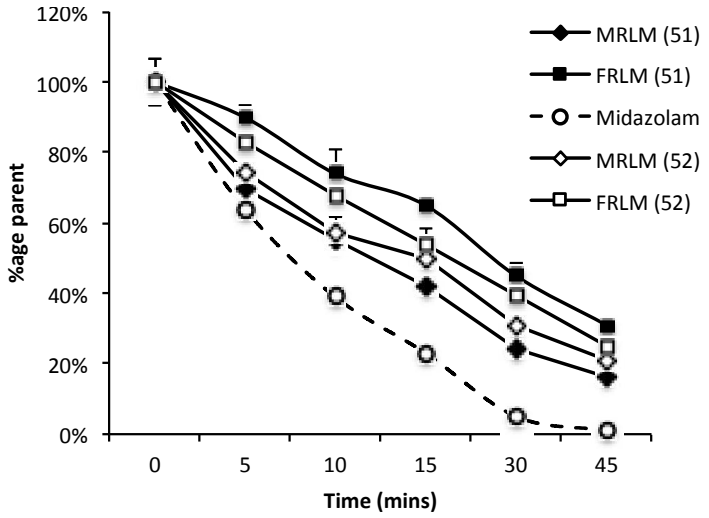


B

| Compound | In vitro system | $T_{1/2}$ (min) | $Cl_{int,app}$ (L/h/kg) |
|---|---|---|---|
| **51** | Male RLM | 17.3±1.1 | 16.3±1.1 |
| | Female RLM | 26.3±1.7 | 10.7±0.7 |
| **52** | Male RLM | 21.0±2.2 | 13.5±1.5 |
| | Female RLM | 23.4±0.7 | 12.0±0.4 |

**Figure 11.** *Rat microsomal stability data for **51** and **52**.* (A) Plot of parent remaining against time for male and female mirosomes. (B) The parameters of $T_{1/2}$ and $Cl_{int}$, app values (mean ± SD) for **51** and **52** (3 μM) upon incubation at 37˚C for 45 min in male (MRLM) and female (FRLM) rat liver microsomes.

In conclusion, application of a pharmacophore merging strategy combining HDAC inhibitor **1** with JAK2/FLT3 inhibitor **2** resulted in the design and synthesis of a series of single molecule dual inhibitor macrocyclic carboxylic and hydroxamic acids. Following exploration of a range of aromatic and non-aromatic linkers, preferred compound **51**, applying a merged pharmacophore, was found to be optimal. Compound **51** has single digit nanomolar potency against JAK2 and HDAC6, is selective within the JAK family and in a panel of 97 kinases and has good potency (<100 nM) against HDACs 2 and 10 and sub-micromolar potency against HDACs 1, 8 and 11. Broad antiproliferative potency was observed for **51** across a range of solid and hematological cell lines. This activity translated into inhibition of tumor cell colony formation. In detailed studies in AML, MM and EL cell lines **51** was shown to block both the JAK-STAT and HDAC pathways at concentrations around or below its $IC_{50}$. Apoptosis was shown to be the mechanism of cell death via Annexin V/PI studies and dose and time related increases in cleaved PARP. Compound **51** (EY3238) was also shown to be cleared in rat liver microsomes with a half life of just over 25 minutes. This first detailed demonstration of isoform-selective JAK-HDAC bispecific inhibitors provides useful tool compounds for further studies of multiple pathway inhibition achieved with a single DML molecule.

## EXPERIMENTAL

### Synthesis of compounds

Unless stated otherwise, all non-aqueous reactions were performed in oven-dried round bottom flasks under an inert nitrogen atmosphere. Commercially available AR grade solvents or anhydrous solvents packed in resealable bottles were used as received. All reaction temperatures stated in the procedures are external bath temperatures. Commercial reagents were purchased from Sigma Aldrich, Alfa Aesar, TCI Chemicals or Strem chemicals, and used as received without further purification unless otherwise stated. Yields refer to chromatographically and spectroscopically homogeneous materials, unless otherwise stated. Reaction progress was monitored by analytical thin layer chromatography (TLC) with 0.25 mm Merck pre-coated silica gel plates (60F-254) using UV light (254 nm) as visualizing agent, and ceric ammonium molybdate or potassium permanganate solutions as developing stains. Flash chromatography was performed on silica gel 60 (0.040 – 0.063 mm) purchased from SiliCycle or Merck. $^{1}$H NMR and $^{13}$C NMR spectra were recorded on a Bruker AMX400 (400 MHz) NMR spectrometer at ambient atmosphere. The deuterated solvent used was $CDCl_3$ unless otherwise stated. Chemical shifts are reported in parts per million (ppm), and residual undeuterated solvent peaks were used as internal reference: proton (7.26ppm for

$CDCl_3$, 2.50ppm for DMSO-*d*6), carbon (77.0ppm for $CDCl_3$, 39.52ppm for DMSO-*d*6). $^1$H NMR coupling constants (*J*) are reported in Hertz (Hz), and multiplicities are presented as follows: s (singlet), d (doublet), t (triplet), m (multiplet), and br (broad). Low resolution mass spectra were obtained on an Agilent 6130B Quadrupole LC/MS in ESI mode with an Agilent 1260 Infinity LC system using a ThermoScientific Hypersil 150 x 2.1mm 5 micron column or a Shimadzu LCMS-2020 in ESI mode. Purity of the compounds were assessed by high pressure liquid chromatography by detection at 254 nm using an Agilent 1200 series HPLC system with a Zorbax SB-C18 5 micron 4.6 x 250 mm column using a gradient elution starting from a 5% solution of acetonitrile and 1% trifluoroacetic acid (TFA) and a 95% solution of water and 1% TFA to a 100% solution of acetonitrile and 1% TFA at 0.5 mL per minute over 15mins. HPLC purity is above 99% unless stated. For macrocycles which are isolated as *trans:cis* isomers, only data for the major *trans* isomer is reported below. Compounds **2** and **3** were a gift from S*BIO Pte Ltd. Ruxolitinb and Tubastatin were purchased from Selleckchem (www.selleckchem.com).

**11-(2-Chloroethoxy)-14,19-dioxa-5,7,26-triaza-tetracyclo[19.3.1.1(2,6).1(8,12)]heptacosa-1(25),2(26),3,5,8,10,12(27),16,21,23-decaene (3).** Following the literature procedure[28], 29.4 mg (0.0631 mmol) of the

diallyl compound **S4** (see Supporting Information) and 6.7 mg (0.00789 mmol, 0.13 eq.) of the 2nd generation Grubbs catalyst was dissolved in 14 mL of degassed DCM (5 mM concentration) to obtain an orange solution. 1 mL of 4M hydrochloric acid was added changing the solution to yellow colour. The reaction mixture was refluxed for 3 h. After cooling to rt, the reaction was quenched with saturated sodium bicarbonate solution and extracted with DCM 3 times. The combined organic layer was washed with brine solution and dried with anhydrous sodium sulfate. The organic layer was concentrated and purified by column chromatography using 3:2 Hex/EtOAc to obtain 17.1 mg (62%) in a 87:13 E/Z ratio of macrocycle **3** as a yellow solid. LRMS (ESI) *m/z* 438.0 ($M+H^+$). E isomer only: $^1$H NMR $\delta$ 8.70 (s, 1 H), 8.47 - 8.40 (m, 1 H), 8.30 (s, 1 H), 7.81 (d, $J$ = 7.8 Hz, 1 H), 7.60 (d, $J$ = 7.7 Hz, 1 H), 7.49 (t, $J$ = 7.7 Hz, 1 H), 7.39 (br. s., 1 H), 7.17 (d, $J$ = 5.3 Hz, 1 H), 6.85 (s, 2 H), 5.92 - 5.77 (m, 2 H), 4.66 (d, $J$ = 2.6 Hz, 4 H), 4.26 (t, $J$ = 5.8 Hz, 3 H), 4.17 (d, $J$ = 4.9 Hz, 2 H), 4.07 (d, $J$ = 4.4 Hz, 2 H), 3.87 - 3.80 (m, 2 H). $^{13}$C NMR $\delta$ 164.3, 160.2, 158.7, 151.5, 138.6, 137.1, 134.1, 132.0, 130.9, 129.9, 128.9, 127.9, 127.7, 126.3, 121.4, 119.2, 113.7, 107.9, 70.2, 69.5, 69.3, 67.6, 65.6, 42.2, 29.7.

**11-(2-*N*-(*tert*-Butyl 4-(methoxycarbonyl)phenylcarbamate)-ethoxy)-14,19-dioxa-5,7,26-triaza-tetracyclo[19.3.1.1(2,6).1(8,12)]heptacosa-1(25),2(26),3,5,8,10,12(27),16,21,23-decaene (4).** 0.147 g (0.335 mmol) of

macrocycle chloride (**3**), 0.183 g (0.562 mmol, 1.7 eq.) of caesium carbonate, 0.122 g (0.330 mmol, 1.0 eq.) of tetrabutylammonium iodide and 0.129 g (0.514 mmol, 1.5 eq.) of **4a** was mixed and 3 mL of DMF was added. The mixture was stirred at 120 °C for 16 h. The mixture was cooled to rt and diluted with water. It was extracted with ethyl acetate 3 times. The combined organic layer was washed with brine solution and dried with anhydrous sodium sulfate. The organic layer was concentrated and purified by column chromatography using 2:1 to 1:1 to 2:3 Hex/EtOAc solution to obtain 117 mg (53%) of **4** as a yellow solid. TLC (1:1 Hex/EtOAc) $R_f$ = 0.31. LRMS (ESI) *m/z* 653.3 ($M+H^+$). $^1$H NMR $\delta$ 8.60 (d, *J* = 2.6 Hz, 1 H), 8.38 (d, *J* = 5.1 Hz, 1 H), 8.25 (s, 1 H), 8.06 - 8.01 (m, 2 H), 7.82 - 7.76 (m, 2 H), 7.58 (d, *J* = 7.7 Hz, 1 H), 7.47 (t, *J* = 7.7 Hz, 1 H), 7.42 - 7.37 (m, *J* = 8.7 Hz, 2 H), 7.13 (d, *J* = 5.3 Hz, 1 H), 6.83 (dd, *J* = 2.6, 8.7 Hz, 1 H), 6.77 (d, *J* = 8.7 Hz, 1 H), 5.81 - 5.76 (m, 2 H), 4.62 (s, 2 H), 4.33 (s, 2 H), 4.19 - 4.14 (m, 2 H), 4.04 (d, *J* = 4.0 Hz, 2 H), 4.01 (d, *J* = 4.5 Hz, 2 H), 3.91 (s, 3 H), 1.45 (s, 9 H). $^{13}$C NMR $\delta$ 166.5, 164.3, 160.0, 158.4, 154.0, 151.6, 147.3, 138.5, 137.0, 133.4, 132.0, 130.9, 130.1, 129.8, 128.8, 127.6, 127.1, 126.9, 126.3, 126.2, 121.4, 119.2, 111.9, 107.6, 81.1, 70.1, 69.2, 67.4, 66.8, 65.3, 52.0, 49.6, 28.2.

**11-(2-(*tert*-Butyl 3-(methoxycarbonyl)phenylcarbamate)-ethoxy)-14,19-dioxa-5,7,26-triaza-tetracyclo[19.3.1.1(2,6).1(8,12)]heptacosa-1(25),2(26),3,5,8,10,12(27),16,21,23-decaene (5).** Synthesised following the

procedure for **4** using 190 mg (0.434 mmol) of **3**, 447 mg (1.37 mmol, 3.2 eq.) of caesium carbonate, 201 mg (0.544 mmol, 1.3 eq.) of tetrabutylammonium iodide and 171 mg (0.678 mmol, 1.6 eq.) of **5a**. The compound was purified by column chromatography using 2:1 to 1:1 Hex/EtOAc solution to obtain 127 mg (45%) of **5** as a yellow solid. TLC (1:1 Hex/EtOAc) $R_f$ = 0.24. LRMS (ESI) *m/z* 653.3 ($M+H^+$). $^1$H NMR  8.44 (d, *J* = 2.64 Hz, 1H), 8.25 (d, *J* = 5.15 Hz, 1H), 8.13 (s, 1H), 7.83 (s, 1H), 7.75 - 7.80 (m, 1H), 7.68 (d, *J* = 7.91 Hz, 1H), 7.48 (d, *J* = 9.29 Hz, 2H), 7.32 - 7.40 (m, 2H), 7.30 (d, *J* = 7.78 Hz, 1H), 7.13 (s, 1H), 7.03 (d, *J* = 5.27 Hz, 1H), 6.72 (dd, *J* = 2.70, 8.72 Hz, 1H), 6.66 (d, *J* = 8.66 Hz, 1H), 5.66 (q, *J* = 5.14 Hz, 2H), 4.50 (s, 2H), 4.23 (s, 2H), 4.01 - 4.06 (m, 2H), 3.95 - 4.01 (m, 3H), 3.92 (d, *J* = 4.52 Hz, 2H), 3.88 (d, *J* = 4.77 Hz, 2H), 3.79 (s, 3H), 1.28 - 1.36 (m, 9H). $^{13}$C NMR  166.5, 164.7, 159.7, 157.8, 154.3, 151.8, 143.2, 138.6, 136.9, 133.1, 132.1, 131.8, 131.1, 130.9, 129.8, 129.0, 128.7, 127.9, 127.7, 127.1, 127.1, 126.3, 121.4, 119.4, 112.0, 107.6, 81.0, 70.1, 69.2, 67.5, 66.7, 65.3, 52.2, 49.6, 28.3.

**11-(2-(Methyl 4-hydroxybenzoate))- 14,19-dioxa-5,7,26-triaza-tetracyclo [19.3.1.1(2,6).1(8,12)] heptacosa-1(25),2(26),3,5,8,10,12(27),16,21,23-decaene (6).** Synthesised following the procedure for **4** using 201 mg (0.459 mmol) of **3**, 307 mg (0.943 mmol, 2.0 eq.) of caesium carbonate, 169 mg (0.457 mmol, 1.0 eq.) of tetrabutylammonium iodide and 142 mg (0.932 mmol, 2.0 eq.) of **6a**. The crude

product was purified by column chromatography using 2:1 to 2:3 to 1:2 Hex/EtOAc solution to obtain 206 mg (82%) of **6** as a yellow solid. TLC (1:1 Hex/EtOAc) $R_f$ = 0.22. LRMS (ESI) *m/z* 554.2 ($M+H^+$). $^1$H NMR $\delta$ 8.65 (d, *J* = 2.3 Hz, 1 H), 8.40 (br. s., 1 H), 8.28 (s, 1 H), 8.05 - 7.99 (m, 2 H), 7.81 (d, *J* = 7.7 Hz, 1 H), 7.60 (d, *J* = 7.3 Hz, 2 H), 7.52 - 7.45 (m, 1 H), 7.17 (d, *J* = 5.3 Hz, 1 H), 7.02 - 6.96 (m, 2 H), 6.95 - 6.84 (m, 2 H), 5.87 - 5.78 (m, 2 H), 4.66 - 4.60 (m, 2 H), 4.59 (s, 2 H), 4.43 - 4.33 (m, 4 H), 4.09 (d, *J* = 4.5 Hz, 2 H), 4.05 (d, *J* = 4.0 Hz, 2 H), 3.93 - 3.84 (m, 3 H). $^{13}$C NMR $\delta$ 166.8, 164.7, 162.5, 159.7, 157.9, 151.9, 138.7, 136.9, 133.7, 131.9, 131.6, 131.1, 129.9, 129.0, 127.9, 127.7, 126.4, 122.9, 121.4, 119.5, 114.3, 113.6, 107.8, 70.1, 69.3, 68.0, 67.6, 66.7, 65.6.

**11-(2-*N*-(*tert*-Butyl 4-nitrophenylcarbamate)- ethoxy)-14,19-dioxa-5,7,26-triaza-tetracyclo[19.3.1.1(2,6).1(8,12)]heptacosa-1(25),2(26),3,5,8,10,12(27),16,21,23-decaene (7).** Synthesised following the procedure for **4** using 432 mg (0.988 mmol) of **3**, 387 mg (1.19 mmol, 1.2 eq.) of caesium carbonate, 185 mg (0.502 mmol, 0.51 eq.) of tetrabutylammonium iodide and 275 mg (1.15 mmol, 1.2 eq.) of **7a** in 4 mL of DMF. The crude product was purified by column chromatography using 1:1 Hex/EtOAc solution to obtain 395 mg (62%) of **7** as a light yellow solid. TLC (1:1 Hex/EtOAc) $R_f$ = 0.18. LRMS (ESI) *m/z* 640.3 ($M+H^+$). $^1$H NMR $\delta$ 8.64 (d, *J* = 2.4 Hz, 1 H), 8.40 (d, *J* = 5.3 Hz, 1 H), 8.26 (s, 1 H), 8.25 - 8.19 (m, 2 H), 7.80 (d, *J* = 7.8 Hz, 1 H), 7.62 -

7.52 (m, 4 H), 7.51 - 7.45 (m, 1 H), 7.15 (d, *J* = 5.3 Hz, 1 H), 6.86 - 6.77 (m, 2 H), 5.82 - 5.77 (m, 2 H), 4.63 (s, 2 H), 4.34 (s, 2 H), 4.24 - 4.19 (m, 2 H), 4.17 - 4.11 (m, 2 H), 4.06 (d, *J* = 3.9 Hz, 2 H), 4.01 (d, *J* = 4.3 Hz, 2 H), 1.52 - 1.45 (m, 9 H). $^{13}$C NMR $\delta$ 164.4, 160.1, 158.5, 153.5, 151.6, 149.1, 144.7, 138.6, 137.1, 133.7, 131.6, 131.0, 130.1, 128.9, 127.6, 126.9, 126.6, 126.3, 124.1, 121.5, 119.2, 112.2, 107.8, 82.0, 70.1, 69.4, 67.6, 67.0, 65.4, 49.9, 28.2.

**11-(2-(Methyl isonipecotate)-ethoxy)- 14,19-dioxa-5,7,26-triaza-tetracyclo[19.3.1.1(2,6).1(8,12)]heptacosa-1(25),2(26),3,5,8,10,12(27),16,21,23-decaene (8).** 1.00 g (2.29 mmol) of **3** was dissolved in 20 mL of acetonitrile. 0.90 mL (6.66 mmol, 2.9 eq.) of **8a** was added to the solution and it was refluxed for 64 h. The solution was cooled to rt and concentrated. The crude product was purified by column chromatography using 45:55 to 3:7 Hex/EtOAc to EtOAc to 9:1 EtOAc/MeOH to give 255 mg (25%) of recovered **1** and 771mg (62%) of **8** as a yellow solid. TLC (10:1 EtOAc/MeOH) $R_f$ = 0.16. LRMS (ESI) *m/z* 544.3 ($M+H^+$). $^1$H NMR □ 8.68 (s, 1 H), 8.40 (d, *J* = 5.1 Hz, 1 H), 8.29 (s, 1 H), 7.79 (d, *J* = 7.8 Hz, 1 H), 7.61 - 7.55 (m, 2 H), 7.51 - 7.44 (m, 1 H), 7.14 (d, *J* = 5.3 Hz, 1 H), 6.86 - 6.82 (m, 2 H), 5.91 - 5.77 (m, 2 H), 4.64 (s, 2 H), 4.60 (s, 2 H), 4.20 - 4.10 (m, 4 H), 4.06 (d, *J* = 4.5 Hz, 2 H), 3.70 - 3.65 (m, 3 H), 3.09 - 3.00 (m, 2 H), 2.89 (t, *J* = 5.6 Hz, 2 H), 2.41 - 2.30 (m, 3 H), 2.02 - 1.93 (m, 2 H), 1.92 - 1.80 (m, 2 H). $^{13}$C NMR □ 175.1, 164.2, 160.2, 158.7, 151.9, 138.6, 137.1, 133.5, 131.9,

130.9, 129.9, 128.9, 127.6, 127.0, 126.2, 121.4, 119.2, 112.7, 107.7, 77.2, 70.0, 69.3, 67.6, 66.7, 65.8, 57.2, 53.1, 51.6, 40.3, 27.8.

**11-(2-*N*-(*tert*-Butyl 4-aminophenylcarbamate)-ethoxy)-14,19-dioxa-5,7,26-triaza-tetracyclo[19.3.1.1(2,6).1(8,12)]heptacosa-1(25),2(26),3,5,8,10,12(27),16,21,23-decaene (9).** 395 mg (0.617 mmol) of **7**, 140 mg (2.51 mmol, 4.0 eq.) of iron and 219 mg (4.10 mmol, 6.6 eq.) of ammonium chloride in 10 mL of ethanol, 5 mL of ethyl acetate and 3 mL of water. Compound **9** was used without further purification. TLC (1:1 Hex/EtOAc) $R_f$ = 0.09. LRMS (ESI) *m/z* 610.3 ($M+H^+$).

**11-(2-(*tert*-Butyl 4-(methyl 7-carbamoylpentanoyl)phenylcarbamate))-ethoxy)-14,19-dioxa-5,7,26-triaza-tetracyclo[19.3.1.1(2,6).1(8,12)]heptacosa-1(25),2(26),3,5,8,10,12(27),16,21, 23-decaene (10).** 100.3 mg (0.1645 mmol) of aniline **9**, 30 µL (0.2025 mmol, 1.2 eq.) of monomethyl adipate (**10a**), 85.1 mg (0.224 mmol, 1.4 eq.) of HATU and 43 µL (0.307 mmol, 1.9 eq.) of triethylamine were dissolved in 2 mL of DMF and stirred at 60 ºC for 18 h. The reaction was cooled to rt, diluted with water and extracted with ethyl acetate 3 times. The combined organic layer was washed with brine solution and dried with anhydrous sodium sulfate.. The crude product was purified by column chromatography using 2:3 to 1:4 Hex/EtOAc to EtOAc solution to obtain 97.5 mg (79%) of **10** as a yellow amorphous solid (contains 1:1 DMF). TLC (2:3 Hex/EtOAc) $R_f$ = 0.51.

LRMS (ESI) *m/z* 752.4 ($M+H^+$). $^1$H NMR □ 8.48 (d, *J* = 2.51 Hz, 1H), 8.35 (d, *J* = 5.65 Hz, 1H), 8.23 (s, 1H), 8.10 (s, 1H), 7.78 - 7.87 (m, 2H), 7.62 (d, *J* = 7.78 Hz, 1H), 7.47 - 7.57 (m, 3H), 7.16 - 7.23 (m, 3H), 6.87 (dd, *J* = 2.70, 8.72 Hz, 1H), 6.78 (d, *J* = 8.78 Hz, 1H), 5.73 - 5.87 (m, 2H), 4.62 (s, 2H), 4.48 (s, 2H), 4.08 - 4.15 (m, 4H), 3.99 - 4.06 (m, 4H), 3.67 (s, 3H), 2.32 - 2.43 (m, 4H), 1.63 - 1.80 (m, 4H). $^{13}$C NMR □ 174.0, 171.0, 162.7, 158.1, 155.5, 154.8, 152.3, 138.8, 136.2, 131.8, 129.7, 129.1, 127.9, 127.7, 127.3, 126.7, 121.8, 120.0, 112.0, 107.5, 80.6, 70.2, 69.2, 67.6, 66.3, 65.4, 51.6, 49.5, 38.6, 37.0, 36.5, 33.6, 28.3, 24.9, 24.4, 24.2.

**11-(2-(*tert*-Butyl 4-(methyl 7-carbamoylhexanoyl)phenylcarbamate))-ethoxy)-14,19-dioxa-5,7,26-triaza-tetracyclo[19.3.1.1(2,6).1(8,12)]heptacosa-1(25),2(26),3,5,8,10,12(27),16,21,23-decaene (11).** Synthesised using the method for **10** with 83.3 mg (0.137 mmol) of **9**, 36 µL (0.203 mmol, 1.5 eq.) of ethyl hydrogen pimelate (**11a**), 63.3 mg (0.166 mmol, 1.2 eq.) of HATU and 40 µL (0.285 mmol, 2.1 eq.) of triethylamine. The crude product was purified by column chromatography using 3:7 to 1:3 Hex/EtOAc solution to obtain 78.0 mg (73%) of **11** as a pale yellow solid. TLC (2:3 Hex/EtOAc) $R_f$ = 0.36. LRMS (ESI) *m/z* 780.4 ($M+H^+$). $^1$H NMR □ 8.58 (d, *J* = 2.51 Hz, 1H), 8.33 - 8.42 (m, 1H), 8.27 (s, 1H), 7.75 - 7.85 (m, 2H), 7.55 - 7.67 (m, 2H), 7.43 - 7.55 (m, 3H), 7.11 - 7.23 (m, 3H), 6.85 (dd, *J* = 2.76, 8.66 Hz, 1H), 6.78 (d, *J* = 8.78 Hz, 1H), 5.72 - 5.89 (m, 2H),

4.63 (s, 2H), 4.48 (s, 2H), 3.97 - 4.20 (m, 12H), 3.25 - 3.42 (m, 1H), 2.24 - 2.42 (m, 7H), 1.56 - 1.78 (m, 7H), 1.32 - 1.56 (m, 13H), 1.19 - 1.31 (m, 5H). $^{13}$C NMR  173.7, 171.2, 164.8, 159.7, 157.7, 154.8, 151.9, 138.6, 136.9, 136.2, 132.1, 131.1, 129.7, 128.9, 127.7, 127.7, 127.1, 126.3, 121.4, 119.9, 119.5, 112.1, 107.6, 70.1, 69.2, 67.5, 66.4, 65.5, 60.2, 60.1, 49.6, 37.2, 34.1, 34.0, 32.8, 28.9, 28.5, 28.3, 25.1, 25.0, 24.7, 24.6, 24.4, 14.2.

**11-(2-(*tert*-Butyl 4-(methyl 7-carbamoylheptanoyl)phenylcarbamate))-ethoxy)-14,19-dioxa-5,7,26-triaza-tetracyclo[19.3.1.1(2,6).1(8,12)]heptacosa-1(25),2(26),3,5,8,10,12(27), 16,21,23-decaene (12).** 73.5 mg (0.391 mmol, 1.7 eq.) of monomethyl suberate, 140 mg (0.229 mmol), aniline **9**, 158 mg (0.414 mmol, 1.8 eq.) and 90 μL (0.642 mmol, 2.8 eq.) of triethylamine. The crude product was purified by column chromatography using 2:3 (**12a**) to 1:4 Hex/EtOAc solution to obtain 105 mg (59%) of **12** as a pale yellow solid. TLC (3:7 Hex/EtOAc) $R_f$ = 0.33. LRMS (ESI) *m/z* 780.4 ($M+H^+$). $^1$H NMR $\delta$ 8.60 (d, $J$ = 2.4 Hz, 1 H), 8.38 (d, $J$ = 4.5 Hz, 1 H), 8.27 (s, 1 H), 7.80 (d, $J$ = 7.8 Hz, 1 H), 7.63 (s, 1 H), 7.59 (d, $J$ = 7.7 Hz, 1 H), 7.53 - 7.45 (m, 4 H), 7.19 (d, $J$ = 7.7 Hz, 2 H), 7.14 (d, $J$ = 5.3 Hz, 1 H), 6.83 (dd, $J$ = 2.6, 8.7 Hz, 1 H), 6.78 (d, $J$ = 8.7 Hz, 1 H), 5.80 (q, $J$ = 4.8 Hz, 2 H), 4.63 (s, 2 H), 4.48 (s, 2 H), 4.15 - 4.07 (m, 4 H), 4.07 - 3.98 (m, 4 H), 3.65 (s, 3 H), 2.35 - 2.27 (m, 4 H), 1.76 - 1.66 (m, 2 H), 1.62 (td, $J$ = 7.3, 14.3 Hz, 2 H), 1.49 - 1.40 (m, 9 H), 1.40 - 1.32 (m, 6 H). $^{13}$C NMR $\delta$ 174.2, 171.2, 164.5, 160.0, 158.2,

154.8, 151.8, 138.6, 137.0, 133.2, 132.1, 131.0, 129.8, 128.9, 127.7, 127.1, 126.3, 121.4, 119.9, 119.4, 112.1, 107.6, 80.5, 70.2, 69.2, 67.5, 66.4, 65.5, 51.5, 49.6, 37.4, 33.9, 29.6, 28.7, 28.7, 28.3, 25.3, 24.6.

**2-((Allyloxy)methyl)-4-nitrophenol (14).** 2.00 g (12.0 mmol) of 2-hydroxy-5-nitrobenzaldehyde (**13**) was dissolved in 30 mL of DCM and cooled to 0 °C. 2.5 mL (17.8 mmol, 1.5 eq.) of triethylamine and 1.1 mL (14.5 mmol, 1.2 eq.) of chloromethyl methyl ether was added and the solution was allowed to warm to rt and stirred for 18 h at rt. The solution was concentrated and the crude product used directly in the next step. TLC (4:1 Hex/EtOAc) $R_f$ = 0.13. The crude mixture was redissolved in 30 mL of methanol and cooled to 0 °C. 0.461 g (12.2 mmol, 1.0 eq.) of sodium borohydride was added portionwise and the mixture was stirred at rt for 1 h. The reaction was quenched with saturated ammonium chloride solution. This was extracted 4 times with dichloromethane. The combined organic layer was washed with brine solution and dried with anhydrous sodium sulfate. The solution was concentrated and the crude product used directly in the next step. TLC (1:1 Hex/EtOAc) $R_f$ = 0.54. The crude product was redissolved in 10 mL of DCM. 0.845 g (3.71 mmol, 0.3 eq.) of triethylbenzylammonium chloride, 3.1 mL (35.8 mmol, 3.0 eq.) of allyl bromide and 19 mL (363 mmol, 30 eq.) of concentrated sodium hydroxide solution was added sequentially at rt. The biphasic mixture was stirred at rt for 66 h. This was extracted 3 times with dichloromethane.

The combined organic layer was washed with brine solution and dried with anhydrous sodium sulfate. The solution was concentrated and the crude product used directly in the next step. TLC (3:1 Hex/EtOAc) $R_f$ = 0.59. The crude product was redissolved in 20 mL of THF and 10 mL of 4 M HCl was added to the solution. The solution was refluxed for 3 h after which it was cooled to rt. This was extracted 3 times with dichloromethane. The combined organic layer was washed with saturated sodium bicarbonate solution and dried with anhydrous sodium sulfate. The solution was concentrated and the product was purified using column chromatography starting from 9:1 to 85:15 to 3:1 to 2:1 Hex/EtOAc solutions to obtain 1.81g (72% over 4 steps) of the product as a yellow oil. TLC (2:1 Hex/EtOAc) $R_f$ = 0.30; LRMS (ESI) *m/z* 152.0 ($M+H^+$). $^1$H NMR $\delta$ 8.09 (dd, $J$ = 2.7, 9.0 Hz, 1 H), 7.98 (d, $J$ = 2.6 Hz, 1 H), 6.92 (d, $J$ = 9.0 Hz, 1 H), 6.00 - 5.86 (m, 1 H), 5.38 - 5.25 (m, 2 H), 4.75 (s, 2 H), 4.12 (d, $J$ = 5.8 Hz, 2 H). $^{13}$C NMR $\delta$ 161.9, 140.7, 132.7, 125.4, 124.1, 122.7, 119.0, 116.8, 71.9, 70.3.

**Methyl 4-(2-((allyloxy)methyl)-4-nitrophenoxy)butanoate (15).** 0.126 g (0.602 mmol) of phenol **14** was dissolved in 6 mL of acetonitrile. 0.172 g (1.24 mmol, 2.1 eq.) of potassium carbonate and 0.11 mL (0.888 mmol, 1.5 eq.) of methyl 4-bromobutyrate (**15a**) was added to the solution. The mixture was refluxed for 18 h with stirring. The solution was cooled to rt, diluted water and extracted 3 times with DCM. The combined organic layer was washed with brine solution and dried

with anhydrous sodium sulfate. The organic layer was concentrated and purified by column chromatography using 3:1 to 2:1 Hex/EtOAc to obtain 0.151 g (100%) of **15** as a light yellow oil. TLC (2:1 Hex/EtOAc) $R_f$ = 0.28; LRMS (ESI) *m/z* 310.1 ($M+H^+$), 332.1 ($M+Na^+$). $^1$H NMR $\delta$ 8.29 (d, *J* = 2.9 Hz, 1 H), 8.12 (dd, *J* = 2.8, 9.0 Hz, 1 H), 6.87 (d, *J* = 9.0 Hz, 1 H), 6.02 - 5.90 (m, 1 H), 5.33 (qd, *J* = 1.6, 17.2 Hz, 1 H), 5.22 (qd, *J* = 1.3, 10.4 Hz, 1 H), 4.52 (s, 2 H), 4.15 - 4.08 (m, 4 H), 3.67 (s, 3 H), 2.52 (t, *J* = 7.2 Hz, 2 H), 2.20 - 2.10 (m, 2 H). $^{13}$C NMR $\delta$ 173.1, 160.6, 141.3, 134.3, 128.3, 124.7, 123.9, 117.3, 110.3, 71.9, 67.6, 65.9, 51.6, 30.1, 24.2.

**Methyl 5-(2-((allyloxy)methyl)-4-nitrophenoxy)pentanoate (16).** Synthesised using the procedure for **15** using 145 mg (0.691 mmol) of **14**, 0.15 mL (1.05 mmol, 1.5eq.) of methyl 5-bromopentanoate (**16a**) and 209 mg (1.51 mmol, 2.2eq.) of potassium carbonate in 6 mL of acetonitrile. The compound was purified by flash column chromatography using 4:1 to 2:1 Hex/EtOAc solution to obtain 165 mg (90%) of **16** as a light yellow oil. TLC (7:3 Hex/EtOAc) $R_f$ = 0.32. LRMS (ESI) *m/z* 346.1 ($M+Na^+$). $^1$H NMR $\delta$ 8.27 (d, *J* = 2.8 Hz, 1 H), 8.10 (dd, *J* = 2.8, 9.0 Hz, 1 H), 6.85 (d, *J* = 9.2 Hz, 1 H), 6.01 - 5.89 (m, 1 H), 5.32 (qd, *J* = 1.6, 17.2 Hz, 1 H), 5.20 (qd, *J* = 1.4, 10.4 Hz, 1 H), 4.51 (s, 2 H), 4.12 - 4.03 (m, 4 H), 3.64 (s, 3 H), 2.38 (t, *J* = 7.0 Hz, 2 H), 1.91 - 1.76 (m, 4 H). $^{13}$C NMR $\delta$ 173.5, 160.8, 141.2, 134.3, 128.3, 124.6, 123.8, 117.2, 110.2, 71.8, 68.3, 65.9, 51.4, 33.3, 28.2, 21.3.

**Ethyl 6-(2-((allyloxy)methyl)-4-nitrophenoxy)hexanoate (17).** Synthesised using the procedure for **15** using 429 mg (2.05 mmol) of **14**, 0.45 mL (2.53 mmol, 1.2eq.) of ethyl 6-bromohexanoate (**17a**) and 730 mg (5.28 mmol, 2.6eq.) of potassium carbonate in 10 mL of acetonitrile. The compound was purified by flash column chromatography using 9:1 to 85:15 Hex/EtOAc solution to obtain 631 mg (88%) of **17** as a yellow solid. TLC (7:3 Hex/EtOAc) $R_f$ = 0.34. LRMS (ESI) *m/z* 374.1 ($M+Na^+$). $^1$H NMR $\delta$ 8.31 - 8.25 (m, 1 H), 8.10 (td, *J* = 3.2, 9.0 Hz, 1 H), 6.85 (dd, *J* = 1.6, 9.0 Hz, 1 H), 6.01 - 5.89 (m, 1 H), 5.37 - 5.28 (m, 1 H), 5.24 - 5.17 (m, 1 H), 4.51 (d, *J* = 2.1 Hz, 2 H), 4.14 - 4.01 (m, 6 H), 2.31 (dt, *J* = 1.9, 7.4 Hz, 2 H), 1.88 - 1.77 (m, 2 H), 1.74 - 1.63 (m, 2 H), 1.54 - 1.44 (m, 2 H), 1.22 (dt, *J* = 2.3, 7.2 Hz, 3 H). $^{13}$C NMR $\delta$ 173.3, 160.9, 141.2, 134.3, 128.3, 124.6, 123.8, 117.2, 110.2, 71.8, 68.5, 65.9, 60.1, 34.0, 28.5, 25.4, 24.5, 14.1.

**Methyl 7-(2-((allyloxy)methyl)-4-nitrophenoxy)heptanoate (18).** Synthesised using the procedure for **15** using 409 mg (1.96 mmol) of **14**, 0.42 mL (2.37 mmol, 1.2eq.) of methyl 7-bromoheptanoate (**18a**) and 579 mg (4.19 mmol, 2.1eq.) of potassium carbonate in 15 mL of acetonitrile. The crude product was purified using flash column chromatography using 9:1 to 4:1 Hex/EtOAc solution to obtain 576 mg (84%) of **18** as a light yellow oil. TLC (2:1 Hex/EtOAc) $R_f$ = 0.42. LRMS (ESI) *m/z* 374.1 ($M+Na^+$). $^1$H NMR $\delta$ 8.33 - 8.28 (m, 1 H), 8.16 - 8.10 (m, 1 H), 6.86 (d, *J* = 9.0 Hz, 1 H), 6.03 - 5.91 (m, 1 H), 5.34 (qd, *J* = 1.6, 17.3 Hz, 1 H),

5.26 - 5.20 (m, 1 H), 4.53 (s, 2 H), 4.15 - 4.09 (m, 2 H), 4.06 (t, *J* = 6.3 Hz, 2 H), 3.68 - 3.63 (m, 3 H), 2.35 - 2.28 (m, 2 H), 1.87 - 1.78 (m, 2 H), 1.70 - 1.59 (m, 2 H), 1.53 - 1.44 (m, 2 H), 1.44 - 1.35 (m, 3 H). $^{13}$C NMR $\delta$ 174.0, 161.0, 141.2, 134.4, 128.3, 124.7, 123.9, 117.3, 110.2, 71.9, 68.7, 66.0, 51.4, 33.8, 28.7, 25.6, 24.7.

**Methyl 8-(2-((allyloxy)methyl)-4-nitrophenoxy)octanoate (19).** Synthesised using the procedure for **15** using 188 mg (0.901 mmol) of **14**, 254 mg (1.07 mmol, 1.2eq.) of methyl 8-bromooctanoate (**19a**) and 284 mg (2.06 mmol, 2.3eq.) of potassium carbonate in 5 mL of acetonitrile. The crude product was purified by flash column chromatography using 5:1 to 4:1 Hex/EtOAc solution to obtain 286 mg (87%) of **19** as a yellow oil. TLC (2:1 Hex/EtOAc) $R_f$ = 0.54; LRMS (ESI) *m/z* 366.1 ($M+H^+$). $^1$H NMR $\delta$ 8.30 - 8.24 (m, 1 H), 8.13 - 8.06 (m, 1 H), 6.84 (d, *J* = 9.2 Hz, 1 H), 6.01 - 5.87 (m, 1 H), 5.36 - 5.27 (m, 1 H), 5.23 - 5.15 (m, 1 H), 4.51 (s, 2 H), 4.09 (dd, *J* = 1.3, 5.6 Hz, 2 H), 4.07 - 4.00 (m, 2 H), 3.63 (s, 3 H), 2.28 (t, *J* = 7.5 Hz, 2 H), 1.85 - 1.76 (m, 2 H), 1.61 (quin, *J* = 7.2 Hz, 2 H), 1.50 - 1.41 (m, 2 H), 1.41 - 1.28 (m, 4 H). $^{13}$C NMR $\delta$ 174.0, 160.9, 141.1, 134.3, 128.3, 124.6, 123.7, 117.1, 110.2, 71.8, 68.7, 65.9, 51.3, 33.8, 28.8, 28.8, 28.7, 25.6, 24.7.

**Methyl 4-(4-(4-(3-((allyloxy)methyl)phenyl)pyrimidin-2-ylamino)-2-((allyloxy)methyl) phenoxy)butanoate (21).** 196 mg (0.634 mmol) of **15** was dissolved in 10 mL of methanol and 5 mL of water (on bigger scale, a small

volume of ethyl acetate was added to aid the dissolution of the compound). 108 mg (1.94 mmol, 3.1 eq.) of iron and 216 mg (4.04 mmol, 6.4 eq.) of ammonium chloride was added and the reaction mixture was refluxed for 4 h. The reaction mixture was cooled to rt and filtered through a pad of celite, washing with DCM. Saturated sodium bicarbonate was added to the filtrate and it was extracted 3 times with DCM. The combined organic layers were washed with brine solution and dried over anhydrous sodium sulfate. The combined organic layer was concentrated and dissolved in 10 mL of dioxane. 459 mg (1.76 mmol, 2.8 eq.) of pyrimidine **20** (see Supporting Information and *J. Med. Chem.* **2011**, *54*, 4638) and 97.4 mg (0.512 mmol, 0.81 eq.) of PTSA was added to the solution. The reaction mixture was stirred at 95 °C for 16 h. The reaction was cooled to rt and quenched with saturated sodium bicarbonate solution and extracted 3 times with DCM. The combined organic layers were washed with brine solution and dried over anhydrous sodium sulfate. The crude product was purified using flash column chromatography using 3:1 to 7:3 to 3:2 Hex/EtOAc solution to obtain 186 mg (58%) of **21** as a brown amorphous solid and 107 mg of pyrimidine starting material. TLC (2:1 Hex/EtOAc) $R_f$ = 0.23; LRMS (ESI) *m/z* 504.2 ($M+H^+$). $^1H$ NMR $\delta$ 8.41 (d, $J$ = 5.3 Hz, 1 H), 8.05 - 7.98 (m, 2 H), 7.63 (s, 2 H), 7.61 - 7.59 (m, 1 H), 7.50 - 7.43 (m, 3 H), 7.12 (d, $J$ = 5.3 Hz, 1 H), 6.85 (d, $J$ = 8.8 Hz, 1 H), 6.04 - 5.91 (m, 2 H), 5.35 (q, $J$ = 1.6 Hz, 1 H), 5.30 (q, $J$ = 1.6 Hz, 1 H), 5.20

(dddd, *J* = 1.3, 3.0, 10.6, 14.0 Hz, 2 H), 4.60 (s, 2 H), 4.58 (s, 2 H), 4.50 - 4.46 (m, 1 H), 4.36 (s, 1 H), 4.08 (tdd, *J* = 1.4, 5.6, 12.4 Hz, 4 H), 4.02 (t, *J* = 6.0 Hz, 2 H), 3.88 - 3.83 (m, 1 H), 3.69 (s, 3 H), 2.54 (t, *J* = 7.3 Hz, 2 H), 2.17 - 2.08 (m, 2 H). $^{13}$C NMR $\delta$ 173.6, 164.9, 160.3, 158.1, 152.0, 139.0, 137.2, 134.9, 134.6, 132.6, 130.0, 128.9, 127.5, 126.4, 126.3, 121.2, 120.1, 117.2, 116.8, 111.7, 107.9, 71.8, 71.5, 71.3, 68.5, 67.2, 66.8, 66.2, 62.6, 51.6, 30.5, 24.7.

**Methyl 5-(4-(4-(3-((allyloxy)methyl)phenyl)pyrimidin-2-ylamino)-2-((allyloxy)methyl)phenoxy) pentanoate (22).** Synthesised using the procedure for **21** using 209 mg (0.646 mmol) of **16**, 110 mg (1.97 mmol, 3.0eq.) of iron and 315 mg (5.89 mmol, 9.1 eq.) of ammonium chloride in 6 mL of methanol and 3 mL of water; for the second step, 264 mg (1.01 mmol, 1.5 eq.) of **20** and 110 mg (0.577 mmol, 0.89 eq.) of PTSA in 5 mL of dioxane was used. The crude product was purified by flash column chromatography using 3:1 to 3:2 Hex/EtOAc solution to obtain 93.7mg (28%) of **22** as a yellow oil. TLC (aniline **16**) (7:3 Hex/EtOAc) $R_f$ = 0.11; TLC (**22**) (1:1 Hex/EtOAc) $R_f$ = 0.43; LRMS (ESI) *m/z* 518.2 ($M+H^+$). $^1$H NMR $\delta$ 8.42 (d, *J* = 5.3 Hz, 1 H), 8.05 - 7.97 (m, 2 H), 7.66 - 7.60 (m, 2 H), 7.50 - 7.44 (m, 3 H), 7.10 (d, *J* = 5.1 Hz, 1 H), 6.87 - 6.80 (m, 1 H), 5.97 (tdd, *J* = 5.4, 10.6, 17.3 Hz, 2 H), 5.37 - 5.28 (m, 2 H), 5.25 - 5.15 (m, 2 H), 4.59 (d, *J* = 3.6 Hz, 4 H), 4.49 - 4.43 (m, 1 H), 4.36 (s, 1 H), 4.08 (tdd, *J* = 1.3, 5.6, 14.4 Hz, 4 H), 3.98 (br. s., 2 H), 3.84 (dd, *J* = 4.2, 5.2 Hz, 1 H), 3.67 (s, 3 H), 2.40 (t, *J* = 6.8 Hz,

2 H), 1.87 - 1.79 (m, 4 H). $^{13}$C NMR $\delta$ 173.8, 164.6, 160.5, 158.5, 152.0, 138.9, 137.3, 134.9, 134.6, 132.6, 129.8, 128.8, 127.4, 126.3, 126.2, 121.0, 120.0, 117.1, 116.7, 111.6, 107.8, 71.8, 71.4, 71.2, 68.4, 67.8, 66.8, 66.2, 62.5, 51.4, 33.6, 28.7, 21.6.

**Methyl 5-(4-(4-(3-((allyloxy)methyl)phenyl)pyrimidin-2-ylamino)-2-((allyloxy)methyl)phenoxy)hexanoate (23).** Synthesised using the procedure for **21** using 193 mg (0.549 mmol) of **17**, 115 mg (2.05 mmol, 3.7 eq.) of iron and 162 mg (3.02 mmol, 5.5 eq.) of ammonium chloride in 6 mL of methanol and 3 mL of water; for the second step, 244 mg (0.934 mmol, 1.7 eq.) of **20** and 81.2 mg (0.427 mmol, 0.78 eq.) of PTSA in 5 mL of dioxane was used. The crude product was purified by flash column chromatography using 7:3 to 3:2 Hex/EtOAc solution to obtain 122 mg (41%) of **23** as a yellow oil. TLC (aniline **17**) (1:1 Hex/EtOAc) $R_f$ = 0.33; TLC (**23**) (1:1 Hex/EtOAc) $R_f$ = 0.33; LRMS (ESI) *m/z* 545.4 ($M+H^+$). $^1$H NMR $\delta$ 8.43 (d, $J$ = 5.1 Hz, 1 H), 8.06 - 7.97 (m, 2 H), 7.66 - 7.60 (m, 2 H), 7.51 - 7.42 (m, 3 H), 7.11 (d, $J$ = 5.1 Hz, 1 H), 6.87 - 6.81 (m, 1 H), 6.04 - 5.92 (m, 2 H), 5.35 (d, $J$ = 1.4 Hz, 1 H), 5.31 (d, $J$ = 1.3 Hz, 1 H), 5.25 - 5.15 (m, 2 H), 4.60 (d, $J$ = 4.1 Hz, 4 H), 4.18 - 4.04 (m, 6 H), 3.97 (t, $J$ = 6.3 Hz, 2 H), 2.34 (t, $J$ = 7.5 Hz, 2 H), 1.86 - 1.76 (m, 2 H), 1.76 - 1.66 (m, 2 H), 1.57 - 1.49 (m, 2 H), 1.30 - 1.21 (m, 2 H). $^{13}$C NMR $\delta$ 173.5, 164.7, 160.6, 158.5, 152.2, 138.9, 137.3, 135.0, 134.6, 132.6, 129.8, 128.8, 127.4, 126.3, 126.2, 121.0, 120.0,

117.1, 116.7, 111.7, 107.8, 71.8, 71.4, 71.2, 68.1, 66.8, 60.1, 34.2, 29.0, 25.7, 24.7, 14.2.

**Methyl 5-(4-(4-(3-((allyloxy)methyl)phenyl)pyrimidin-2-ylamino)-2-((allyloxy)methyl)phenoxy)heptanoate (24).** Synthesised using the procedure for **21** using 440 mg (1.25 mmol) of **18**, 212 mg (3.79 mmol, 3.0 eq.) of iron and 407 mg (7.61 mmol, 6.1 eq.) of ammonium chloride in 6 mL of methanol and 6 mL of water; for the second step, 496 mg (1.90 mmol, 1.5 eq.) of **20** and 195 mg (1.02 mmol, 0.82 eq.) of PTSA in 6 mL of dioxane was used. The crude product was purified by flash column chromatography using 3:1 to 7:3 to 3:2 to 1:1 Hex/EtOAc solution to obtain 390 mg (57%) of **24** as a dark yellow oil and 97.9 mg (24%) of the aniline **18** as a yellow oil. TLC (aniline **18**) (1:1 Hex/EtOAc) $R_f$ = 0.27; TLC (**23**) (1:1 Hex/EtOAc) $R_f$ = 0.46; LRMS (ESI) *m/z* 546.3 ($M+H^+$). $^1$H NMR $\delta$ 8.41 (d, $J$ = 5.1 Hz, 1 H), 8.02 (s, 1 H), 7.99 (td, $J$ = 2.0, 6.4 Hz, 1 H), 7.76 (br. s., 1 H), 7.66 - 7.57 (m, 2 H), 7.47 - 7.41 (m, 2 H), 7.08 (d, $J$ = 5.3 Hz, 1 H), 6.82 (d, $J$ = 8.5 Hz, 1 H), 6.02 - 5.89 (m, 2 H), 5.31 (tdd, $J$ = 1.7, 3.7, 17.2 Hz, 2 H), 5.22 - 5.13 (m, 2 H), 4.61 - 4.55 (m, 4 H), 4.13 - 4.07 (m, 2 H), 4.07 - 4.02 (m, 2 H), 3.93 (t, $J$ = 6.3 Hz, 2 H), 3.64 (s, 3 H), 2.35 - 2.27 (m, 2 H), 1.81 - 1.72 (m, 2 H), 1.65 (td, $J$ = 7.5, 15.0 Hz, 2 H), 1.52 - 1.42 (m, 2 H), 1.42 - 1.33 (m, 2 H). $^{13}$C NMR $\delta$ 173.9, 170.8, 164.5, 160.5, 158.4, 152.0, 138.8, 137.2, 134.9, 134.5, 132.6, 129.7, 128.7, 127.3, 126.2, 126.1, 120.9, 119.9, 117.0, 116.5,

111.5, 107.6, 71.7, 71.3, 71.2, 71.1, 68.1, 66.7, 60.1, 51.2, 33.8, 29.0, 28.7, 25.6, 24.7, 20.8, 14.0.

**Methyl 5-(4-(4-(3-((allyloxy)methyl)phenyl)pyrimidin-2-ylamino)-2-((allyloxy)methyl)phenoxy)octanoate (25).** Synthesised using the procedure for **21** using 328 mg (0.896 mmol) of **19**, 188 mg (3.37 mmol, 3.8 eq.) of iron and 407 mg (5.60 mmol, 6.3 eq.) of ammonium chloride in 5 mL of methanol and 5 mL of water; for the second step, 351 mg (1.35 mmol, 1.5 eq.) of **20** and 136 mg (0.715 mmol, 0.80 eq.) of PTSA in 5 mL of dioxane was used. The crude product was purified by flash column chromatography using 3:1 to 7:3 to 65:35 Hex/EtOAc solution to obtain 311 mg (62%) of **25** as a yellow solid. TLC (aniline **19**) (1:1 Hex/EtOAc) $R_f$ =; TLC (**25**) (1:1 Hex/EtOAc) $R_f$ = 0.45; LRMS (ESI) *m/z* 560.3 ($M+H^+$). $^1$H NMR $\delta$ 8.43 (d, $J$ = 5.3 Hz, 1 H), 8.04 (s, 1 H), 8.03 - 7.98 (m, 1 H), 7.72 (br. s., 1 H), 7.66 - 7.60 (m, 2 H), 7.49 - 7.41 (m, 2 H), 7.09 (d, $J$ = 5.1 Hz, 1 H), 6.84 (d, $J$ = 8.8 Hz, 1 H), 5.97 (dtdd, $J$ = 2.6, 5.5, 10.6, 17.2 Hz, 2 H), 5.33 (td, $J$ = 1.6, 17.3 Hz, 2 H), 5.20 (ddd, $J$ = 1.6, 10.5, 13.6 Hz, 2 H), 4.59 (d, $J$ = 2.0 Hz, 4 H), 4.11 (td, $J$ = 1.3, 5.5 Hz, 2 H), 4.06 (td, $J$ = 1.3, 5.6 Hz, 2 H), 3.95 (t, $J$ = 6.4 Hz, 2 H), 3.66 (s, 3 H), 2.32 (t, $J$ = 7.5 Hz, 2 H), 1.82 - 1.73 (m, 2 H), 1.69 - 1.61 (m, 2 H), 1.52 - 1.43 (m, 2 H), 1.43 - 1.31 (m, 4 H). $^{13}$C NMR $\delta$ 174.0, 164.5, 160.5, 158.4, 152.1, 138.8, 137.3, 134.9, 134.5, 132.5, 129.7, 128.7, 127.3, 126.3,

126.2, 120.9, 119.9, 117.0, 116.6, 111.6, 107.7, 71.8, 71.3, 71.1, 68.3, 66.7, 51.3, 33.9, 29.2, 28.9, 28.9, 25.8, 24.7.

**11-(4-(Butanoate)oxy)-14,19-dioxa-5,7,26-triaza-tetracyclo[19.3.1.1(2,6).1(8,12)]heptacosa-1(25),2(26),3,5,8,10,12(27),16,21,23-decaene methyl ester (26).** Following the literature procedure (*J. Med. Chem.* **2011**, *54*, 4638), 29.4 mg (0.0631 mmol) of **21** and 6.7 mg (0.00789 mmol, 0.13 eq.) of the 2nd generation Grubbs catalyst (see Supporting Information for structure) was dissolved in 14 mL of degassed DCM (5 mM concentration) to obtain an orange solution. 1 mL of 4 M hydrochloric acid was added changing it to a yellow solution. The reaction mixture was refluxed for 3 h. After cooling to rt, the reaction was quenched with saturated sodium bicarbonate solution and extracted with DCM 3 times. The combined organic layer was washed with brine solution and dried with anhydrous sodium sulfate. The organic layer was concentrated and purified by column chromatography using 3:2 Hex/EtOAc to obtain 17.1 mg (62%) of **26** in an 87:13 *E/Z* ratio as a yellow solid. LRMS (ESI) *m/z* 476.2 ($M+H^+$).

(*E* isomer only) $^1$H NMR $\delta$ 8.64 (d, $J$ = 2.4 Hz, 1 H), 8.43 - 8.37 (m, 1 H), 8.29 (s, 1 H), 7.80 (d, $J$ = 7.8 Hz, 1 H), 7.71 - 7.67 (m, 1 H), 7.59 (d, $J$ = 7.7 Hz, 1 H), 7.48 (t, $J$ = 7.7 Hz, 1 H), 7.14 (d, $J$ = 5.1 Hz, 1 H), 6.88 - 6.79 (m, 2 H), 5.88 - 5.82 (m, 2 H), 4.64 (s, 2 H), 4.62 (s, 2 H), 4.16 (d, $J$ = 4.8 Hz, 2 H), 4.08 - 4.00 (m, 4 H),

3.70 (s, 3 H), 2.57 (t, $J$ = 7.3 Hz, 2 H), 2.18 - 2.10 (m, 2 H). $^{13}$C NMR $\delta$ 173.7, 164.4, 160.1, 158.3, 152.0, 138.6, 137.1, 133.2, 132.0, 131.0, 129.8, 128.9, 127.7, 127.1, 126.3, 121.4, 119.3, 112.4, 107.6, 70.1, 69.3, 67.6, 67.5, 65.7, 51.6, 30.6, 24.7.

**11-(5-(Pentanoate)oxy)-14,19-dioxa-5,7,26-triaza-tetracyclo[19.3.1.1(2,6).1(8,12)]heptacosa-1(25),2(26),3,5,8,10,12(27),16,21,23-decaene methyl ester (27).** Synthesised using the procedure for **26** using 156.5 mg (0.302 mmol) of **22** and 25.9 mg (0.0305 mmol, 0.10 eq.) of Grubbs II catalyst in 30 mL of DCM and 3 mL of 4 M HCl. The crude product was purified by flash column chromatography using 1:1 to 2:3 Hex/EtOAc solution to obtain 104 mg (70%) (5:1 *E/Z* isomers) of **27** as a yellowish green solid. TLC (1:1 Hex/EtOAc) $R_f$ = 0.23. LRMS (ESI) *m/z* 490.2 ($M+H^+$). (*E* isomer only) $^1$H NMR $\delta$ 8.65 (d, $J$ = 2.4 Hz, 1 H), 8.39 (d, $J$ = 5.3 Hz, 1 H), 8.29 (s, 1 H), 7.95 (s, 1 H), 7.78 (d, $J$ = 7.8 Hz, 1 H), 7.58 (d, $J$ = 7.7 Hz, 1 H), 7.49 - 7.45 (m, 1 H), 7.12 (d, $J$ = 5.3 Hz, 1 H), 6.87 - 6.77 (m, 2 H), 5.87 - 5.82 (m, 2 H), 4.63 (s, 4 H), 4.16 (d, $J$ = 4.4 Hz, 2 H), 4.05 (d, $J$ = 4.1 Hz, 2 H), 3.98 (m., 2 H), 3.69 - 3.65 (s, 3 H), 2.42 (t, $J$ = 7.0 Hz, 2 H), 1.88 - 1.81 (m, 4 H). $^{13}$C NMR $\delta$ 173.8, 164.1, 160.2, 158.5, 152.0, 138.5, 137.1, 133.2, 132.0, 130.8, 129.7, 128.8, 127.6, 126.9, 126.1, 121.5, 119.2, 112.2, 107.5, 70.0, 69.2, 68.1, 67.5, 65.6, 51.4, 33.6, 28.6, 21.6.

**11-(6-(Hexanoate)oxy)-14,19-dioxa-5,7,26-triaza-tetracyclo[19.3.1.1(2,6).1(8,12)]heptacosa-1(25),2(26),3,5,8,10,12(27),16,21,23-decaene methyl ester (28).** Synthesised using the procedure for **26** using 151 mg (0.277 mmol) of **23** and 26.4 mg (0.0311 mmol, 0.11 eq.) of Grubbs II catalyst in 30 mL of DCM and 3 mL of 4 M HCl. The crude product was purified by flash column chromatography using 1:1 to 2:3 Hex/EtOAc solution to obtain 113 mg (79%) (5:1 *E/Z* isomers) of **28** as a green amorphous solid. TLC (1:1 Hex/EtOAc) $R_f$ = 0.20; LRMS (ESI) *m/z* 518.3 ($M+H^+$). (*E* isomer only) $^1$H NMR $\delta$ 8.64 (d, $J$ = 2.0 Hz, 1 H), 8.40 (d, $J$ = 5.1 Hz, 1 H), 8.29 (s, 1 H), 7.80 (d, $J$ = 7.7 Hz, 1 H), 7.67 (s, 1 H), 7.58 (d, $J$ = 7.7 Hz, 1 H), 7.51 - 7.41 (m, 1 H), 7.13 (d, $J$ = 5.1 Hz, 1 H), 6.88 - 6.78 (m, 2 H), 5.88 - 5.81 (m, 2 H), 4.68 - 4.60 (m, 4 H), 4.19 - 4.09 (m, 4 H), 4.06 (d, $J$ = 4.0 Hz, 2 H), 3.98 (t, $J$ = 6.3 Hz, 2 H), 2.35 (t, $J$ = 7.5 Hz, 3 H), 1.88 - 1.78 (m, 2 H), 1.72 (quin, $J$ = 7.6 Hz, 2 H), 1.59 - 1.47 (m, 2 H), 1.31 - 1.21 (m, 3 H). $^{13}$C NMR $\delta$ 173.6, 164.2, 160.2, 158.6, 152.2, 138.5, 137.1, 133.1, 132.1, 130.8, 129.7, 128.8, 127.7, 127.0, 126.2, 121.4, 119.3, 112.4, 107.6, 70.1, 69.2, 68.5, 67.5, 65.7, 60.2, 34.2, 29.0, 25.7, 24.7, 14.2.

**11-(7-(Heptanoate)oxy)-14,19-dioxa-5,7,26-triaza-tetracyclo[19.3.1.1(2,6).1(8,12)]heptacosa-1(25),2(26),3,5,8,10,12(27),16,21,23-decaene methyl ester (29).** Synthesised using the procedure for **26** using 390 mg (0.715 mmol) of **24** and 31.3 mg (0.0369 mmol, 0.05 eq.) of Grubbs II catalyst in

40 mL of DCM and 4 mL of 4M HCl. The crude product was purified by flash column chromatography using 65:35 to 3:2 to 1:1 Hex/EtOAc solution to obtain 266 mg (72%) (10:3 *E/Z* isomers) of **29** as a green amorphous solid. TLC (1:1 Hex/EtOAc) $R_f$ = 0.24; LRMS (ESI) *m/z* 518.2 ($M+H^+$). (*E* isomer only) $^1$H NMR $\delta$ 8.63 (d, *J* = 2.3 Hz, 1 H), 8.42 - 8.37 (m, 1 H), 8.29 (s, 1 H), 7.79 (d, *J* = 7.8 Hz, 1 H), 7.73 (s, 1 H), 7.58 (d, *J* = 7.7 Hz, 1 H), 7.47 (t, *J* = 7.7 Hz, 1 H), 7.13 (d, *J* = 5.1 Hz, 1 H), 6.89 - 6.78 (m, 2 H), 5.84 (q, *J* = 4.7 Hz, 2 H), 4.66 - 4.60 (m, 4 H), 4.16 (d, *J* = 4.8 Hz, 2 H), 4.05 (d, *J* = 4.1 Hz, 2 H), 3.97 (t, *J* = 6.4 Hz, 2 H), 3.66 (s, 3 H), 2.36 - 2.29 (m, 2 H), 1.85 - 1.76 (m, 2 H), 1.72 - 1.63 (m, 2 H), 1.54 - 1.45 (m, 2 H), 1.45 - 1.36 (m, 2 H). $^{13}$C NMR $\delta$ 174.1, 164.1, 160.3, 158.6, 152.2, 138.5, 137.1, 133.0, 132.1, 130.8, 129.7, 128.8, 127.6, 127.0, 126.2, 121.4, 119.3, 112.4, 107.5, 70.1, 69.2, 68.6, 67.5, 65.6, 60.3, 51.4, 33.9, 29.1, 28.8, 25.7, 24.8, 14.1.

**11-(8-(Octanoate)oxy)-14,19-dioxa-5,7,26-triaza-tetracyclo[19.3.1.1(2,6).1(8,12)]heptacosa-1(25),2(26),3,5,8,10,12(27),16,21,23-decaene methyl ester (30).** Synthesised using the procedure for **26** using 311 mg (0.555 mmol) of **25** and 48.3 mg (0.0569 mmol, 0.10 eq.) of Grubbs II catalyst in 55 mL of DCM and 5.5 mL of 4M HCl. The crude product was purified using flash column chromatography using 1:1 to 45:55 Hex/EtOAc solution to obtain 246 mg (83%) (4:1 *E/Z* isomers) of **30** as a brown amorphous solid. TLC (1:1 Hex/EtOAc)

$R_f$ = 0.29; LRMS (ESI) *m/z* 532.3 ($M+H^+$). (*E* isomer only) $^1$H NMR $\delta$ 8.66 - 8.62 (m, 1 H), 8.40 (d, *J* = 5.1 Hz, 1 H), 8.29 (s, 1 H), 7.83 - 7.71 (m, 2 H), 7.58 (d, *J* = 7.5 Hz, 1 H), 7.47 (t, *J* = 7.7 Hz, 1 H), 7.13 (d, *J* = 5.1 Hz, 1 H), 6.88 - 6.78 (m, 2 H), 5.91 - 5.81 (m, 2 H), 4.66 - 4.60 (m, 3 H), 4.16 (d, *J* = 4.5 Hz, 2 H), 4.05 (d, *J* = 4.0 Hz, 2 H), 3.96 (t, *J* = 6.4 Hz, 2 H), 3.66 (s, 3 H), 2.32 (t, *J* = 7.5 Hz, 2 H), 1.85 - 1.75 (m, 2 H), 1.69 - 1.60 (m, 2 H), 1.54 - 1.44 (m, 2 H), 1.44 - 1.31 (m, 4 H). $^{13}$C NMR $\delta$ 174.1, 164.1, 160.2, 158.6, 152.3, 138.5, 137.1, 133.0, 132.1, 130.8, 129.7, 128.8, 127.6, 127.0, 126.2, 121.4, 119.2, 112.3, 107.5, 70.0, 69.2, 68.7, 67.5, 65.6, 51.3, 34.0, 29.2, 29.0, 28.9, 25.8, 24.8.

**11-(4-(4-Aminobenzoic acid)ethoxy)-14,19-dioxa-5,7,26-triaza-tetracyclo[19.3.1.1(2,6).1(8,12)]heptacosa-1(25),2(26),3,5,8,10,12(27),16,21,23-decaene hydrochloride (31).** 117 mg (0.179 mmol) of **4** was dissolved in 4 mL of THF and 0.811 g (5.69 mmol, 32 eq.) of 90% potassium trimethylsilanoate was added. The resultant orange suspension was stirred at rt for 2 h, after which 1.5 mL of concentrated hydrochloric acid was added to the reaction and a yellow precipitate was formed. The reaction was stirred for a further 24 h at rt. 5 mL of water was added to the mixture and stirred at rt for 1 h. The solid was filtered and washed successively 3 times each with water, ethyl acetate and acetone. The resulting solid was dried under vacuum overnight to obtain 69.9 mg (56%) of **31** as a yellow solid. LRMS (ESI) *m/z* 539.2 ($M+H^+$). HPLC purity >99%. $^1$H NMR

(DMSO-$d_6$) □□ 9.54 (s, 1 H), 8.51 (d, *J* = 5.0 Hz, 1 H), 8.47 (br. s., 1 H), 8.15 (s, 1 H), 8.01 (d, *J* = 4.0 Hz, 1 H), 7.70 (d, *J* = 8.4 Hz, 2 H), 7.55 (br. s., 2 H), 7.39 (d, *J* = 5.0 Hz, 1 H), 7.10 (d, *J* = 6.3 Hz, 1 H), 7.00 - 6.95 (m, 1 H), 6.68 (d, *J* = 8.5 Hz, 2 H), 5.79 (d, *J* = 14.9 Hz, 1 H), 5.66 (d, *J* = 15.2 Hz, 1 H), 4.53 (s, 2 H), 4.43 (s, 3 H), 4.11 (br. s., 3 H), 3.99 (br. s., 4 H), 3.52 (br. s., 2 H). $^{13}$C NMR (DMSO-$d_6$) □ 167.4, 163.0, 160.0, 159.2, 152.6, 151.1, 138.5, 136.7, 133.9, 131.1, 130.8, 129.8, 129.1, 126.6, 126.5, 120.6, 119.6, 117.1, 113.1, 111.0, 107.4, 69.1, 68.9, 67.9, 67.0, 65.0, 41.8.

**11-(4-(3-Aminobenzoic acid)ethoxy)-14,19-dioxa-5,7,26-triaza-tetracyclo[19.3.1.1(2,6).1(8,12)]heptacosa-1(25),2(26),3,5,8,10,12(27),16,21,23-decaene hydrochloride (32).** Synthesised using the procedure for **31** using 58.2 mg (0.0892 mmol) of ester **5**, 416 mg of potassium trimethylsilanoate (2.92 mmol, 33 eq.). 37.7 mg (72%) of **32** was isolated as a light yellow solid. LRMS (ESI) *m/z* 539.2 ($M+H^+$). HPLC purity 95.6%. $^1$H NMR (DMSO-$d_6$) □ 9.55 (s, 1 H), 8.51 (d, *J* = 5.1 Hz, 1 H), 8.46 (d, *J* = 2.5 Hz, 1 H), 8.15 (s, 1 H), 8.02 (dd, *J* = 1.8, 5.9 Hz, 1 H), 7.58 - 7.53 (m, 2 H), 7.39 (d, *J* = 5.3 Hz, 1 H), 7.27 (s, 1 H), 7.21 (t, *J* = 7.7 Hz, 1 H), 7.16 (d, *J* = 7.5 Hz, 1 H), 7.10 (dd, *J* = 2.6, 8.8 Hz, 1 H), 6.98 (d, *J* = 8.8 Hz, 1 H), 6.93 - 6.88 (m, 1 H), 5.83 - 5.75 (m, 1 H), 5.71 - 5.61 (m, 1 H), 4.53 (s, 2 H), 4.44 (s, 2 H), 4.11 (t, *J* = 5.3 Hz, 2 H), 3.99 (d, *J* = 5.0 Hz, 4 H), 3.48 (t, *J* = 5.3 Hz, 2 H). $^{13}$C NMR (DMSO-$d_6$) □ 167.9, 163.0, 160.0, 159.1,

151.1, 148.8, 138.6, 136.7, 133.8, 131.4, 130.8, 129.8, 129.1, 129.0, 126.6, 126.5, 126.5, 120.6, 119.6, 116.9, 116.4, 113.1, 112.8, 107.4, 69.1, 68.9, 67.9, 67.0, 64.9, 54.9, 42.3.

**11-(2-(4-Hydroxybenzoate))-14,19-dioxa-5,7,26-triaza-tetracyclo[19.3.1.1(2,6).1(8,12)]heptacosa-1(25),2(26),3,5,8,10,12(27),16,21,23-decaene hydrochloride (33).** Synthesised using the procedure for **31** using 133 mg (0.241 mmol) of **6** and 1.06 g of potassium trimethylsilanoate (7.43 mmol, 31 eq.) in 5 mL of THF and 1.5 mL of conc. HCl. 66.8 mg (47%) of **33** was isolated as a light yellow solid. LRMS (ESI) *m/z* 540.2 ($M+H^+$). HPLC purity 95.7%. $^1$H NMR (DMSO-$d_6$) □ 9.67 (s, 1 H), 8.53 (d, *J* = 5.3 Hz, 1 H), 8.45 (d, *J* = 2.6 Hz, 1 H), 8.14 (s, 1 H), 8.03 (d, *J* = 5.8 Hz, 1 H), 7.91 (d, *J* = 8.8 Hz, 2 H), 7.59 - 7.54 (m, 2 H), 7.43 (d, *J* = 5.4 Hz, 1 H), 7.15 - 7.08 (m, 3 H), 7.07 - 7.02 (m, 1 H), 5.83 - 5.74 (m, 1 H), 5.69 - 5.60 (m, 1 H), 4.52 (s, 2 H), 4.44 - 4.39 (m, 4 H), 4.36 - 4.31 (m, 2 H), 3.98 (d, *J* = 4.9 Hz, 4 H). $^{13}$C NMR (DMSO-$d_6$) □ 166.9, 163.4, 162.1, 159.5, 158.5, 151.0, 138.6, 136.5, 133.8, 131.3, 131.0, 130.7, 129.8, 129.1, 126.9, 126.6, 126.6, 123.1, 120.7, 119.8, 114.4, 113.7, 107.4, 69.2, 68.9, 67.8, 67.0, 66.7, 64.8.

**11-(2-(Isonipecotate)-ethoxy)-14,19-dioxa-5,7,26-triaza-tetracyclo[19.3.1.1(2,6).1(8,12)]heptacosa-1(25),2(26),3,5,8,10,12(27),16,21,23-decaene hydrochloride (34).** Synthesised using the procedure for **31** using 182 mg (0.335 mmol) of **8** and 1.30 g of potassium trimethylsilanoate (9.12 mmol, 27 eq.).

157 mg (83%) of **31** was isolated as a light yellow solid. LRMS (ESI) *m/z* 531.2 ($M+H^+$). $^1$H NMR (DMSO-$d_6$) □ 11.21 (br. s., 1 H), 9.89 (s, 1 H), 8.56 - 8.49 (m, 2 H), 8.14 (s, 1 H), 8.01 (d, *J* = 6.9 Hz, 1 H), 7.60 - 7.49 (m, 2 H), 7.43 (d, *J* = 5.5 Hz, 1 H), 7.16 (dd, *J* = 2.3, 8.7 Hz, 1 H), 7.00 (dd, *J* = 3.9, 8.7 Hz, 1 H), 5.88 - 5.75 (m, 1 H), 5.71 - 5.63 (m, 1 H), 4.52 (s, 2 H), 4.47 (s, 2 H), 4.40 (br. s., 3 H), 4.03 (d, *J* = 5.1 Hz, 4 H), 3.97 (d, *J* = 5.0 Hz, 2 H), 3.65 - 3.52 (m, 2 H), 3.47 - 3.38 (m, 2 H), 3.16 - 3.01 (m, 2 H), 2.07 – 1.92 (m, 4 H). $^{13}$C NMR (DMSO-$d_6$) □ 174.6, 164.2, 158.8, 157.6, 150.7, 138.7, 136.4, 133.8, 131.2, 130.9, 129.9, 129.2, 126.9, 126.8, 126.3, 120.9, 119.8, 112.9, 107.5, 69.0, 68.9, 67.2, 67.0, 65.6, 63.2, 55.0, 54.9, 51.6, 37.8, 25.2, 25.1.

**11-(2-(7-(4-Aminophenylcarbamoyl)hexanoic acid))-ethoxy)-14,19-dioxa-5,7,26-triaza-tetracyclo[19.3.1.1(2,6).1(8,12)]heptacosa-1(25),2(26),3,5,8,10,12(27),16,21,23-decaene (35).** Synthesised using the procedure for **31** using 82.0 mg (0.105 mmol) of **11** and 461 mg (3.23 mmol, 31 eq.) of potassium trimethylsilanoate in 5 mL of THF and 1.5 mL of concentrated HCl. 52.2 mg (76%) of **35** was obtained as a light yellow solid. LRMS (ESI) *m/z* 652.3 ($M+H^+$). HPLC purity >99%. $^1$H NMR (DMSO-$d_6$) □ 9.98 (br. s., 1H), 9.62 (s, 1H), 8.52 (d, *J* = 5.14 Hz, 1H), 8.46 (d, *J* = 2.76 Hz, 1H), 8.14 (s, 1H), 7.99 - 8.05 (m, 1H), 7.62 (d, *J* = 8.66 Hz, 2H), 7.52 - 7.59 (m, 2H), 7.41 (d, *J* = 5.40 Hz, 1H), 7.25 (d, *J* = 6.65 Hz, 2H), 7.10 (dd, *J* = 2.64, 8.78 Hz, 1H), 6.96

(d, *J* = 8.91 Hz, 1H), 5.81 (td, *J* = 5.47, 15.65 Hz, 1H), 5.67 (td, *J* = 6.04, 15.65 Hz, 1H), 4.54 (s, 2H), 4.43 (s, 2H), 4.18 (t, *J* = 4.89 Hz, 2H), 4.01 (dd, *J* = 5.58, 15.62 Hz, 4H), 2.28 (t, *J* = 7.40 Hz, 2H), 2.19 (t, *J* = 7.34 Hz, 2H), 1.46 - 1.61 (m, 4H), 1.26 - 1.34 (m, 2H). $^{13}$C NMR (DMSO-$d_6$) □ 174.4, 163.3, 159.7, 158.8, 150.6, 138.6, 136.6, 134.1, 131.0, 129.8, 129.2, 126.7, 126.6, 126.6, 120.7, 120.1, 119.7, 113.1, 107.5, 69.2, 68.8, 67.0, 64.8, 36.2, 33.5, 28.2, 24.8, 24.3.

**11-(2-(7-(4-Aminophenylcarbamoyl)heptanoic acid))-ethoxy)-14,19-dioxa-5,7,26-triaza-tetracyclo[19.3.1.1(2,6).1(8,12)]heptacosa-1(25),2(26),3,5,8,10,12(27),16,21,23-decaene (36).** Synthesised using the procedure for **31** using 41.6 mg (0.0533 mmol) of **12** and 231 mg (1.62 mmol, 30 eq.) of potassium trimethylsilanoate in 3 mL of THF and 1 mL of concentrated HCl. 26.7 mg (75%) of **36** was obtained as a light yellow solid. LRMS (ESI) *m/z* 666.3 ($M+H^+$). HPLC purity 91%. $^1$H NMR (DMSO-$d_6$) $\delta$ 12.25 (br. s., 2 H), 9.53 (s, 1 H), 9.47 (s, 1 H), 8.54 - 8.47 (m, 2 H), 8.16 (s, 1 H), 8.04 - 7.98 (m, 1 H), 7.59 - 7.52 (m, 2 H), 7.41 - 7.35 (m, 1 H), 7.32 (d, *J* = 8.8 Hz, 1 H), 7.16 - 7.07 (m, 1 H), 6.96 (d, *J* = 8.9 Hz, 1 H), 6.60 (d, *J* = 8.7 Hz, 2 H), 5.91 - 5.78 (m, 1 H), 5.73 - 5.63 (m, 1 H), 4.54 (s, 2 H), 4.50 - 4.43 (m, 2 H), 4.12 - 3.94 (m, 6 H), 3.46 - 3.38 (m, 2 H), 2.76 (d, *J* = 15.4 Hz, 2 H), 2.66 (d, *J* = 15.4 Hz, 2 H), 2.20 (q, *J* = 7.6 Hz, 2 H), 1.62 - 1.43 (m, 4 H), 1.28 (br. s., 4 H). $^{13}$C NMR (DMSO-$d_6$) □ 174.5, 174.4, 171.2, 170.2, 162.9, 160.2, 159.4, 151.2, 138.6, 136.8, 133.9, 131.0, 130.8, 129.8,

129.1, 126.6, 126.5, 126.5, 120.8, 120.5, 119.6, 113.2, 112.2, 107.4, 72.4, 69.1, 68.9, 68.0, 67.0, 65.1, 42.7, 42.6, 36.2, 33.6, 28.4, 28.3, 25.1, 24.4.

**11-(4-(Butanoate)oxy)-14,19-dioxa-5,7,26-triaza-tetracyclo[19.3.1.1(2,6).1(8,12)]heptacosa-1(25),2(26),3,5,8,10,12(27),16,21,23-decaene hydrochloride (37).** Synthesised using the procedure for **31** using 58.5 mg (0.123 mmol) of **26** and 527 mg (3.70 mmol, 30 eq.) of potassium trimethylsilanoate in 5 mL of THF and 1.5 mL of concentrated HCl. 50.1 mg (80%) of **37** was obtained as an orange solid. LRMS (ESI) *m/z* 462.3 ($M+H^+$). HPLC purity >99% (ratio of 77.9%. acid to 22.1% ester) $^1$H NMR (DMSO-$d_6$) □ 10.01 (br. s., 1 H), 8.56 (d, *J* = 5.3 Hz, 1 H), 8.41 - 8.36 (m, 1 H), 8.18 - 8.10 (m, 1 H), 8.05 (d, *J* = 6.7 Hz, 1 H), 7.60 - 7.54 (m, 2 H), 7.53 - 7.44 (m, 1 H), 7.11 (dd, *J* = 2.3, 8.7 Hz, 1 H), 6.95 (d, *J* = 8.8 Hz, 1 H), 5.87 - 5.75 (m, 1 H), 5.67 (td, *J* = 5.8, 15.8 Hz, 1 H), 4.52 (s, 2 H), 4.51 - 4.44 (m, 2 H), 4.11 - 4.03 (m, 2 H), 4.02 - 3.93 (m, 4 H), 1.97 (quin, *J* = 6.4 Hz, 2 H). $^{13}$C NMR (DMSO-$d_6$) □ 173.1, 164.9, 158.0, 156.3, 151.6, 138.7, 136.1, 132.5, 131.5, 130.8, 129.8, 129.2, 127.0, 126.8, 126.5, 121.1, 120.1, 112.6, 107.3, 69.1, 68.8, 67.2, 67.1, 64.9, 51.3, 29.9, 24.3.

**11-(5-(Pentanoate)oxy)-14,19-dioxa-5,7,26-triaza-tetracyclo[19.3.1.1(2,6).1(8,12)]heptacosa-1(25),2(26),3,5,8,10,12(27),16,21,23-decaene hydrochloride (38).** Synthesised using the procedure for **31** using 330 mg (0.674 mmol) of **27** and 2.90 g (20.3 mmol, 30 eq.) of potassium trimethylsilanoate

in 10 mL of THF and 2 mL of concentrated HCl. 288 mg (83%) of **38** was obtained as a yellow soild. LRMS (ESI) *m/z* 476.2 ($M+H^+$). HPLC purity >99%. $^1$H NMR (DMSO-$d_6$) $\delta$ 9.60 (s, 1 H), 8.52 (d, $J$ = 5.3 Hz, 1 H), 8.48 (d, $J$ = 2.6 Hz, 1 H), 8.17 (s, 1 H), 8.03 (td, $J$ = 2.2, 6.2 Hz, 1 H), 7.58 - 7.54 (m, 2 H), 7.41 (d, $J$ = 5.4 Hz, 1 H), 7.11 (dd, $J$ = 2.7, 8.7 Hz, 1 H), 6.98 - 6.93 (m, 1 H), 5.88 - 5.80 (m, 1 H), 5.74 - 5.65 (m, 1 H), 4.55 (s, 2 H), 4.51 - 4.47 (m, 2 H), 4.06 (d, $J$ = 6.0 Hz, 3 H), 3.98 (dd, $J$ = 5.7, 13.7 Hz, 7 H), 2.31 (t, $J$ = 7.1 Hz, 2 H), 1.80 - 1.65 (m, 5 H). $^{13}$C NMR (DMSO-$d_6$) $\delta$ 174.4, 163.3, 159.7, 158.7, 151.5, 138.6, 136.6, 133.4, 131.0, 130.9, 129.8, 129.1, 126.6, 126.3, 120.7, 119.7, 112.7, 107.3, 69.1, 68.9, 68.0, 67.1, 65.1, 33.3, 28.2, 21.3.

**11-(6-(Hexanoate)oxy)-14,19-dioxa-5,7,26-triaza-tetracyclo[19.3.1.1(2,6).1(8,12)]heptacosa-1(25),2(26),3,5,8,10,12(27),16,21,23-decaene hydrochloride (39).** Synthesised using the procedure for **31** using 113 mg (0.218 mmol) of **28** and 951 mg (6.67 mmol, 31 eq.) of potassium trimethylsilanoate in 5 mL of THF and 1.5 mL of concentrated HCl. 51.4 mg (44%) of **39** was obtained as a yellow solid. LRMS (ESI) *m/z* 490.2 ($M+H^+$). HPLC purity 91.7%. $^1$H NMR (DMSO-$d_6$) $\delta$ 9.81 (s, 1 H), 8.57 - 8.53 (m, 1 H), 8.43 (d, $J$ = 2.6 Hz, 1 H), 8.16 (s, 1 H), 8.04 (td, $J$ = 1.9, 6.8 Hz, 1 H), 7.61 - 7.54 (m, 2 H), 7.45 (d, $J$ = 5.5 Hz, 1 H), 7.11 (dd, $J$ = 2.8, 8.8 Hz, 1 H), 6.99 - 6.92 (m, 1 H), 5.88 - 5.79 (m, 1 H), 5.74 - 5.64 (m, 1 H), 4.54 (s, 2 H), 4.52 - 4.47 (m, 2 H),

4.06 (d, $J$ = 5.8 Hz, 2 H), 4.02 - 3.93 (m, 4 H), 2.25 (t, $J$ = 7.3 Hz, 2 H), 1.72 (quin, $J$ = 6.9 Hz, 2 H), 1.58 (td, $J$ = 7.3, 15.0 Hz, 2 H), 1.51 - 1.40 (m, 2 H). $^{13}$C NMR (DMSO-$d_6$) $\delta$ 174.4, 164.1, 158.9, 157.5, 151.7, 138.7, 136.4, 132.9, 131.2, 130.9, 129.8, 129.2, 126.8, 126.7, 126.4, 120.9, 119.9, 112.7, 107.3, 69.1, 68.8, 68.2, 67.1, 65.1, 33.7, 28.5, 25.2, 24.2.

**11-(7-(Heptanoate)oxy)-14,19-dioxa-5,7,26-triaza-tetracyclo[19.3.1.1(2,6).1(8,12)]heptacosa-1(25),2(26),3,5,8,10,12(27),16,21,23-decaene hydrochloride (40).** Synthesised using the procedure for **31** using 266 mg (0.514 mmol) of **29** and 2.24g (15.7 mmol, 30 eq.) of potassium trimethylsilanoate in 10 mL of THF and 2 mL of concentrated HCl. 203 mg (72%) of **40** was obtained as a light yellow solid. LRMS (ESI) *m/z* 504.2 ($M+H^+$). HPLC purity >99%. $^1$H NMR (DMSO-$d_6$) $\delta$ 9.85 (br. s., 1 H), 8.55 (d, $J$ = 5.4 Hz, 1 H), 8.41 (d, $J$ = 2.4 Hz, 1 H), 8.23 - 8.12 (m, 2 H), 8.05 (d, $J$ = 6.8 Hz, 1 H), 7.62 - 7.55 (m, 2 H), 7.55 - 7.50 (m, 1 H), 7.49 - 7.42 (m, 1 H), 7.16 - 7.05 (m, 1 H), 6.96 (d, $J$ = 8.8 Hz, 1 H), 5.89 - 5.78 (m, 1 H), 5.74 - 5.63 (m, 1 H), 4.58 - 4.44 (m, 4 H), 4.12 - 4.02 (m, 2 H), 4.02 - 3.91 (m, 4 H), 2.22 (t, $J$ = 7.3 Hz, 2 H), 1.78 - 1.65 (m, 2 H), 1.53 (quin, $J$ = 7.3 Hz, 2 H), 1.44 (td, $J$ = 7.2, 14.4 Hz, 2 H), 1.38 - 1.28 (m, 2 H). $^{13}$C NMR (DMSO-$d_6$) $\delta$ 174.4, 164.4, 158.5, 157.1, 151.8, 138.7, 136.3, 132.7, 131.3, 130.8, 130.0, 129.8, 129.2, 128.7, 126.9, 126.8, 126.4, 121.0, 120.1, 112.6, 107.3, 69.2, 68.8, 68.2, 67.1, 65.0, 33.6, 28.6, 28.2, 25.3, 24.4.

**11-(8-(Octanoate)oxy)-14,19-dioxa-5,7,26-triaza-tetracyclo[19.3.1.1(2,6).1(8,12)]heptacosa-1(25),2(26),3,5,8,10,12(27),16,21,23-decaene hydrochloride (41).** Synthesised using the procedure for **31** using 246 mg (0.463 mmol) of **30** and 2.00 g (14.0 mmol, 30 eq.) of potassium trimethylsilanoate in 10 mL of THF and 2 mL of concentrated HCl. 136 mg (51%) of **41** was obtained as a light yellow solid. LRMS (ESI) *m/z* 518.2 ($M+H^+$). HPLC purity >99%. $^1$H NMR (DMSO-d6) $\delta$ 9.93 (br. s., 1 H), 8.56 (d, $J$ = 5.4 Hz, 1 H), 8.39 (d, $J$ = 2.5 Hz, 1 H), 8.14 (s, 1 H), 8.06 (d, $J$ = 6.9 Hz, 1 H), 7.62 - 7.53 (m, 2 H), 7.53 - 7.44 (m, 1 H), 7.11 (dd, $J$ = 2.6, 8.8 Hz, 1 H), 6.96 (d, $J$ = 8.8 Hz, 1 H), 5.88 - 5.77 (m, 1 H), 5.74 - 5.62 (m, 1 H), 4.53 (s, 2 H), 4.51 - 4.45 (m, 2 H), 4.06 (d, $J$ = 5.9 Hz, 2 H), 4.01 - 3.91 (m, 4 H), 2.21 (t, $J$ = 7.3 Hz, 2 H), 1.78 - 1.64 (m, 2 H), 1.57 - 1.48 (m, 2 H), 1.48 - 1.39 (m, 2 H), 1.39 - 1.26 (m, 4 H). $^{13}$C NMR (DMSO-d6) $\delta$ 174.4, 164.7, 158.2, 156.7, 151.9, 138.7, 136.2, 132.5, 131.5, 130.8, 129.8, 129.2, 127.0, 126.8, 126.5, 121.1, 120.2, 112.6, 107.3, 69.2, 68.8, 68.2, 67.1, 65.0, 33.7, 28.7, 28.5, 28.4, 25.4, 24.4.

**11-(2-(4-Aminophenylhydroxamate)ethoxy)-14,19-dioxa-5,7,26-triaza-tetracyclo[19.3.1.1(2,6).1(8,12)]heptacosa-1(25),2(26),3,5,8,10,12(27),16,21,23-decaene (42).** 39.4 mg (0.0732 mmol) of **31**, 12.0 mg (0.102 mmol, 1.4 eq.) of *O*-(tetrahydro-2*H*-pyran-2-yl)hydroxylamine, 33.8 mg (0.0889 mmol, 1.2 eq.) of HATU and 21 µL (0.150 mmol, 2.0 eq.) of triethylamine were dissolved in 2 mL

of DMF. The solution was stirred at rt for 24 h after which it was diluted with water to precipitate out a yellow solid. There were two methods to obtain the crude product. The solid obtained could be filtered under vacuum to obtain the product. However, if the precipitate cannot be filtered easily, extraction of the mixture with 10% methanol in ethyl acetate 3 times was performed. The combined organic layer was washed with brine and dried with anhydrous sodium sulfate. The crude product was purified by flash column chromatography using 2:3 Hex/EtOAC to EtOAc to 40:1 to 20:1 DCM/MeOH to obtain 11.8 mg of the THP protected hydroxamate as a pale yellow solid. TLC (2:3 Hex/EtOAc) $R_f$ = 0.17. LRMS (ESI) *m/z* 638.4 ($M+H^+$). This product was dissolved in 5 mL of dioxane and 1 mL of 4 M HCl in dioxane was added. An orange precipitate formed immediately upon addition of the acid solution. The mixture was stirred for 18 h at rt. The reaction was quenched with saturated sodium bicarbonate solution to precipitate out a yellow solid. The mixture was concentrated to remove the volatile organic solvent. The precipitate was then filtered and dried under vacuum to obtain 6.7 mg (23%) of **42** as a yellow solid. LRMS (ESI) *m/z* 554.2 ($M+H^+$). HPLC purity >99%. $^1$H NMR (DMSO-$d_6$) □ 9.53 (br. s., 1H), 8.42 - 8.59 (m, 2H), 8.16 (s, 1H), 8.01 (d, *J* = 6.15 Hz, 1H), 7.49 - 7.61 (m, 4H), 7.39 (d, *J* = 4.52 Hz, 1H), 7.07 - 7.14 (m, 1H), 6.97 (d, *J* = 8.78 Hz, 1H), 6.60 - 6.73 (m, 2H), 6.29 (br. s., 1H), 5.79 (br. s., 1H), 5.69 (s, 1H), 4.50 - 4.61 (m, 2H), 4.40 - 4.50 (m, 2H), 4.10 (t, *J* = 5.08 Hz, 2H),

4.00 (d, *J* = 4.27 Hz, 4H), 3.49 (d, *J* = 5.27 Hz, 2H). $^{13}$C NMR (DMSO-$d_6$) □ 162.8, 160.2, 159.4, 151.2, 151.1, 138.6, 136.8, 134.0, 130.9, 130.9, 130.8, 129.8, 129.1, 128.2, 126.6, 126.5, 126.4, 120.5, 119.6, 119.3, 115.4, 114.0, 113.2, 111.0, 107.4, 69.1, 68.9, 67.9, 67.0, 65.0, 41.9.

**11-(2-(3-Aminophenylhydroxamate)ethoxy)-14,19-dioxa-5,7,26-triaza-tetracyclo[19.3.1.1(2,6).1(8,12)]heptacosa-1(25),2(26),3,5,8,10,12(27),16,21,23-decaene (43).** Synthesised following the procedure for **42**. 163 mg (0.302 mmol) of **32**, 36.3 mg (0.310 mmol, 1.0 eq.) of *O*-(tetrahydro-2*H*-pyran-2-yl)hydroxylamine, 128 mg (0.336 mmol, 1.1 eq.) of HATU and 130 µL (0.928 mmol, 3.1 eq.) of triethylamine was dissolved in 3 mL of DMF. The crude product was purified by flash column chromatography using 1:4 Hex/EtOAC to 25:1 to 25:1.5 to 25:2 DCM/MeOH to obtain 17.6 mg of the THP protected hydroxamate as a yellow solid. TLC (2:3 Hex/EtOAc) $R_f$ = 0.16. LRMS (ESI) *m/z* 638.4 ($M+H^+$). This product was dissolved in 4 mL of dioxane and 0.5 mL of 4 M HCl in dioxane was added to give 12.4 mg (7%) of **43** as a yellow solid. LRMS (ESI) *m/z* 554.2 ($M+H^+$). HPLC purity >99%. $^1$H NMR (DMSO-$d_6$) □ 9.52 (s, 1H), 8.46 - 8.54 (m, 2H), 8.16 (s, 1H), 8.01 (d, *J* = 3.89 Hz, 1H), 7.52 - 7.60 (m, 2H), 7.39 (d, *J* = 5.14 Hz, 1H), 7.08 - 7.17 (m, 2H), 7.04 (s, 1H), 6.98 (d, *J* = 8.78 Hz, 1H), 6.93 (d, *J* = 7.53 Hz, 1H), 6.77 (dd, *J* = 1.69, 7.97 Hz, 1H), 5.92 (t, *J* = 5.40 Hz, 1H), 5.73 - 5.88 (m, 1H), 5.61 - 5.73 (m, 1H), 4.54 (s, 2H), 4.47 (s, 2H), 4.12 (t, *J* = 5.27

Hz, 2H), 3.96 - 4.04 (m, 4H), 3.43 - 3.50 (m, 2H). $^{13}$C NMR (101 MHz, DMSO-$d_6$) □ 162.9, 160.2, 159.4, 151.1, 148.7, 138.6, 136.8, 133.9, 130.9, 130.8, 129.8, 129.1, 128.8, 126.6, 126.5, 126.4, 120.5, 119.6, 114.9, 114.2, 113.2, 110.3, 107.4, 69.1, 68.9, 67.8, 67.0, 66.3, 65.0, 42.0.

**11-(2-(4-Hydroxyphenyl hydroxamate))-14,19-dioxa-5,7,26-triaza-tetracyclo[19.3.1.1(2,6).1(8,12)]heptacosa-1(25),2(26),3,5,8,10,12(27),16,21,23-decaene hydrochloride (44).** Synthesised following the procedure for **42**. 33.9 mg (0.0628 mmol) of **33**, 11.0 mg (0.0.0939 mmol, 1.5 eq.) of *O*-(tetrahydro-2*H*-pyran-2-yl)hydroxylamine, 47.7 mg (0.125 mmol, 2.0 eq.) of HATU and 26 µL (0.186 mmol, 3.0 eq.) of triethylamine was dissolved in 2 mL of DMF. The crude product was purified by flash column chromatography using DCM to 30:1 to 20:1 DCM/MeOH to obtain 31.0 mg of the THP protected hydroxamate as a yellow solid. TLC (2:3 Hex/EtOAc) $R_f$ = 0.19; LRMS (ESI) *m/z* 639.4 ($M+H^+$). This product was dissolved in 5 mL of dioxane and 0.5 mL of 4M HCl in dioxane was added to give 6.5 mg (18%) of **44** as a yellow solid. LRMS (ESI) *m/z* 555.2 ($M+H^+$). HPLC purity >99%. $^1$H NMR (DMSO-$d_6$) □ 9.55 (s, 1H), 8.47 - 8.56 (m, 2H), 8.17 (s, 1H), 8.02 (d, *J* = 3.39 Hz, 1H), 7.77 (t, *J* = 9.35 Hz, 2H), 7.53 - 7.61 (m, 2H), 7.40 (d, *J* = 5.15 Hz, 1H), 7.00 - 7.18 (m, 4H), 5.75 - 5.86 (m, 1H), 5.61 - 5.72 (m, 1H), 4.54 (s, 2H), 4.45 (d, *J* = 3.14 Hz, 2H), 4.39 (br. s., 2H), 4.34 (br. s., 2H), 3.99 (d, *J* = 5.14 Hz, 4H). $^{13}$C NMR (DMSO-$d_6$) □ 162.9, 161.1, 160.2,

159.4, 150.9, 138.6, 136.7, 134.2, 130.8, 130.8, 129.9, 129.1, 129.0, 128.6, 126.8, 126.5, 126.5, 120.5, 119.7, 114.3, 114.3, 113.8, 107.4, 101.0, 69.1, 68.9, 67.9, 67.0, 66.7, 66.3, 64.9, 61.4.

**11-(2-(*N*-Hydroxy-1-piperidine-4-carboxamide)-ethoxy)-14,19-dioxa-5,7,26-triaza-tetracyclo[19.3.1.1(2,6).1(8,12)]heptacosa-1(25),2(26),3,5,8,10,12(27),16,21,23-decaene hydrochloride (45).** Synthesised following the procedure for **42**. 70.9 mg (0.134 mmol) of **34**, 24.6 mg (0.210 mmol, 1.6 eq.) of *O*-(tetrahydro-2*H*-pyran-2-yl)hydroxylamine, 78.1 mg (0.205 mmol, 1.5 eq.) of HATU and 100 μL (0.714 mmol, 5.3 eq.) of triethylamine was dissolved in 5 mL of DMF. The crude product was purified by flash column chromatography using EtOAC to 25:1 to 22:3 DCM/MeOH to obtain 68.8 mg of the THP protected hydroxamate as a yellow solid. TLC (9:1 DCM/MeOH) $R_f$ = 0.18; LRMS (ESI) *m/z* 630.5 ($M+H^+$). This product was dissolved in 5 mL of dioxane and 0.5 mL of 4M HCl in dioxane was added to give 16.4 mg (23%) of **45** as a yellow solid. LRMS (ESI) *m/z* 546.3 ($M+H^+$). HPLC purity 81% (19% carboxylic acid). $^1$H NMR (DMSO-$d_6$) □ 10.38 (br. s., 1H), 9.53 (s, 1H), 8.48 - 8.55 (m, 2H), 8.18 (s, 1H), 7.96 - 8.04 (m, 1H), 7.51 - 7.59 (m, 2H), 7.39 (d, *J* = 5.14 Hz, 1H), 7.08 - 7.15 (m, 1H), 6.97 (d, *J* = 8.78 Hz, 1H), 5.79 - 5.88 (m, 1H), 5.63 - 5.74 (m, 1H), 4.55 (s, 2H), 4.48 (s, 2H), 4.02 - 4.10 (m, 4H), 4.00 (d, *J* = 5.14 Hz, 2H), 2.98 (d, *J* = 11.54 Hz, 1H), 2.68 (t, *J* = 5.58 Hz, 2H), 1.91 - 2.20 (m,

3H), 1.56 - 1.69 (m, 3H). $^{13}$C NMR (DMSO-$d_6$) □ 162.9, 160.2, 159.3, 151.2, 138.6, 136.8, 133.8, 131.0, 130.7, 129.8, 129.1, 126.5, 126.5, 126.3, 120.6, 119.6, 113.1, 107.3, 69.1, 68.9, 67.1, 65.3, 56.9, 53.1, 28.5.

**11-(2-(*N*1-(4-Aminophenyl)-N7-hydroxyheptanediamide)ethoxy)-14,19-dioxa-5,7,26-triaza-tetracyclo[19.3.1.1(2,6).1(8,12)]heptacosa-1(25),2(26),3,5,8,10,12(27),16,21,23-decaene (46).** Synthesised following the procedure for **42**. 25.9 mg (0.0397 mmol) of **35**, 7.0 mg (0.0600 mmol, 1.5 eq.) of *O*-(tetrahydro-2*H*-pyran-2-yl)hydroxylamine, 27.2 mg (0.0715 mmol, 1.8 eq.) of HATU and 20 μL (0.143mmol, 3.6 eq.) of triethylamine was dissolved in 1 mL of DMF. The crude product was purified by flash column chromatography using 1:4 Hex/EtOAC to 25:1 to 25:1.5 DCM/MeOH to obtain 10.5 mg of the THP protected hydroxamate as an off white solid. TLC (2:3 Hex/EtOAc) $R_f$ = 0.05; LRMS (ESI) *m/z* 751.6 ($M+H^+$). This product was dissolved in 5 mL of dioxane and 0.3 mL of 4 M HCl in dioxane was added to give 3.2 mg (12%) of **46** as a pale brown solid. LRMS (ESI) *m/z* 666.4 ($M+H^+$). HPLC purity 93.5%. $^1$H NMR (DMSO-$d_6$) □ 9.52 (br. s., 1H), 9.47 (br. s., 1H), 8.45 - 8.55 (m, 2H), 8.17 (br. s., 1H), 8.01 (br. s., 1H), 7.56 (br. s., 2H), 7.39 (d, *J* = 4.39 Hz, 1H), 7.25 - 7.35 (m, *J* = 8.28 Hz, 2H), 7.10 (d, *J* = 8.91 Hz, 1H), 6.97 (d, *J* = 8.66 Hz, 1H), 6.48 - 6.68 (m, *J* = 8.28 Hz, 2H), 5.83 (d, *J* = 15.81 Hz, 1H), 5.68 (d, *J* = 15.94 Hz, 1H), 4.55 (br. s., 2H), 4.47 (s, 2H), 4.10 (br. s., 2H), 3.90 - 4.07 (m, 5H), 2.21 (t, *J* = 6.90 Hz, 2H), 1.94 (t, *J* =

7.34 Hz, 2H), 1.40 - 1.69 (m, 4H), 1.24 (d, $J$ = 6.90 Hz, 2H). $^{13}$C NMR (DMSO-$d_6$) □ 162.8, 162.4, 160.2, 159.3, 151.2, 138.6, 131.0, 129.8, 129.1, 126.5, 120.8, 120.5, 119.6, 115.7, 113.2, 112.1, 107.3, 68.9, 67.0, 65.1, 42.7, 28.7, 28.3.

**11-(2-(*N*1-(4-Aminophenyl)-N8-hydroxyoctanediamide)ethoxy)-14,19-dioxa-5,7,26-triaza-tetracyclo[19.3.1.1(2,6).1(8,12)]heptacosa-1(25),2(26),3,5,8,10,12(27),16,21,23-decaene (47).** Synthesised following the procedure for **42**. 26.7 mg (0.0496 mmol) of **36**, 11.6 mg (0.0990 mmol, 2.0 eq.) of *O*-(tetrahydro-2*H*-pyran-2-yl)hydroxylamine, 31.1 mg (0.818 mmol, 1.6 eq.) of HATU and 30 μL (0.214mmol, 4.3 eq.) of triethylamine was dissolved in 2 mL of DMF. The crude product was purified by flash column chromatography using 2:3 Hex/EtOAC to 50:1 to 25:1 DCM/MeOH to obtain 29.8 mg of the THP protected hydroxamate as a yellow solid. TLC (2:3 Hex/EtOAc) $R_f$ = 0.18. LRMS (ESI) *m/z* 765.4 ($M+H^+$). This product was dissolved in 4 mL of dioxane and 0.5 mL of 4 M HCl in dioxane was added to give 21.0 mg (62%) of **47** as a yellow solid. LRMS (ESI) *m/z* 681.6 ($M+H^+$). $^1$H NMR (DMSO-$d_6$) □ 9.44 - 9.54 (m, 2H), 8.46 - 8.55 (m, 2H), 8.16 (s, 1H), 8.01 (d, $J$ = 5.27 Hz, 1H), 7.50 - 7.59 (m, 2H), 7.35 - 7.42 (m, 1H), 7.31 (d, $J$ = 8.78 Hz, 2H), 7.10 (dd, $J$ = 2.38, 8.78 Hz, 1H), 6.96 (d, $J$ = 8.78 Hz, 1H), 6.54 - 6.64 (m, 2H), 5.75 - 5.89 (m, 1H), 5.61 - 5.75 (m, 1H), 4.54 (s, 2H), 4.47 (s, 2H), 4.06 - 4.12 (m, 2H), 4.01 (dd, $J$ = 5.14, 14.68 Hz, 4H), 2.13 - 2.25 (m, 2H), 1.79 - 1.98 (m, 2H), 1.37 - 1.61 (m, 4H), 1.16 - 1.33 (m, 4H). $^{13}$C

NMR (DMSO-$d_6$) □ 162.9, 160.2, 159.4, 151.2, 144.8, 138.6, 136.8, 133.9, 131.0, 130.8, 129.8, 129.1, 128.9, 126.6, 126.5, 126.5, 120.8, 120.5, 119.6, 113.2, 112.1, 107.4, 69.1, 68.9, 68.0, 67.1, 65.1, 48.6, 42.7, 36.2, 32.2, 29.0, 28.4, 25.2, 25.0.

**11-(4-(*N*-Hydroxybutanamide)oxy)-14,19-dioxa-5,7,26-triaza-tetracyclo[19.3.1.1(2,6).1(8,12)]heptacosa-1(25),2(26),3,5,8,10,12(27),16,21,23-decaene (48).** Synthesised following the procedure for **42**. 170 mg (0.368 mmol) of **37**, 123 mg (1.05 mmol, 2.9 eq.) of *O*-(tetrahydro-2*H*-pyran-2-yl)hydroxylamine, 228 mg (0.600 mmol, 1.6 eq.) of HATU and 0.24 mL (1.71 mmol, 4.7 eq.) of triethylamine was dissolved in 5 mL of DMF. The crude product was purified by flash column chromatography using 2:3 Hex/EtOAC to 25:1 EOAc/MeOH to obtain 100 mg of the THP protected hydroxamate as a yellow solid. TLC (2:3 Hex/EtOAc) $R_f$ = 0.11; LRMS (ESI) *m/z* 561.2 ($M+H^+$). This product was dissolved in 5 mL of dioxane and 1.2 mL of 4 M HCl in dioxane was added to give 78.2 mg (45%) of **48** as a yellow solid. LRMS (ESI) *m/z* 477.2 ($M+H^+$). HPLC purity >99%. Major E isomer only $^1$H NMR (400 MHz, DMSO-$d_6$) □ 10.42 (br. s., 1H), 9.52 (s, 1H), 8.45 - 8.58 (m, 2H), 8.13 - 8.23 (m, 1H), 8.01 (d, *J* = 5.90 Hz, 1H), 7.52 - 7.62 (m, 2H), 7.45 - 7.52 (m, 1H), 7.38 (d, *J* = 5.27 Hz, 1H), 7.06 - 7.15 (m, 1H), 6.89 - 6.98 (m, 1H), 5.76 - 5.90 (m, 1H), 5.62 - 5.76 (m, 1H), 4.55 (s, 2H), 4.47 - 4.53 (m, 2H), 4.07 (d, *J* = 5.77 Hz, 2H), 3.92 - 4.03 (m, 5H), 2.17 (t, *J* = 7.22 Hz, 1H), 1.94 (quin, *J* = 6.68 Hz, 2H). $^{13}$C NMR (101 MHz,

DMSO-$d_6$) □ 168.7, 163.0, 160.1, 159.2, 151.2, 138.6, 136.8, 133.7, 131.0, 130.8, 129.7, 129.1, 126.5, 126.5, 126.3, 120.5, 119.6, 112.8, 107.3, 69.1, 68.8, 67.7, 67.0, 65.1, 28.8, 24.9.

**11-(4-(*N*-Hydroxypentanamide)oxy)-14,19-dioxa-5,7,26-triaza-tetracyclo[19.3.1.1(2,6).1(8,12)]heptacosa-1(25),2(26),3,5,8,10,12(27),16,21,23-decaene (49).** Synthesised following the procedure for **42**. 103 mg (0.217 mmol) of acid **38**, 38.0 mg (0.324 mmol, 1.5 eq.) of *O*-(tetrahydro-2*H*-pyran-2-yl)hydroxylamine, 128 mg (0.336 mmol, 1.6 eq.) of HATU and 91 µL (0.649 mmol, 3.0 eq.) of triethylamine was dissolved in 3 mL of DMF. The crude product was purified by flash column chromatography using 2:3 Hex/EtOAC to 25:0.5 to 25:1 DCM/MeOH to obtain 131 mg of the THP protected hydroxamate as a yellow oil. TLC (2:3 Hex/EtOAc) $R_f$ = 0.18; LRMS (ESI) *m/z* 575.4 ($M+H^+$). This product was dissolved in 8 mL of dioxane and 1 mL of 4 M HCl in dioxane was added to give 81.9 mg (77%) of **49** as a pale yellow solid. LRMS (ESI) *m/z* 491.3 ($M+H^+$). HPLC purity >99%. $^1$H NMR (DMSO-$d_6$) □ 9.52 (br. s., 1H), 8.44 - 8.60 (m, 2H), 8.12 - 8.21 (m, 1H), 7.99 (d, *J* = 5.77 Hz, 1H), 7.50 - 7.61 (m, 2H), 7.37 (d, *J* = 5.02 Hz, 1H), 7.04 - 7.20 (m, 2H), 6.88 - 6.99 (m, 1H), 5.75 - 5.89 (m, 1H), 5.61 - 5.74 (m, 1H), 4.54 (s, 2H), 4.48 (s, 2H), 4.05 (d, *J* = 5.52 Hz, 2H), 3.90 - 4.01 (m, 4H), 2.02 (t, *J* = 6.15 Hz, 2H), 1.60 - 1.78 (m, 4H). $^{13}$C NMR (DMSO-$d_6$) □ 173.3, 168.7, 162.9, 160.2, 159.3, 151.3, 138.6, 136.8, 133.6, 131.0, 130.7,

130.1, 129.8, 129.1, 128.9, 128.6, 128.2, 126.6, 126.4, 126.2, 126.2, 125.3, 120.6, 119.6, 112.8, 107.3, 69.1, 68.9, 68.0, 67.9, 67.1, 65.8, 65.2, 51.2, 32.9, 32.1, 28.4, 28.2, 21.9, 21.3, 21.0.

**11-(4-(*N*-Hydroxyhexanamide)oxy)-14,19-dioxa-5,7,26-triaza-tetracyclo[19.3.1.1(2,6).1(8,12)]heptacosa-1(25),2(26),3,5,8,10,12(27),16,21,23-decaene (50).** Synthesised following the procedure for **42**. 292 mg (0.597 mmol) of **39**, 106 mg (0.905 mmol, 1.5 eq.) of *O*-(tetrahydro-2*H*-pyran-2-yl)hydroxylamine, 342 mg (0.901 mmol, 1.5 eq.) of HATU and 250 μL (1.78 mmol, 3.0 eq.) of triethylamine was dissolved in 3 mL of DMF. The crude product was purified by flash column chromatography using 1:4 Hex/EtOAC to 50:1 to 25:1 DCM/MeOH to obtain 686 mg of the THP protected hydroxamate as a yellow oil with DMF. TLC (1:3 Hex/EtOAc) $R_f$ = 0.38; LRMS (ESI) *m/z* 589.4 ($M+H^+$). This product was dissolved in 10 mL of dioxane and 2 mL of 4 M HCl in dioxane was added to give 111 mg (37%) of **50** as a yellow solid. LRMS (ESI) *m/z* 505.2 ($M+H^+$). HPLC purity >99%. $^1$H NMR (DMSO-$d_6$) □ 9.52 (br. s., 1H), 8.44 - 8.55 (m, 2H), 8.12 - 8.20 (m, 1H), 7.88 - 8.05 (m, 1H), 7.43 - 7.61 (m, 2H), 7.28 - 7.42 (m, 1H), 7.11 (dd, *J* = 2.57, 8.72 Hz, 1H), 6.85 - 6.98 (m, 1H), 5.74 - 5.89 (m, 1H), 5.68 (td, *J* = 5.93, 15.62 Hz, 1H), 4.53 (s, 2H), 4.48 (s, 2H), 4.01 - 4.09 (m, 2H), 3.79 - 4.01 (m, 4H), 1.84 - 2.02 (m, 2H), 1.62 - 1.78 (m, 2H), 1.48 - 1.62 (m, 2H), 1.32 - 1.48 (m, 2H). $^{13}$C NMR (DMSO-$d_6$) □ 168.7, 162.9, 162.3, 160.2, 159.3,

151.4, 138.6, 136.8, 133.7, 131.1, 130.8, 129.8, 129.1, 126.6, 126.5, 126.3, 120.6, 119.6, 112.8, 107.3, 69.1, 68.9, 68.3, 67.1, 65.2, 40.4, 38.2, 35.8, 32.4, 28.6, 25.3, 25.1.

**11-(4-(*N*-hydroxyheptanamide)oxy)-14,19-dioxa-5,7,26-triaza-tetracyclo[19.3.1.1(2,6).1(8,12)]heptacosa-1(25),2(26),3,5,8,10,12(27),16,21,23-decaene (51).** Synthesised following the procedure for **42**. 46.6 mg (0.0925 mmol) of **40**, 11.2 mg (0.0956 mmol, 1.0 eq.) of *O*-(Tetrahydro-2*H*-pyran-2-yl)hydroxylamine, 49.4 mg (0.130 mmol, 1.4 eq.) of HATU and 20 μL (0.143 mmol, 1.5 eq.) of triethylamine was dissolved in 1.5 mL of DMF. The crude product was purified by flash column chromatography using 2:3 Hex/EtOAC to 50:1 EOAc/MeOH to obtain 30.5 mg of the THP protected hydroxamate as a yellow solid. TLC (2:3 Hex/EtOAc) $R_f$ = 0.18. LRMS (ESI) *m/z* 603.3 ($M+H^+$). This product was dissolved in 2 mL of dioxane and 0.5 mL of 4 M HCl in dioxane was added to give 13.4 mg (36%) of **51** as a yellow solid. LRMS (ESI) *m/z* 519.3 ($M+H^+$). HPLC purity >99%. $^1$H NMR (DMSO-$d_6$) □ 9.51 (s, 1H), 8.46 - 8.54 (m, 2H), 8.13 - 8.23 (m, 1H), 8.01 (d, *J* = 6.15 Hz, 1H), 7.50 - 7.60 (m, 2H), 7.38 (d, *J* = 5.14 Hz, 1H), 7.10 (dd, *J* = 2.57, 8.72 Hz, 1H), 6.94 (d, *J* = 8.78 Hz, 1H), 5.78 - 5.89 (m, 1H), 5.61 - 5.75 (m, 1H), 4.55 (s, 2H), 4.43 - 4.53 (m, 3H), 4.06 (d, *J* = 5.77 Hz, 2H), 3.90 - 4.03 (m, 4H), 1.96 (t, *J* = 7.34 Hz, 2H), 1.64 - 1.79 (m, 2H), 1.52 (td, *J* = 7.26, 14.71 Hz, 2H), 1.43 (td, *J* = 7.39, 14.46 Hz, 2H), 1.26 - 1.37 (m,

2H). $^{13}$C NMR (DMSO-$d_6$) □ 169.1, 162.9, 160.2, 159.3, 151.4, 138.6, 136.8, 133.6, 131.0, 130.7, 129.8, 129.1, 126.5, 126.5, 126.2, 120.6, 119.6, 112.8, 107.3, 69.1, 68.8, 68.2, 67.0, 66.3, 65.2, 40.1, 39.9, 39.7, 39.3, 39.1, 38.9, 32.2, 28.7, 28.3, 25.3, 25.1. HRMS (ESI) *m/*z 541.2425, calc. 541.2421 (diff 0.7 ppm).

**11-(4-(*N*-Hydroxyoctanamide)oxy)-14,19-dioxa-5,7,26-triaza-tetracyclo[19.3.1.1(2,6).1(8,12)]heptacosa-1(25),2(26),3,5,8,10,12(27),16,21,23-decaene (52).** Synthesised following the procedure for **42**. 58.9 mg (0.114 mmol) of **41**, 16.6 mg (0.142 mmol, 1.2 eq.) of *O*-(tetrahydro-2*H*-pyran-2-yl)hydroxylamine, 56.3 mg (0.148 mmol, 1.3 eq.) of HATU and 30 µL (0.214mmol, 1.9 eq.) of triethylamine was dissolved in 1 mL of DMF. The crude product was purified by flash column chromatography using 2:3 Hex/EtOAC to 50:1 EOAc/MeOH to obtain 41.6 mg of the THP protected hydroxamate as a yellow solid. TLC (2:3 Hex/EtOAc) $R_f$ = 0.18; LRMS (ESI) *m/z* 617.4 ($M+H^+$). This product was dissolved in 2 mL of dioxane and 0.5 mL of 4M HCl in dioxane was added to give 24.7 mg (41%) of **52** as a yellow solid. LRMS (ESI) *m/z* 533.3 ($M+H^+$). HPLC purity >99%. $^1$H NMR (400 MHz, DMSO-$d_6$) □ 10.33 (br. s., 1H), 9.51 (s, 1H), 8.66 (br. s., 1H), 8.44 - 8.57 (m, 2H), 8.11 - 8.22 (m, 1H), 8.01 (d, *J* = 5.77 Hz, 1H), 7.48 - 7.59 (m, 2H), 7.38 (d, *J* = 5.02 Hz, 1H), 7.06 - 7.14 (m, 1H), 6.94 (d, *J* = 8.78 Hz, 1H), 5.85 (td, *J* = 5.43, 15.75 Hz, 1H), 5.69 (td, *J* = 5.93, 15.62 Hz, 1H), 4.55 (s, 2H), 4.41 - 4.53 (m, 2H), 4.06 (d, *J* = 5.77 Hz, 2H), 3.88 -

4.02 (m, 4H), 1.95 (t, $J$ = 7.34 Hz, 2H), 1.64 - 1.77 (m, 2H), 1.38 - 1.58 (m, 4H), 1.22 - 1.38 (m, 4H). $^{13}$C NMR (101 MHz, DMSO-$d_6$) □□169.0, 162.9, 160.2, 159.3, 151.4, 138.6, 136.8, 133.6, 131.0, 130.7, 129.8, 129.1, 126.5, 126.4, 126.2, 120.6, 119.6, 112.8, 107.3, 69.1, 68.8, 68.3, 67.0, 66.3, 65.2, 32.2, 28.8, 28.5, 28.4, 25.4, 25.0.

Molecular Modelling

JAK2 modeling is described in (Poulsen et al., 2012). The HDAC1 X-ray structure (ID: 4BKX), HDAC2 structure (4LXZ) and HDAC4 structure (2VQW) was downloaded from the Protein Data Bank (http://www.rcsb.org) and prepared using the protein preparation wizard in Maestro version 10110 using standard settings. This included the addition of hydrogen atoms, bond assignments, removal of water molecules further than 5 Å from the ligand, protonation state assignment, optimization of the hydrogen bond network and restrained minimization using the OPLS2005 force field.111 The proteins were superimposed using structural alignment and the HDAC2 structure ligand SAHA was duplicated into HDAC1 and HDAC4. The HDAC6 protein sequence (ID: Q9UBN7) was downloaded from Uniprot (http://www.uniprot.org). A homology model was built for each of the catalytic domains of HDAC6 using the HDAC4-SAHA complex as template and Prime version 3.8110 with default settings. The two HDAC6 homology models are very similar with 49% sequence identity and 67% homology. Both the C-terminal

catalytic domain model (HDAC 6 residues 482-800) and the N-terminal catalytic domain model (HDAC 6 residues 87-404) were used for modelling. The inhibitors were found to model into both HDAC6 models in a similar conformation and orientation. Following Wiest et al[94] the C-terminal catalytic domain model is discussed unless otherwise stated.

A conformational analysis of each inhibitor was done to obtain a conformational ensemble for docking.[88] Grids for docking were prepared for HDAC1 and HDAC6 using Glide version 6.5[117] with standard settings. Constraints for the zinc atom and the residues that hydrogen bond with the hydroxamate were included. Docking procedures were carried out as previously described.[88] Docking of the hybrid inhibitors with constraints did not produce low energy poses. Docking of **2** without constraints resulted in reasonable poses of low energy conformations binding to the cap-region of HDAC1 and HDAC6. Poses of **2** were then merged with the linker and hydroxamate part of **1**.

The HDAC1 and HDAC6 inhibitor-protein complexes were finally minimized using Macromodel10.6.[117] Distance constraints between the hydroxamate and Zinc (2.3 Å) as well as the 3 residues that hydrogen bond with the hydroxamate (2.8 Å) were included. All residues more than 9 Å from the ligand were constrained before the complex was subjected to 500 steps of Polak-Ribiere-Conjugate-Gradient[118]

(Polak and Ribiere, 1969) minimization using the OPLS2005 force field and GB/SA continuum solvation model (Hasel et al., 1988).[119]

**Enzyme Assays**

Enzyme inhibition assays were carried out by Reaction Biology Corporation (RBC).[120] For HDAC assays: Add 2X of HDAC enzyme into reaction plate except control wells (no enzyme), where buffer (50 mM Tris-HCl, pH8.0, 137 mM NaCl, 2.7 mM KCl, and 1 mM $MgCl_2$) is added instead. Add inhibitors in 100% DMSO into the enzyme mixture via acoustic technology (Echo550; nanoliter range). Spin down and pre-incubate. Add 2X Substrate Mixture: Fluorogenic HDAC General Substrate: 50 µM, Arg-His-Lys-Lys(Ac); HDAC8 only substrate: 50 µM, Arg-His-Lys(Ac)-Lys(Ac); Class2A Substrate: Acetyl-Lys(trifluoroacetyl)-AMC) in all reaction wells to initiate the reaction. Spin and shake. Incubate for 2 h at 30 °C with seal. Add Developer with Trichostatin A to stop the reaction and to generate fluorescent color. Carry out kinetic measurement for 1.5 h with Envision with 15 min interval. (Ex/Em= 360/460 nm). Take endpoint reading for analysis after the development reaches plateau. Kinase assays were carried out according to the published procedures.[121] Briefly, kinase profiling was performed using the "HotSpot" assay platform. Briefly, specific kinase/substrate pairs along with required cofactors were prepared in reaction buffer; 20 mM Hepes pH 7.5, 10 mM $MgCl_2$, 1 mM EGTA, 0.02% Brij35, 0.02 mg/ml BSA, 0.1 mM $Na_3VO_4$, 2 mM

DTT, 1% DMSO. Compounds were delivered into the reaction, followed ~20 min later by addition of a mixture of ATP (Sigma) and $^{33}$P ATP (PerkinElmer) to a final concentration of 10 μM. Reactions were carried out at 25 °C for 120 min, followed by spotting of the reactions onto P81 ion exchange filter paper (Whatman). Unbound phosphate was removed by extensive washing of filters in 0.75% phosphoric acid. After subtraction of background derived from control reactions containing inactive enzyme, kinase activity data were expressed as the percent remaining kinase activity in test samples compared to vehicle (dimethyl sulfoxide) reactions. $IC_{50}$ values and curve fits were obtained using Prism (GraphPad Software).

Kinase profiling was carried out by DiscoveRx according to published protocols.[95]

**Cellular Assays**

**Cell proliferation inhibition assays**

Human breast cancer MCF-7 cells, human breast cancer MDA-MB231 cells, prostate cancer cell line PC-3 and colon cell line HCT-116 cells were purchased from ATCC (Rockville, MD). The first three cell lines were grown in DMEM Media (Invitrogen, Singapore) and the last in Mccoys Media. They were supplemented with 10% fetal bovine serum, 50 μg / mL penicillin and 50 μg/mL streptomycin at 37 °C with 5% $CO_2$. The cells were sub-cultured to 80-90%

confluency and used within 15-20 passages for the assay. Cell viability was assessed with MTT (3-(4,5-dimethylthiazol-2-yl)-2,5-diphenyl tetrazolium bromide) as follows: cells were seeded at 2500 cells per well in a 96-well plate for 24 h. The media was removed and aliquots of test compounds (initially prepared as 10 mM stock solutions in DMSO) were added to each well and the plates were incubated for 72 h. The final amount of DMSO per well was maintained at 0.5% v/v. At the end of the incubation period, the media was removed and replaced with FBS free media (150 μL) and MTT (50 μL of 2 mg/mL solution in phosphate buffer saline, pH 7.4). After incubation for 3 h at 37 °C with 5% $CO_2$, the supernatant was removed and a solution of 100 μL DMSO was added to dissolve the formazan crystals. Absorbance was measured at 570 nm on a micro plate reader (Tecan Infinite 200). Cell viability was determined from readings of treated wells compared to control wells (absence of test compound) with correction of background absorbance. The $IC_{50}$ (concentration required to reduce cell viability to 50% of control/untreated cells) was determined in triplicates on separate occasions, using two different stock solutions. % Viability readings for each test compound were plotted against log concentration on GraphPad Prism (Version 5.0, GraphPad Software, San Diego, CA), with constraints set at $\geq 0$ and $\leq 100\%$. A sigmoidal curve was generated from which the $IC_{50}$ was obtained.

Multiple Myeloma Cell Lines, KMS12BM, OPM2, AML Cell lines KG1 and MOLM14 and NKT-cell lymphoma cell lines, NKYS and KHYG were cultured in were cultured in RPMI 1640 (Biowest) supplemented with 10% Fetal Bovine Serum (Biowest), 100 units/mL penicillin and 100 µg/mL streptomycin. An additional supplementation of IL-2 was required for NKYS (100 units/mL of IL-2) and (200 units/mL of IL-2) for KHYG. All cells were grown in a humidified atmosphere at 37 °C with 5% $CO_2$. KMS12BM, OPM2, KG1, MOLM14, NKYS and KHYG cells were treated in 96 well plates at a density of 25,000 cells per well in triplicates for 48h in a 37 °C incubator with 5% $CO_2$. Cell viability was assessed using the CellTiter-Glo Luminescent Cell Proliferation Assay (CTG assay, Promega, Madison, WI). The luminescence was measured with a Tecan spectrophotometer. Dose response curves were plotted as above.

HEL cells were cultured in RPMI 1640 medium containing 10% FBS (Life Technology) and 55 µM β-mercaptoethanol (Sigma Aldrich). HEL cells ($2.5X10^4$/ 90 µL) were seeded in 96-well plates and inhibitors of various concentrations were added accordingly. As negative control, cells were treated with vehicle (DMSO) only. After 36 h of incubation, 10 µL of PrestoBlue dye were added into each well and further incubated for 2.5 h. Measurement was done according to PrestoBlue dye protocol at 570 nm against 600 nm. This experiment was performed in triplicates and repeated twice. Mean values ± SD for each concentration were

determined. Calculation of cell viability was done according to the protocol (Life Technology).

**Immunoblotting**

*HEL92.1.7 cells*: SDS-PAGE and Western blot analyses were performed as previously described.[122] HEL cells ($5X10^5$/ mL) were seeded into 6-well plate and treated with inhibitor (0, 0.1, 0.5 and 1 μM) for 1 hr. Cells were collected and washed with PBS. Pellet was lysed in RIPA buffer supplemented with phosphatase inhibitor cocktail (Roche Life Science) and protease inhibitor cocktail (Sigma Aldrich). The lysate was loaded into 10% (HEL cells) or 8% (HeLa stable clone) polyacrylamide gel. Proteins were then transferred to PVDF membrane (Milipore) and detected through specific antibodies: anti-Acetylated Tubulin (6-11B-1) (Biolegend), anti-STAT5 (Santa Cruz Biotechnology); anti-H3 (9715S), anti-Acetylated H3 (Lys9/Lys14) (9677S), anti-pJAK2 (Y1007/1008), anti-JAK2 (D2E12), anti-pSTAT5 (Tyr694) and anti-Tubulin (Cell Signaling Technology).

*KMS-12-BM and MOLM-14*: For immunoblotting analysis at least $3x10^6$ cells were seeded for each condition. Cells were treated with **51** at stated concentrations and harvested at indicated timepoints. Equal amounts of protein were separated on an SDS polyacrylamide gel and transferred onto a PVDF membrane. Membrane was then probed with following antibodies: anti-phosho-STAT3 (#9138 Cell Signaling

Technology), anti-STAT3 (#SC-482 Santa Cruz), anti-Acetylated alpha tubulin (#SC-23590, Santa Cruz), anti-Alpha tubulin (#SC-5286), anti-Acetylated Histone 3 (Lys9/Lys14) (#9677 Cell Signaling Technology), anti-Histone (#9715, Novus Biological).

**Colony forming unit assay**

HEL cells (200 cells/ mL) were mixed vigorously with methylcellulose semi-solid medium according to ClonaCell™-TCS Medium (StemCell Technologies). Inhibitors of various concentrations were added accordingly. The mixture was vortexed and aliquoted into 6-well plates for 14-16 days incubation after which colonies werer counted.

**Determination of Toxicity in Transforming growth factor-alpha mouse hepatocyte (TAMH) Cells**

TAMH cells were seeded at a cell density of 12,000 cells/well (60,000 cells/mL) in a 96-well plate (NUNC) a day before drug treatment. Cells were then treated test compounds starting from a concentration of 100 μM (0.5% DMSO concentration: 1.0 μl of **51** and **52** of a 10 mM stock solution in 99 μL of media in each well; drug stock concentration is 10 mM). Drug-treated cells were then incubated at 37 °C for 24 hours after which time cell viability was determined with CellTiter-Glo® Cell Viability Assay (Promega Corporation) as per manufacturer's instructions. The

cell-reagent mixture was then transferred to a solid white flat-bottom 96-well plate (Greiner). Luminescence was then recorded with an integration time of 0.25 seconds (Tecan Infinite® M200 Microplate reader). Either percentage inhibition at the top concentration or an $IC_{50}$ was calculated as for the cell assays above.

**Determination of *in vitro* metabolic stability in male (MRLM) and female rat liver microsomes (FRLM).**

Liver microsomal incubations were conducted in triplicate. Incubation mixtures consisted of 7.5 µL of 20 mg/mL FRLM and MRLM (final: 0.3 mg microsome protein/mL), 2.5 µL of 600 µM **51**/**52** in acetonitrile (final: 3 µM), 440 µL of 0.1 M phosphate buffer (pH 7.4). The mixture was first shaken for 5 min for pre-incubation in a shaking water bath at 37ºC. Reaction was initiated by adding 50 µL of 10 mM NADPH to obtain a final concentration of 1mM NADPH in the mixture. The total volume of the reaction mixture was 500 µL. For metabolic stability studies, aliquots of 50 µL of the incubation sample mixture were collected at 0, 5, 10, 15, 30, and 45 min. After collection of samples, the reaction was terminated with 100 µL of chilled acetonitrile containing the internal standard (1.5 µM compound **1**). The mixture was then centrifuged at 10,000 X g to remove the protein and the supernatant was subsequently applied to LC-MS/MS analysis.

Positive control (PC) samples were prepared as described above, except the test compound was replaced with the known P450 substrate (Midazolam, 3 μM). The samples were assayed for the degradation of midazolam to evaluate the adequacy of the experimental conditions for drug metabolism study. Negative control samples were also prepared as described above but without NADPH.

## ASSOCIATED CONTENT

**Supporting Information**. Additional synthesis of compounds, NMR and HPLC spectra for all final compounds. This material is available free of charge via the Internet at http://pubs.acs.org.

## AUTHOR INFORMATION

### Corresponding Author

*Phone: +6566012495. Email: phadbw@nus.edu.sg

### Author Contributions

The manuscript was written through contributions of all authors. All authors have given approval to the final version of the manuscript.

### Funding Sources

This research was funded by generous grants from the National University of Singapore (Drug Development Unit grant R-711-000-022-133 (MR) and Faculty of

Science start-up grant R-148-000-169-133 to BD). WJC is supported by NMRC Clinician Scientist Investigator award and partly supported by a Singapore Cancer Syndicate Grant, the National Research Foundation Singapore and the Singapore Ministry of Education under the Research Centers of Excellence initiative. JJYY is supported by research grant NSC 102-2320-B-001-007-MY3 from the Ministry of Science and Technology, Taiwan.

ACKNOWLEDGMENTS

The authors gratefully acknowledge Sheela David Packiaraj and Associate Professor Ho Han Kiat for providing TAMH data and Dr Yang Shilli and Professor Paul Ho for RLM data.

ABBREVIATIONS

DML: Designed Multiple Ligand; JAK: Janus Kinase; HDAC: Histone Deacetylase.

REFERENCES

1. Stewart, B. W.; Wild, C. P. *World Cancer Report 2014*. World Health Organization: International Agency for Research on Cancer, 2014.

2. Al-Lazikani, B.; Banerji, U.; Workman, P. Combinatorial drug therapy for cancer in the post-genomic era. *Nat. Biotechnol.* **2012,** *30*, 679-692.

3. Morphy, R.; Kay, C.; Rankovic, Z. From magic bullets to designed multiple ligands. *Drug Discovery Today* **2004,** *9*, 641-651.

4. Zimmermann, G. R.; Lehar, J.; Keith, C. T. Multi-target therapeutics: when the whole is greater than the sum of the parts. *Drug Discovery Today* **2007,** *12*, 34-42.

5. Schwartz, G. K. *Combination Cancer Therapy: Modulators and Potentiators*. Humana Press: Totowa, N.J.: 2005.

6. Morphy, R.; Rankovic, Z. Designed multiple ligands. An emerging drug discovery paradigm. *J. Med. Chem.* **2005,** *48*, 6523-6543.

7. O'Boyle, N. M.; Meegan, M. J. Designed multiple ligands for cancer therapy. *Curr. Med. Chem.* **2011,** *18*, 4722-4737.

8. Anighoro, A.; Bajorath, J.; Rastelli, G. Polypharmacology: challenges and opportunities in drug discovery. *J. Med. Chem.* **2014,** *57*, 7874-7887.

9. Rodrigues, D. A. *Drug-Drug Interactions*. 2nd ed.; CRC Press: New York, USA, 2008.

10. Costantino, L.; Barlocco, D. Designed multiple ligands: basic research vs clinical outcomes. *Curr. Med. Chem.* **2012,** *19*, 3353-3387.

11. Peters, J.-U. *Polypharmacology in Drug Discovery*. Wiley: New Jersey, USA, 2012.

12. Peters, J. U. Polypharmacology - foe or friend? *J. Med. Chem.* **2013,** *56*, 8955-8971.

13. Lai, C. J.; Bao, R.; Tao, X.; Wang, J.; Atoyan, R.; Qu, H.; Wang, D. G.; Yin, L.; Samson, M.; Forrester, J.; Zifcak, B.; Xu, G. X.; DellaRocca, S.; Zhai, H. X.; Cai, X.; Munger, W. E.; Keegan, M.; Pepicelli, C. V.; Qian, C. CUDC-101, a multitargeted inhibitor of histone deacetylase, epidermal growth factor receptor, and human epidermal growth factor receptor 2, exerts potent anticancer activity. *Cancer Res.* **2010,** *70*, 3647-3656.

14. Shimizu, T.; LoRusso, P. M.; Papadopoulos, K. P.; Patnaik, A.; Beeram, M.; Smith, L. S.; Rasco, D. W.; Mays, T. A.; Chambers, G.; Ma, A.; Wang, J.; Laliberte, R.; Voi, M.; Tolcher, A. W. Phase I first-in-human study of CUDC-101, a multitargeted inhibitor of HDACs, EGFR, and HER2 in patients with advanced solid tumors. *Clin. Cancer Res.* **2014,** *20*, 5032-5040.

15. Wang, J.; Pursell, N. W.; Samson, M. E.; Atoyan, R.; Ma, A. W.; Selmi, A.; Xu, W.; Cai, X.; Voi, M.; Savagner, P.; Lai, C. J. Potential advantages of CUDC-101, a multitargeted HDAC, EGFR, and HER2 inhibitor, in treating drug resistance and preventing cancer cell migration and invasion. *Mol. Cancer Ther.* **2013,** *12*, 925-936.

16. Seo, S. Y. Multi-targeted hybrids based on HDAC inhibitors for anti-cancer drug discovery. *Arch. Pharm. Res.* **2012,** *35*, 197-200.

17. Cai, X.; Zhai, H. X.; Wang, J.; Forrester, J.; Qu, H.; Yin, L.; Lai, C. J.; Bao, R.; Qian, C. Discovery of 7-(4-(3-ethynylphenylamino)-7-methoxyquinazolin-6-yloxy)-N-hydroxyheptanamide (CUDC-101) as a potent multi-acting HDAC, EGFR, and HER2 inhibitor for the treatment of cancer. *J. Med. Chem.* **2010,** *53*, 2000-2009.

18. Qian, C.; Lai, C. J.; Bao, R.; Wang, D. G.; Wang, J.; Xu, G. X.; Atoyan, R.; Qu, H.; Yin, L.; Samson, M.; Zifcak, B.; Ma, A. W.; DellaRocca, S.; Borek, M.; Zhai, H. X.; Cai, X.; Voi, M. Cancer network disruption by a single molecule inhibitor targeting both histone deacetylase activity and phosphatidylinositol 3-kinase signaling. *Clin. Cancer Res.* **2012,** *18*, 4104-4113.

19. Dymock, B. W.; Yang, E. G.; Chu-Farseeva, Y.; Yao, L. Selective JAK inhibitors. *Future Med. Chem.* **2014,** *6*, 1439-1471.

20. Dymock, B. W.; See, C. S. Inhibitors of JAK2 and JAK3: an update on the patent literature 2010 - 2012. *Expert Opin. Ther. Pat.* **2013,** *23*, 449-501.

21. James, C.; Ugo, V.; Le Couedic, J. P.; Staerk, J.; Delhommeau, F.; Lacout, C.; Garcon, L.; Raslova, H.; Berger, R.; Bennaceur-Griscelli, A.; Villeval, J. L.; Constantinescu, S. N.; Casadevall, N.; Vainchenker, W. A unique clonal JAK2 mutation leading to constitutive signalling causes polycythaemia vera. *Nature* **2005,** *434*, 1144-1148.

22. Kralovics, R.; Passamonti, F.; Buser, A. S.; Teo, S. S.; Tiedt, R.; Passweg, J. R.; Tichelli, A.; Cazzola, M.; Skoda, R. C. A gain-of-function mutation of JAK2 in myeloproliferative disorders. *N. Engl. J. Med.* **2005,** *352*, 1779-1790.

23. Baxter, E. J.; Scott, L. M.; Campbell, P. J.; East, C.; Fourouclas, N.; Swanton, S.; Vassiliou, G. S.; Bench, A. J.; Boyd, E. M.; Curtin, N.; Scott, M. A.; Erber, W. N.; Green, A. R.; Cancer Genome, P. Acquired mutation of the tyrosine kinase JAK2 in human myeloproliferative disorders. *Lancet* **2005,** *365*, 1054-1061.

24. Zhao, R.; Xing, S.; Li, Z.; Fu, X.; Li, Q.; Krantz, S. B.; Zhao, Z. J. Identification of an acquired JAK2 mutation in polycythemia vera. *J. Biol. Chem.* **2005,** *280*, 22788-22792.

25. Harrison, C.; Kiladjian, J. J.; Al-Ali, H. K.; Gisslinger, H.; Waltzman, R.; Stalbovskaya, V.; McQuitty, M.; Hunter, D. S.; Levy, R.; Knoops, L.; Cervantes, F.; Vannucchi, A. M.; Barbui, T.; Barosi, G. JAK inhibition with ruxolitinib versus best available therapy for myelofibrosis. *N. Engl. J. Med.* **2012,** *366*, 787-798.

26. Mesa, R. A.; Yasothan, U.; Kirkpatrick, P. Ruxolitinib. *Nat. Rev. Drug Discovery* **2012,** *11*, 103-104.

27. Dowty, M. E.; Jesson, M. I.; Ghosh, S.; Lee, J.; Meyer, D. M.; Krishnaswami, S.; Kishore, N. Preclinical to clinical translation of tofacitinib, a Janus kinase inhibitor, in rheumatoid arthritis. *J. Pharmacol. Exp. Ther.* **2014,** *348*, 165-173.

28. William, A. D.; Lee, A. C.; Blanchard, S.; Poulsen, A.; Teo, E. L.; Nagaraj, H.; Tan, E.; Chen, D.; Williams, M.; Sun, E. T.; Goh, K. C.; Ong, W. C.; Goh, S. K.; Hart, S.; Jayaraman, R.; Pasha, M. K.; Ethirajulu, K.; Wood, J. M.; Dymock, B. W. Discovery of the macrocycle 11-(2-pyrrolidin-1-yl-ethoxy)-14,19-dioxa-5,7,26-triaza-tetracyclo[19.3.1.1(2,6). 1(8,12)]heptacosa-1(25),2(26),3,5,8,10,12(27),16,21,23-decaene (SB1518), a potent Janus kinase 2/fms-like tyrosine kinase-3 (JAK2/FLT3) inhibitor for the treatment of myelofibrosis and lymphoma. *J. Med. Chem.* **2011,** *54*, 4638-4658.

29. Hart, S.; Goh, K. C.; Novotny-Diermayr, V.; Hu, C. Y.; Hentze, H.; Tan, Y. C.; Madan, B.; Amalini, C.; Loh, Y. K.; Ong, L. C.; William, A. D.; Lee, A.; Poulsen, A.; Jayaraman, R.; Ong, K. H.; Ethirajulu, K.; Dymock, B. W.; Wood, J. W. SB1518, a novel macrocyclic pyrimidine-based JAK2 inhibitor for the treatment of myeloid and lymphoid malignancies. *Leukemia* **2011,** *25*, 1751-1759.

30. Padrnos, L.; Mesa, R. A. A closer look at pacritinib: a JAK2/FLT3 inhibitor for the treatment of myelofibrosis. *Expert Op. Orphan Drugs* **2014,** *2*, 725-733.

31. Oral pacritinib versus best available therapy to treat myelofibrosis with thrombocytopenia (PAC326). https://www.clinicaltrials.gov/ct2/show/NCT02055781?term=pacritinib&rank=2 (accessed April10 , 2016).

32. CTI BioPharma initiates rolling submission of U.S. new drug application for pacritinib for the treatment of patients with myelofibrosis. http://investors.ctibiopharma.com/phoenix.zhtml?c=92775&p=RssLanding&cat=news&id=2114525 (accessed April 10, 2016).

33. Koppikar, P.; Bhagwat, N.; Kilpivaara, O.; Manshouri, T.; Adli, M.; Hricik, T.; Liu, F.; Saunders, L. M.; Mullally, A.; Abdel-Wahab, O.; Leung, L.; Weinstein, A.; Marubayashi, S.;

Goel, A.; Gonen, M.; Estrov, Z.; Ebert, B. L.; Chiosis, G.; Nimer, S. D.; Bernstein, B. E.; Verstovsek, S.; Levine, R. L. Heterodimeric JAK-STAT activation as a mechanism of persistence to JAK2 inhibitor therapy. *Nature* **2012,** *489*, 155-159.

34. LaFave, L. M.; Levine, R. L. JAK2 the future: therapeutic strategies for JAK-dependent malignancies. *Trends Pharmacol. Sci.* **2012,** *33*, 574-582.

35. Santos, F. P.; Verstovsek, S. What is next beyond janus kinase 2 inhibitors for primary myelofibrosis? *Curr. Opin. Hematol.* **2013,** *20*, 123-129.

36. Meyer, S. C.; Levine, R. L. Molecular pathways: molecular basis for sensitivity and resistance to JAK kinase inhibitors. *Clin. Cancer Res.* **2014,** *20*, 2051-2059.

37. Bartalucci, N.; Tozzi, L.; Bogani, C.; Martinelli, S.; Rotunno, G.; Villeval, J. L.; Vannucchi, A. M. Co-targeting the PI3K/mTOR and JAK2 signalling pathways produces synergistic activity against myeloproliferative neoplasms. *J. Cell Mol. Med.* **2013,** *17*, 1385-1396.

38. Choong, M. L.; Pecquet, C.; Pendharkar, V.; Diaconu, C. C.; Yong, J. W.; Tai, S. J.; Wang, S. F.; Defour, J. P.; Sangthongpitag, K.; Villeval, J. L.; Vainchenker, W.; Constantinescu, S. N.; Lee, M. A. Combination treatment for myeloproliferative neoplasms using JAK and pan-class I PI3K inhibitors. *J. Cell Mol. Med.* **2013,** *17*, 1397-1409.

39. Waibel, M.; Solomon, V. S.; Knight, D. A.; Ralli, R. A.; Kim, S. K.; Banks, K. M.; Vidacs, E.; Virely, C.; Sia, K. C.; Bracken, L. S.; Collins-Underwood, R.; Drenberg, C.; Ramsey, L. B.; Meyer, S. C.; Takiguchi, M.; Dickins, R. A.; Levine, R.; Ghysdael, J.; Dawson, M. A.; Lock, R. B.; Mullighan, C. G.; Johnstone, R. W. Combined targeting of JAK2 and Bcl-2/Bcl-xL to cure mutant JAK2-driven malignancies and overcome acquired resistance to JAK2 inhibitors. *Cell Rep.* **2013,** *5*, 1047-1059.

40. Grunstein, M. Histone acetylation in chromatin structure and transcription. *Nature* **1997,** *389*, 349-352.

41. de Ruijter, A. J.; van Gennip, A. H.; Caron, H. N.; Kemp, S.; van Kuilenburg, A. B. Histone deacetylases (HDACs): characterization of the classical HDAC family. *Biochem. J.* **2003,** *370*, 737-749.

42. Witt, O.; Deubzer, H. E.; Milde, T.; Oehme, I. HDAC family: What are the cancer relevant targets? *Cancer Lett.* **2009,** *277*, 8-21.

43. Wagner, J. M.; Hackanson, B.; Lubbert, M.; Jung, M. Histone deacetylase (HDAC) inhibitors in recent clinical trials for cancer therapy. *Clin. Epigenetics* **2010,** *1*, 117-136.

44. Marks, P. A.; Breslow, R. Dimethyl sulfoxide to vorinostat: development of this histone deacetylase inhibitor as an anticancer drug. *Nat. Biotechnol.* **2007,** *25*, 84-90.

45. Pazdur, R. FDA Approval for Romidepsin, National Cancer Institute. http://www.cancer.gov/about-cancer/treatment/drugs/fda-romidepsin (accessed April 10, 2016).

46. Belinostat, U.S. Food and Drug Administration. http://www.fda.gov/Drugs/InformationOnDrugs/ApprovedDrugs/ucm403960.htm (accessed April 10, 2016).

47. Garnock-Jones, K. P. Panobinostat: first global approval. *Drugs* **2015,** *75*, 695-704.

48. Guha, M. HDAC inhibitors still need a home run, despite recent approval. *Nat. Rev. Drug Discovery* **2015,** *14*, 225-226.

49. Yao, T. P.; Seto, E. *Histone Deacetylases: the Biology and Clinical Implication*. Springer-Verlag: Berlin Heidelberg, Germany, 2011.

50. Malvaez, M.; McQuown, S. C.; Rogge, G. A.; Astarabadi, M.; Jacques, V.; Carreiro, S.; Rusche, J. R.; Wood, M. A. HDAC3-selective inhibitor enhances extinction of cocaine-seeking behavior in a persistent manner. *Proc. Natl. Acad. Sci. U. S. A.* **2013,** *110*, 2647-2652.

51. Decroos, C.; Clausen, D. J.; Haines, B. E.; Wiest, O.; Williams, R. M.; Christianson, D. W. Variable active site loop conformations accommodate the binding of macrocyclic largazole analogues to HDAC8. *Biochemistry* **2015,** *54*, 2126-2135.

52. Huang, W. J.; Wang, Y. C.; Chao, S. W.; Yang, C. Y.; Chen, L. C.; Lin, M. H.; Hou, W. C.; Chen, M. Y.; Lee, T. L.; Yang, P.; Chang, C. I. Synthesis and biological evaluation of ortho-aryl N-hydroxycinnamides as potent histone deacetylase (HDAC) 8 isoform-selective inhibitors. *ChemMedChem* **2012,** *7*, 1815-1824.

53. Suzuki, T.; Muto, N.; Bando, M.; Itoh, Y.; Masaki, A.; Ri, M.; Ota, Y.; Nakagawa, H.; Iida, S.; Shirahige, K.; Miyata, N. Design, synthesis, and biological activity of NCC149 derivatives as histone deacetylase 8-selective inhibitors. *ChemMedChem* **2014,** *9*, 657-664.

54. Butler, K. V.; Kalin, J.; Brochier, C.; Vistoli, G.; Langley, B.; Kozikowski, A. P. Rational design and simple chemistry yield a superior, neuroprotective HDAC6 inhibitor, tubastatin A. *J. Am. Chem. Soc.* **2010,** *132*, 10842-10846.

55. Aldana-Masangkay, G. I.; Sakamoto, K. M. The role of HDAC6 in cancer. *J. Biomed. Biotechnol.* **2011,** *2011*, 875824.

56. Kalin, J. H.; Bergman, J. A. Development and therapeutic implications of selective histone deacetylase 6 inhibitors. *J. Med. Chem.* **2013,** *56*, 6297-6313.

57. Haakenson, J.; Zhang, X. HDAC6 and Ovarian Cancer. *Int. J. Mol. Sci.* **2013,** *14*, 9514-9535.

58. Dallavalle, S.; Pisano, C.; Zunino, F. Development and therapeutic impact of HDAC6-selective inhibitors. *Biochemical Pharmacol.* **2012,** *84*, 756-765.

59. Rey, M.; Irondelle, M.; Waharte, F.; Lizarraga, F.; Chavrier, P. HDAC6 is required for invadopodia activity and invasion by breast tumor cells. *Eur. J. Cell Biol.* **2011,** *90*, 128-135.

60. Castro-Castro, A.; Janke, C.; Montagnac, G.; Paul-Gilloteaux, P.; Chavrier, P. ATAT1/MEC-17 acetyltransferase and HDAC6 deacetylase control a balance of acetylation of alpha-tubulin and cortactin and regulate MT1-MMP trafficking and breast tumor cell invasion. *Eur. J. Cell Biol.* **2012,** *91*, 950-960.

61. Wang, L.; Xiang, S.; Williams, K. A.; Dong, H.; Bai, W.; Nicosia, S. V.; Khochbin, S.; Bepler, G.; Zhang, X. Depletion of HDAC6 enhances cisplatin-induced DNA damage and apoptosis in non-small cell lung cancer cells. *PLoS One* **2012,** *7*, e44265.

62. Bergman, J. A.; Woan, K.; Perez-Villarroel, P.; Villagra, A.; Sotomayor, E. M.; Kozikowski, A. P. Selective histone deacetylase 6 inhibitors bearing substituted urea linkers inhibit melanoma cell growth. *J. Med. Chem.* **2012,** *55*, 9891-9899.

63. Wickstrom, S. A.; Masoumi, K. C.; Khochbin, S.; Fassler, R.; Massoumi, R. CYLD negatively regulates cell-cycle progression by inactivating HDAC6 and increasing the levels of acetylated tubulin. *EMBO J.* **2010,** *29*, 131-144.

64. Kijima, M.; Yoshida, M.; Sugita, K.; Horinouchi, S.; Beppu, T. Trapoxin, an antitumor cyclic tetrapeptide, is an irreversible inhibitor of mammalian histone deacetylase. *J. Biol. Chem.* **1993,** *268*, 22429-22435.

65. Kozikowski, A. P.; Tapadar, S.; Luchini, D. N.; Kim, K. H.; Billadeau, D. D. Use of the nitrile oxide cycloaddition (NOC) reaction for molecular probe generation: a new class of

enzyme selective histone deacetylase inhibitors (HDACIs) showing picomolar activity at HDAC6. *J. Med. Chem.* **2008,** *51*, 4370-4373.

66. Guerini, V.; Barbui, V.; Spinelli, O.; Salvi, A.; Dellacasa, C.; Carobbio, A.; Introna, M.; Barbui, T.; Golay, J.; Rambaldi, A. The histone deacetylase inhibitor ITF2357 selectively targets cells bearing mutated JAK2(V617F). *Leukemia* **2008,** *22*, 740-747.

67. Amaru Calzada, A.; Todoerti, K.; Donadoni, L.; Pellicioli, A.; Tuana, G.; Gatta, R.; Neri, A.; Finazzi, G.; Mantovani, R.; Rambaldi, A.; Introna, M.; Lombardi, L.; Golay, J.; Investigators, A. The HDAC inhibitor Givinostat modulates the hematopoietic transcription factors NFE2 and C-MYB in JAK2(V617F) myeloproliferative neoplasm cells. *Exp. Hematol.* **2012,** *40*, 634-645.

68. Xiong, H.; Du, W.; Zhang, Y. J.; Hong, J.; Su, W. Y.; Tang, J. T.; Wang, Y. C.; Lu, R.; Fang, J. Y. Trichostatin A, a histone deacetylase inhibitor, suppresses JAK2/STAT3 signaling via inducing the promoter-associated histone acetylation of SOCS1 and SOCS3 in human colorectal cancer cells. *Mol. Carcinog.* **2012,** *51*, 174-184.

69. Wang, Y.; Fiskus, W.; Chong, D. G.; Buckley, K. M.; Natarajan, K.; Rao, R.; Joshi, A.; Balusu, R.; Koul, S.; Chen, J.; Savoie, A.; Ustun, C.; Jillella, A. P.; Atadja, P.; Levine, R. L.; Bhalla, K. N. Cotreatment with panobinostat and JAK2 inhibitor TG101209 attenuates JAK2V617F levels and signaling and exerts synergistic cytotoxic effects against human myeloproliferative neoplastic cells. *Blood* **2009,** *114*, 5024-5033.

70. Novotny-Diermayr, V.; Hart, S.; Goh, K. C.; Cheong, A.; Ong, L. C.; Hentze, H.; Pasha, M. K.; Jayaraman, R.; Ethirajulu, K.; Wood, J. M. The oral HDAC inhibitor pracinostat (SB939) is efficacious and synergistic with the JAK2 inhibitor pacritinib (SB1518) in preclinical models of AML. *Blood Cancer J.* **2012,** *2*, e69.

71. Evrot, E.; Ebel, N.; Romanet, V.; Roelli, C.; Andraos, R.; Qian, Z.; Dolemeyer, A.; Dammassa, E.; Sterker, D.; Cozens, R.; Hofmann, F.; Murakami, M.; Baffert, F.; Radimerski, T. JAK1/2 and Pan-deacetylase inhibitor combination therapy yields improved efficacy in preclinical mouse models of JAK2V617F-driven disease. *Clin. Cancer Res.* **2013,** *19*, 6230-6241.

72. Ohlson, S. Designing transient binding drugs: a new concept for drug discovery. *Drug Discovery Today* **2008,** *13*, 433-439.

73. Ganesan, A. Macrocyclic Inhibitors of Zinc-dependent Histone Deacetylases (HDACs). In *Macrocycles in Drug Discovery*, Levin, J., Ed. The Royal Society of Chemistry: Cambridge, UK, 2015; pp 109 - 140.

74. Haggarty, S. J.; Koeller, K. M.; Wong, J. C.; Grozinger, C. M.; Schreiber, S. L. Domain-selective small-molecule inhibitor of histone deacetylase 6 (HDAC6)-mediated tubulin deacetylation. *Proc. Natl. Acad. Sci. U. S. A.* **2003,** *100*, 4389-4394.

75. Wagner, F. F.; Olson, D. E.; Gale, J. P.; Kaya, T.; Weiwer, M.; Aidoud, N.; Thomas, M.; Davoine, E. L.; Lemercier, B. C.; Zhang, Y. L.; Holson, E. B. Potent and selective inhibition of histone deacetylase 6 (HDAC6) does not require a surface-binding motif. *J. Med. Chem.* **2013,** *56*, 1772-1776.

76. Auzzas, L.; Larsson, A.; Matera, R.; Baraldi, A.; Deschenes-Simard, B.; Giannini, G.; Cabri, W.; Battistuzzi, G.; Gallo, G.; Ciacci, A.; Vesci, L.; Pisano, C.; Hanessian, S. Non-natural macrocyclic inhibitors of histone deacetylases: design, synthesis, and activity. *J. Med. Chem.* **2010,** *53*, 8387-8399.

77. Darkin-Rattray, S. J.; Gurnett, A. M.; Myers, R. W.; Dulski, P. M.; Crumley, T. M.; Allocco, J. J.; Cannova, C.; Meinke, P. T.; Colletti, S. L.; Bednarek, M. A.; Singh, S. B.; Goetz,

M. A.; Dombrowski, A. W.; Polishook, J. D.; Schmatz, D. M. Apicidin: a novel antiprotozoal agent that inhibits parasite histone deacetylase. *Proc. Natl. Acad. Sci. U. S. A.* **1996,** *93*, 13143-13147.

78. Colletti, S. L.; Myers, R. W.; Darkin-Rattray, S. J.; Gurnett, A. M.; Dulski, P. M.; Galuska, S.; Allocco, J. J.; Ayer, M. B.; Li, C.; Lim, J.; Crumley, T. M.; Cannova, C.; Schmatz, D. M.; Wyvratt, M. J.; Fisher, M. H.; Meinke, P. T. Broad spectrum antiprotozoal agents that inhibit histone deacetylase: structure-activity relationships of apicidin. Part 1. *Bioorg. Med. Chem. Lett.* **2001,** *11*, 107-111.

79. Colletti, S. L.; Myers, R. W.; Darkin-Rattray, S. J.; Gurnett, A. M.; Dulski, P. M.; Galuska, S.; Allocco, J. J.; Ayer, M. B.; Li, C.; Lim, J.; Crumley, T. M.; Cannova, C.; Schmatz, D. M.; Wyvratt, M. J.; Fisher, M. H.; Meinke, P. T. Broad spectrum antiprotozoal agents that inhibit histone deacetylase: structure-activity relationships of apicidin. Part 2. *Bioorg Med Chem Lett* **2001,** *11*, 113-117.

80. Gu, W.; Cuetob, M.; Jensenb, P. R.; Fenicalb, W.; Silvermana, R. B. Microsporins A and B: new histone deacetylase inhibitors from the marine-derived fungus Microsporum cf. gypseum and the solid-phase synthesis of microsporin A. *Tetrahedron* **2007,** *63*, 6535 - 6541.

81. Nakajima, H.; Kim, Y. B.; Terano, H.; Yoshida, M.; Horinouchi, S. FR901228, a potent antitumor antibiotic, is a novel histone deacetylase inhibitor. *Exp. Cell Res.* **1998,** *241*, 126-133.

82. Masuoka, K.; Nagai, A.; Shin-ya, K.; Furihata, K.; Nagai, K.; Suzuki, K.-I.; Hayakawa, Y.; Seto, H. Spiruchostatins A and B, novel gene expression-enhancing substances produced by Pseudomonas sp. *Tetrahedron Lett.* **2001,** *42*, 41 - 44.

83. Taori, K.; Paul, V. J.; Luesch, H. Structure and activity of largazole, a potent antiproliferative agent from the Floridian marine cyanobacterium Symploca sp. *J. Am. Chem. Soc.* **2008,** *130*, 1806-1807.

84. Nakao, Y.; Yoshida, S.; Matsunaga, S.; Shindoh, N.; Terada, Y.; Nagai, K.; Yamashita, J. K.; Ganesan, A.; van Soest, R. W.; Fusetani, N. Azumamides A-E: histone deacetylase inhibitory cyclic tetrapeptides from the marine sponge Mycale izuensis. *Angew. Chem. Int. Ed.* **2006,** *45*, 7553-7557.

85. Liu, T.; Kapustin, G.; Etzkorn, F. A. Design and synthesis of a potent histone deacetylase inhibitor. *J. Med. Chem.* **2007,** *50*, 2003-2006.

86. Pirali, T.; Faccio, V.; Mossetti, R.; Grolla, A. A.; Di Micco, S.; Bifulco, G.; Genazzani, A. A.; Tron, G. C. Synthesis, molecular docking and biological evaluation as HDAC inhibitors of cyclopeptide mimetics by a tandem three-component reaction and intramolecular [3+2] cycloaddition. *Mol. Diversity* **2010,** *14*, 109-121.

87. Ning, C. Q.; Lu, C.; Hu, L.; Bi, Y. J.; Yao, L.; He, Y. J.; Liu, L. F.; Liu, X. Y.; Yu, N. F. Macrocyclic compounds as anti-cancer agents: Design and synthesis of multi-acting inhibitors against HDAC, FLT3 and JAK2. *Eur. J. Med. Chem.* **2015,** *95*, 104-115.

88. Poulsen, A.; William, A.; Blanchard, S.; Lee, A.; Nagaraj, H.; Wang, H.; Teo, E.; Tan, E.; Goh, K. C.; Dymock, B. Structure-based design of oxygen-linked macrocyclic kinase inhibitors: discovery of SB1518 and SB1578, potent inhibitors of Janus kinase 2 (JAK2) and Fms-like tyrosine kinase-3 (FLT3). *J. Comput. Aided Mol. Des.* **2012,** *26*, 437-450.

89. Nolan, S. P.; Clavier, H. Chemoselective olefin metathesis transformations mediated by ruthenium complexes. *Chem. Soc. Rev.* **2010,** *39*, 3305-3316.

90. Bermudez-Lugo, J. A.; Perez-Gonzalez, O.; Rosales-Hernandez, M. C.; Ilizaliturri-Flores, I.; Trujillo-Ferrara, J.; Correa-Basurto, J. Exploration of the valproic acid binding site on histone deacetylase 8 using docking and molecular dynamic simulations. *J. Mol. Model.* **2012,** *18*, 2301-2310.

91. Bieliauskas, A. V.; Pflum, M. K. Isoform-selective histone deacetylase inhibitors. *Chem. Soc. Rev.* **2008,** *37*, 1402-1413.

92. Hopkins, A. L.; Keseru, G. M.; Leeson, P. D.; Rees, D. C.; Reynolds, C. H. The role of ligand efficiency metrics in drug discovery. *Nat. Rev. Drug Discovery* **2014,** *13*, 105-121.

93. Vishwakarma, S.; Iyer, L. R.; Muley, M.; Singh, P. K.; Shastry, A.; Saxena, A.; Kulathingal, J.; Vijaykanth, G.; Raghul, J.; Rajesh, N. Tubastatin, a selective histone deacetylase 6 inhibitor shows anti-inflammatory and anti-rheumatic effects. *Int. Immunopharmacol.* **2013,** *16*, 72-78.

94. Estiu, G.; Greenberg, E.; Harrison, C. B.; Kwiatkowski, N. P.; Mazitschek, R.; Bradner, J. E.; Wiest, O. Structural origin of selectivity in class II-selective histone deacetylase inhibitors. *J. Med. Chem.* **2008,** *51*, 2898-2906.

95. Fabian, M. A.; Biggs, W. H.; Treiber, D. K.; Atteridge, C. E.; Azimioara, M. D.; Benedetti, M. G.; Carter, T. A.; Ciceri, P.; Edeen, P. T.; Floyd, M. A small molecule–kinase interaction map for clinical kinase inhibitors. *Nature biotechnology* **2005,** *23*, 329-336.

96. Vanhaesebroeck, B.; Whitehead, M. A.; Piñeiro, R. Molecules in medicine mini-review: isoforms of PI3K in biology and disease. *Journal of Molecular Medicine* **2016,** *94*, 5-11.

97. Karaman, M. W.; Herrgard, S.; Treiber, D. K.; Gallant, P.; Atteridge, C. E.; Campbell, B. T.; Chan, K. W.; Ciceri, P.; Davis, M. I.; Edeen, P. T. A quantitative analysis of kinase inhibitor selectivity. *Nature biotechnology* **2008,** *26*, 127-132.

98. Hurwitz, H. I.; Uppal, N.; Wagner, S. A.; Bendell, J. C.; Beck, J. T.; Wade, S. M.; Nemunaitis, J. J.; Stella, P. J.; Pipas, J. M.; Wainberg, Z. A. Randomized, double-blind, phase II study of ruxolitinib or placebo in combination with capecitabine in patients with metastatic pancreatic cancer for whom therapy with gemcitabine has failed. *Journal of Clinical Oncology* **2015,** *33*, 4039-4047.

99. Panobinostat and Ruxolitinib in MPN clinical trial, http://clinicaltrials.gov/ct2/show/NCT01433445. http://clinicaltrials.gov/ct2/show/NCT01433445 (accessed April 10, 2016).

100. Yi, X.; Wei, W.; Wang, S.-Y.; Du, Z.-Y.; Xu, Y.-J.; Yu, X.-D. Histone deacetylase inhibitor SAHA induces ERα degradation in breast cancer MCF-7 cells by CHIP-mediated ubiquitin pathway and inhibits survival signaling. *Biochem. Pharmacol.* **2008,** *75*, 1697-1705.

101. Carlisi, D.; Lauricella, M.; D'Anneo, A.; Buttitta, G.; Emanuele, S.; Di Fiore, R.; Martinez, R.; Rolfo, C.; Vento, R.; Tesoriere, G. The synergistic effect of SAHA and parthenolide in MDA-MB231 breast cancer cells. *J. Cell. Physiol.* **2015,** *230*, 1276-1289.

102. Wang, H.; Yu, N.; Chen, D.; Lee, K. C. L.; Lye, P. L.; Chang, J. W. W.; Deng, W.; Ng, M. C. Y.; Lu, T.; Khoo, M. L. Discovery of (2 E)-3-{2-butyl-1-[2-(diethylamino) ethyl]-1 H-benzimidazol-5-yl}-N-hydroxyacrylamide (SB939), an orally active histone deacetylase inhibitor with a superior preclinical profile. *J. Med. Chem.* **2011,** *54*, 4694-4720.

103. Ehrentraut, S.; Nagel, S.; Scherr, M. E.; Schneider, B.; Quentmeier, H.; Geffers, R.; Kaufmann, M.; Meyer, C.; Prochorec-Sobieszek, M.; Ketterling, R. P. t (8; 9)(p22; p24)/PCM1-JAK2 Activates SOCS2 and SOCS3 via STAT5. *PloS one* **2013,** *8*, e53767.

104. Katagiri, S.; Yonezawa, T.; Kuyama, J.; Kanayama, Y.; Nishida, K.; Abe, T.; Tamaki, T.; Ohnishi, M.; Tarui, S. Two distinct human myeloma cell lines originating from one patient with myeloma. *Int. J. Cancer* **1985,** *36*, 241-246.

105. Otsuki, T.; Hata, H.; Harada, N.; Matsuzaki, H.; Yata, K.; Wada, H.; Yawata, Y.; Ueki, A.; Yamada, O. Cellular biological differences between human myeloma cell lines KMS-12-PE and KMS-12-BM established from a single patient. *Int. J. Hematol.* **2000,** *72*, 216-222.

106. Matsuo, Y.; MacLeod, R.; Uphoff, C.; Drexler, H.; Nishizaki, C.; Katayama, Y.; Kimura, G.; Fujii, N.; Omoto, E.; Harada, M. Two acute monocytic leukemia (AML-M5a) cell lines (MOLM-13 and MOLM-14) with interclonal phenotypic heterogeneity showing MLL-AF9 fusion resulting from an occult chromosome insertion, ins (11; 9)(q23; p22p23). *Leukemia* **1997,** *11*, 1469-1477.

107. Koeffler, H.; Golde, D. Human myeloid leukemia cell lines: a review. *Blood* **1980,** *56*, 344-350.

108. Iqbal, J.; Kucuk, C.; Srivastava, G.; Tam, W.; Geng, H.; Klinkebiel, D.; Christman, J.; Patel, K.; Cao, K.; Shen, L. Genomic analyses reveal global functional alterations that promote tumor growth and novel tumor suppressor genes in natural killer-cell malignancies. *Leukemia* **2009,** *23*, 1139-1151.

109. Chiang, A. K.; Chan, A. C.; Srivastava, G.; Ho, F. C. Nasal T/natural killer(NK)-cell lymphomas are derived from Epstein-Barr virus-infected cytotoxic lymphocytes of both NK- and T-cell lineage. *Int. J Cancer* **1997,** *73*, 332-338.

110. Karube, K.; Tsuzuki, S.; Yoshida, N.; Arita, K.; Kato, H.; Katayama, M.; Ko, Y.-H.; Ohshima, K.; Nakamura, S.; Kinoshita, T. Comprehensive gene expression profiles of NK cell neoplasms identify vorinostat as an effective drug candidate. *Cancer Lett.* **2013,** *333*, 47-55.

111. West, A. C.; Johnstone, R. W. New and emerging HDAC inhibitors for cancer treatment. *The Journal of clinical investigation* **2014,** *124*, 30-39.

112. Hubbert, C.; Guardiola, A.; Shao, R.; Kawaguchi, Y.; Ito, A.; Nixon, A.; Yoshida, M.; Wang, X.-F.; Yao, T.-P. HDAC6 is a microtubule-associated deacetylase. *Nature* **2002,** *417*, 455-458.

113. Kerr, J. F.; Wyllie, A. H.; Currie, A. R. Apoptosis: a basic biological phenomenon with wide-ranging implications in tissue kinetics. *Br. J. Cancer* **1972,** *26*, 239-257.

114. Vermes, I.; Haanen, C.; Steffens-Nakken, H.; Reutelingsperger, C. A novel assay for apoptosis. Flow cytometric detection of phosphatidylserine expression on early apoptotic cells using fluorescein labelled Annexin V. *J. Immunol. Methods* **1995,** *184*, 39-51.

115. D'Amours, D.; Sallmann, F. R.; Dixit, V. M.; Poirier, G. G. Gain-of-function of poly(ADP-ribose) polymerase-1 upon cleavage by apoptotic proteases: implications for apoptosis. *J. Cell Sci.* **2001,** *114*, 3771-3778.

116. Danial, N. N.; Korsmeyer, S. J. Cell death: critical control points. *Cell* **2004,** *116*, 205-219.

117. Schrödinger, LLC., 2014. New York, NY, USA, http://www.schrodinger.com. (accessed April 10, 2016).

118. Polak, E.; Ribiere, G. Note sur la convergence de méthodes de directions conjuguées. *Revue française d'informatique et de recherche opérationnelle, série rouge* **1969,** *3*, 35-43.

119. Hasel, W.; Hendrickson, T. F.; Still, W. C. A rapid approximation to the solvent accessible surface areas of atoms. *Tetrahedron Comp. Methodol.* **1988,** *1*, 103-116.

120. Lobera, M.; Madauss, K. P.; Pohlhaus, D. T.; Wright, Q. G.; Trocha, M.; Schmidt, D. R.; Baloglu, E.; Trump, R. P.; Head, M. S.; Hofmann, G. A. Selective class IIa histone deacetylase inhibition via a nonchelating zinc-binding group. *Nat. Chem. Biol.* **2013,** *9*, 319-325.

121. Anastassiadis, T.; Deacon, S. W.; Devarajan, K.; Ma, H.; Peterson, J. R. Comprehensive assay of kinase catalytic activity reveals features of kinase inhibitor selectivity. *Nat. Biotechnol.* **2011,** *29*, 1039-1045.

122. Chen, P.-H.; Chien, F.-C.; Lee, S.-P.; Chan, W.-E.; Lin, I.-H.; Liu, C.-S.; Lee, F.-J.; Lai, J.-S.; Chen, P.; Yang-Yen, H.-F. Identification of a novel function of the clathrin-coated structure at the plasma membrane in facilitating GM-CSF receptor-mediated activation of JAK2. *Cell Cycle* **2012,** *11*, 3611-3626.

Table of Contents Graphic